Biomaterials Translational

Proper animal experimental designs for preclinical research of biomaterials for intervertebral disc regeneration

Yizhong Peng[1], Xiangcheng Qing[1], Hongyang Shu[2,3], Shuo Tian[1], Wenbo Yang[1], Songfeng Chen[4], Hui Lin[1], Xiao Lv[1], Lei Zhao[1], Xi Chen[1], Feifei Pu[1], Donghua Huang[4], Xu Cao[5,], Zengwu Shao[1,*]*

Key Words:
animal model; biomaterials; intervertebral disc; preclinical evaluation; translational medicine

From the Contents

ABSTRACT

Low back pain is a vital musculoskeletal disease that impairs life quality, leads to disability and imposes heavy economic burden on the society, while it is greatly attributed to intervertebral disc degeneration (IDD). However, the existing treatments, such as medicines, chiropractic adjustments and surgery, cannot achieve ideal disc regeneration. Therefore, advanced bioactive therapies are implemented, including stem cells delivery, bioreagents administration, and implantation of biomaterials etc. Among these researches, few reported unsatisfying regenerative outcomes. However, these advanced therapies have barely achieved successful clinical translation. The main reason for the inconsistency between satisfying preclinical results and poor clinical translation may largely rely on the animal models that cannot actually simulate the human disc degeneration. The inappropriate animal model also leads to difficulties in comparing the efficacies among biomaterials in different reaches. Therefore, animal models that better simulate the clinical charateristics of human IDD should be acknowledged. In addition, in vivo regenerative outcomes should be carefully evaluated to obtain robust results. Nevertheless, many researches neglect certain critical characteristics, such as adhesive properties for biomaterials blocking annulus fibrosus defects and hyperalgesia that is closely related to the clinical manifestations, e.g., low back pain. Herein, in this review, we summarized the animal models established for IDD, and highlighted the proper models and parameters that may result in acknowledged IDD models. Then, we discussed the existing biomaterials for disc regeneration and the characteristics that should be considered for regenerating different parts of discs. Finally, well-established assays and parameters for in vivo disc regeneration are explored.

***Corresponding authors:**
Zengwu Shao, szwpro@163.com;
Xu Cao, xcao11@jhmi.edu.

http://doi.org/10.12336/biomatertransl.2021.02.003

How to cite this article:
Peng, Y.; Qing, X.; Shu, H.; Tian, S.; Yang, W.; Chen, S.; Lin, H.; Lv, X.; Zhao, L.; Chen, X.; Pu, F.; Huang, D.; Cao, X.; Shao, Z. Proper animal experimental designs for preclinical research of biomaterials for intervertebral disc regeneration. *Biomater Transl.* **2021**, *2*(2), 91-142.

Introduction

The Global Burden of Diseases, Injuries, and Risk Factors Study conducted in 2019 reported that low back pain (LBP) was the leading cause of loss of years to disability from 1990 through 2019, affecting 568 million individuals and with an estimated 64 million years to disability globally.[1] Among 204 countries, LBP is reportedly the leading health condition contributing to the need for rehabilitation services in 160 countries.[1] Statistically, intervertebral disc (IVD) degeneration (IDD) contributes to 40% of LBP.[2] With aging, the economic and social burdens imposed by IDD, which is an age-related disease, are expected to progressively increase in the coming decades.[3] Traditional treatments for IDD include physiotherapy, nonsteroidal anti-inflammatory drugs, lumbar epidural steroid injections, chiropractic adjustments, decompression, spinal fusion, and discectomy.[4-6] Although these therapies, especially surgical interventions, have presented favorable outcomes in terms of pain relief and disability improvement, gastrointestinal and cardiovascular adverse effects following prolonged nonsteroidal anti-inflammatory drug administration, the incidence of reherniation and recurrent back pain after discectomy, and the adjacent disc degeneration observed in spinal fusion render traditional therapies less effective.[7-9]

Therefore, several advanced strategies that emphasize the regeneration of disc integrity and modification of the unfavorable microenvironment of degenerated discs have gained momentum. First, intradiscal administration of autologous or allogeneic stem cells/mature disc cells was

performed.[10, 11] Numerous clinical trials have shown that intradiscal injection of stem cells favors pain relief, with a 1–6-year follow-up period.[11-18] However, the sample sizes in these clinical trials were extremely small (less than 30), and long-term outcomes remained debatable. Bioactive reagents present an additional option for intradiscal administration. As an avascular organ, IVDs appear to prolong the retention of injected reagents when compared with that in articular joints.[19] Ideally, extended exposure to bioactive molecules prevents repetitive injections that may predispose the discs to degeneration.[20-22] The application of biomaterials, such as nanoparticles, can help alter the original drug release pattern and even regulate release based on specific stimulation in the microenvironment.[23, 24]

Numerous biomaterials for disc regeneration have been developed to modify the intradiscal microenvironment to favor cell survival, promote cell reparative effects, and control the release of therapeutic molecules, while others with satisfactory mechanical properties aid in the mechanical repair of impaired discs.[25-28] Preclinical evaluation of these biomaterials is critical for their further application in clinical trials. Animal models that resemble the characteristics of human disc degeneration play a pivotal role in preclinical experiments. Currently, numerous animal models with either spontaneous, mechanical alteration, or disc injury have been established for the preclinical evaluation of therapeutic strategies.[29-33] However, not all models satisfactorily simulate human disc degeneration. Factors, including animal age, disc geometry, size, and mechanical properties for selected animal models, could contribute to the bias of preclinical studies and clinical applications.[34, 35] Apart from spinal fracture-related disc injuries, age-related human disc degeneration is an overall degeneration that influences all discs, specifically the lumbar discs, which hinders the efficiency of local administration.[36, 37] However, most existing biomaterials for disc repair cannot be systemically administered. Therefore, for the *in vivo* evaluation of these biomaterials, animal models with regional degeneration (e.g., disc injury) are preferred, which is not often the clinical case primarily identified in age-related disc degeneration. Therefore, selecting an appropriate animal model that not only resembles human disc degeneration but also facilitates the *in vivo* evaluation of novel biomaterials remains a challenge. In addition, evaluation protocols and parameters for the outcomes of *in vivo* disc regeneration are to yet be unified, resulting in incomparable results among different studies and limiting clinical translation.

The articles about the establishment of animal models for intervertebral disc degeneration were retrieved by the search terms: Intervertebral disc (MeSH Terms) AND (Animal (MeSH Terms) OR Models, Animal (MeSH Terms) OR Animal Experimentation (MeSH Terms)). Then, the articles about biomaterials for disc regeneration were retrieved by the search terms: Intervertebral disc (MeSH Terms) AND Biomaterials (MeSH Terms). Then, the articles related to the characteristics that determines the outcome of intervertebral disc regeneration were retrieved by the search terms: Intervertebral disc (MeSH Terms) AND (Pain (MeSH Terms) OR Hyperalgesia (MeSH Terms) OR Allodynia (MeSH Terms) OR Biocompatibility (All Fields) OR X-ray (MeSH Terms) OR computed tomography (MeSH Terms) OR CT (MeSH Terms) OR Magnetic Resonance Imaging (MeSH Terms) OR Histology (MeSH Terms) OR Anatomy (MeSH Terms) OR Mechanical Tests(MeSH Terms) OR Torsion, Mechanical (MeSH Terms) OR Stress, Mechanical (MeSH Terms) OR Adhesives (MeSH Terms)). All these searches were perfromed on PubMed, Embase, Web of Science and CNKI databases prior to Feburary, 2021. The results were further screened by title and abstract. Irrelevant articles were excluded. In the end, 810 articles were included in this review (**Figure 1**). This review aims to provide cues for appropriate animal experimental designs for preclinical evaluation of biomaterials for IVD regeneration. We summarized the basic pathological characteristics of human degenerated discs, animal models that resemble human disc regeneration, and discussed suitable animal models for the preclinical evaluation of specific biomaterials. We then highlighted the existing biomaterials for disc regeneration and the characteristics that should be considered for regenerating different parts of discs. Finally, we explored well-established assays and parameters for *in vivo* disc regeneration (**Figure 2**).

Pathological Alteration of Intervertebral Disc

Nucleus pulposus

Young and healthy human nucleus pulposus (NP) is a gel-like tissue with an 80% water content and contains two types of cells: notochordal cells and mature NP cells.[38] The former are large vacuolated cells that originate from the embryonic notochord and gradually disappear in an age-related manner. The latter type of cells are the major residents in the adult disc.[39] Both cell types play a vital role in maintaining the integrity of the NP matrix. The extracellular matrix (ECM) in healthy NP and the inner annulus fibrosus (AF) is mainly composed of loosely arranged type II collagen fibers and proteoglycans.[40] Proteoglycans and glycosaminoglycans (GAGs) maintain high osmotic pressure and hydration in NP tissues.[41] Their interaction with cells and cytokines regulates cell biology through various signaling pathways.[42]

Cellular changes during nucleus pulposus degeneration

In NP tissues, the change in cell types begins in childhood, and notochord cells gradually disappear with age. Notochord cells play a crucial role in protecting NP cells and promoting their anabolism.[43, 44] The elimination of notochord cells is predominant in the initiation and development of IDD.[45] Reduced cell numbers and impaired cell viability in degenerative discs are closely related to the excessive activation of multiple programmed cell death pathways, including apoptosis and

1 Department of Orthopaedics, Union Hospital, Tongji Medical College, Huazhong University of Science and Technology, Wuhan, Hubei Province, China; 2 Division of Cardiology, Department of Internal Medicine, Tongji Hospital, Tongji Medical College, Huazhong University of Science and Technology, Wuhan, Hubei Province, China; 3 Hubei Key Laboratory of Genetics and Molecular Mechanism of Cardiologic Disorders, Huazhong University of Science and Technology, Wuhan, Hubei Province, China; 4 Department of Orthopaedic Surgery, The First Affiliated Hospital of Zhengzhou University, Zhengzhou, Henan Province, China; 5 Department of Orthopaedic Surgery, Institute for Cell Engineering, Johns Hopkins University, Baltimore, MD, USA.

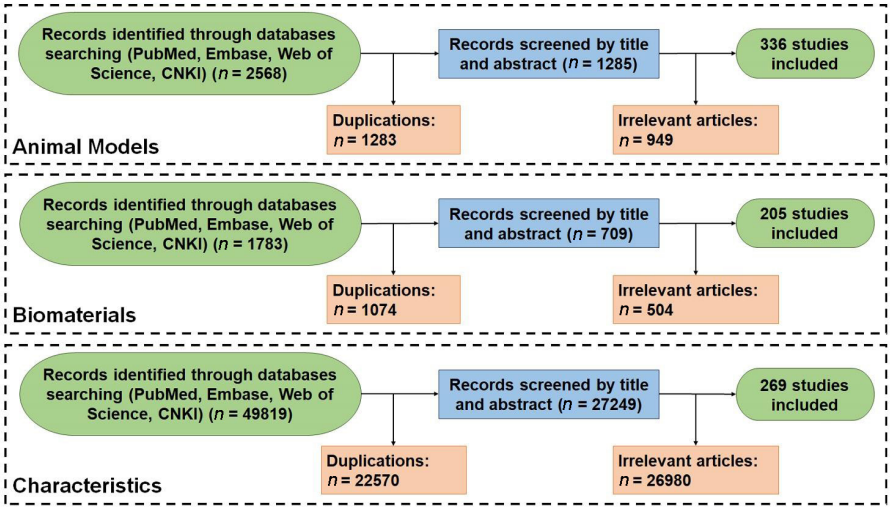

Figure 1. The flow diagram of enrolling articles.

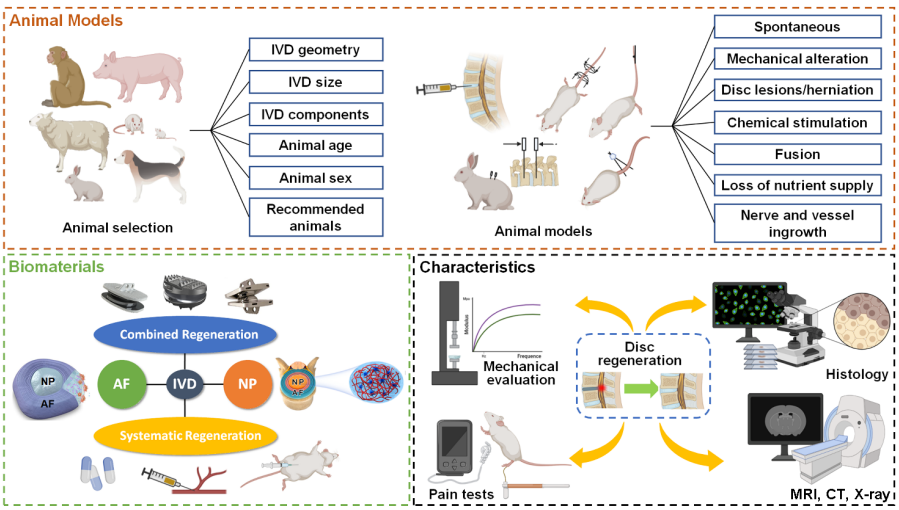

Figure 2. The structural diagram of this review. AF: annulus fibrosus; CT: computed tomography; IVD: intervertebral disc; MRI: magnetic resonance imaging; NP: nucleus pulposus.

necroptosis. Our research group is committed to investigating NP cell death and underlying mechanisms, such as the dysfunction of autophagy and abnormal activation of heat shock protein 90.[46-48] Identifying the underlying mechanism of notochord cell reduction and cell death in an unfavorable intradiscal microenvironment provides further information and alternative targets for biomaterial design and fabrication.

In IDD, disc cells undergo cell death and demonstrate dysfunction in an age-related manner. Among dysfunctional cells, senescent cells play a crucial role in the pathology of IDD.[49] Cell senescence is characterized by a cell state of proliferating arrest and secretion of senescence-associated secretory phenotype.[50] Senescent cells are detrimental to tissue renewal and repair and are known to secrete several proinflammatory factors, including chemokines, cytokines, protein enzymes, and other bioactive factors, which further destroy the living environment of surrounding cells and place degenerated discs at risk of a vicious circle.[51] Contrary to the effective self-clearance of senescent cells in other tissues, the avascular nature of discs partly limits immune-mediated clearance and causes abnormal accumulation.[52, 53] Although senescent cells are characterized by permanent cell cycle arrest, temporary replication stagnation can be reversed when intervened during early stages with reduced risk factors.[54] Instead of reversing senescent cells and restoring their function, another strategy focusing on removing these cells, called senolysis, has been proven effective in prolonging life expectancy[55-57] and ameliorating various age-associated disorders, including cognitive impairment, vascular disease, and cardiac dysfunction.[58-60] Strategies that target cellular senescence in the field of IVD regeneration warrant further research.

During IDD, the NP cell phenotype changes as microenvironments become increasingly unfavorable, such as accumulating ECM degradation products and lactic acid.[61, 62] Phenotypic changes in NP cells, such as the production of proinflammatory cytokines and chemokines, lead to an increase in ECM degradation, with a decrease in the level of anabolic factors and synthesis of healthy ECM.[63-67] In addition to synthesizing matrix metalloproteinases (MMPs) and a

disintegrin and metalloproteinase with thrombospondin motifs (ADAMTSs) that mediate ECM degradation, NP cells secrete chemokines, C-C chemokine ligand (CCL)2, CCL3, and (C-X-C motif) ligand 10, to stimulate the recruitment of immune cells that produce interleukin (IL)-1β and tumor necrosis factor (TNF)-α, which further stimulates the production of MMPs and ADAMTSs, thus amplifying the pro-catabolic alteration of ECM.[68-70] Additionally, inflammatory factors can promote cell apoptosis, further accelerating IDD.[71] Therefore, although the IVD is considered an avascular tissue, inflammatory factors secreted by invading inflammatory cells and NP cells form a continuous inflammatory microenvironment, which plays a vital role in the development of IDD.[72-74] The alleviation of inflammation in the IVD is a crucial issue in delaying IDD.

Disruption of extracellular matrix homeostasis

The NP tissue is composed of abundant ECM that maintains a dynamic balance between synthesis and proteases-induced degradation.[75] Following IDD, ECM anabolism gradually decreases, while catabolism is accelerated, which eventually leads to an imbalance in ECM metabolism. The catabolism of NP ECM is mainly mediated by two enzymes: MMP and ADAMTS. As mentioned above, inflammatory factors can promote MMP and ADAMTS secretion, fostering ECM degradation. An increase in ECM degradation products can also induce the secretion of IL-1β, TNF-α, IL-6, and other inflammatory factors, which further promotes ECM catabolism and accelerates IDD.[63] The metabolic imbalance of ECM leads to a gradual decrease in the proteoglycan content, with alterations in collagen types and organization.[76-78] Eventually, the gel-like tissue is gradually replaced by a consolidated fibrous structure that fails to distribute the axial pressure evenly and limits segmental motion.[79, 80]

Furthermore, ECM homeostasis depends on cytokines. Transforming growth factor-β (TGF-β) signaling plays a protective role in ECM homeostasis by stimulating matrix synthesis, inhibiting matrix catabolism, inflammatory response, and cell loss.[81] TGF-β is also known as one of the most potent inhibitors of TNF-α-induced MMP upregulation and matrix degradation.[82] However, excessive TGF-β activation can accelerate disc degeneration.[83, 84] Aberrant mechanical loading resulted in excessive activation of TGF-β signaling and IDD, while suppressing TGF-β signaling attenuated IDD, which may be attributed to variations in Smad activation.[85-87] Moreover, the bone morphogenetic protein (BMP) family, including BMP-2 and growth and differentiation factor-5 (GDF-5), can reportedly promote the synthesis of ECM components and reduce MMP expression.[88, 89]

Annulus fibrosus

AF consists of a unique and complex structure of 15–25 concentric layers that are generated from packed collagen fibers (mainly type I collagen).[90] Type I collagen increases from the inner to the outer AF, and the opposite trend can be observed with regards to the content of type II collagen and aggrecan.[40, 91] The interlamellar matrix between adjacent layers is composed of elastic fibers, cells, water, lipids and proteoglycans, etc.[92] Although the primary resident cell type, often referred to as AF cells, is annulocytes,[93] various other cell types are present within the AF, such as the AF stem/progenitor cells and cells in the interlamellar matrix with different cell morphologies, which are influenced by the mechanical loads, elastic fiber orientation, and density.[92, 94, 95] AF cells are characterized as elongated and spindle fibroblasts with extended cytoplasmic processes. During degeneration, AF cells become more rounded and chondrocytic, developing multiple cytoplasmic processes that extend extracellularly.[96, 97] The structural integrity of the AF tissue is critical for confining the NP, as well as for maintaining the physiological loading pressure of the spine.[27] With aging, the AF structure gradually becomes disordered, and the cartilage-like matrix accumulates, resulting in weakened tensile strength.[98]

Mechanical disturbance of degenerated annulus fibrosus

Biomechanical "wear and tear" plays a vital role in AF tissue degeneration. When exposed to higher mechanical stress, type I collagen and aggrecan production decreased, while tissue inhibitor of metalloproteinase-1 increased, which could induce ECM remodeling to a degenerative state.[99] With progressing IDD, the mechanical stress is shifted from hydrostatic pressure to shear stress, which reportedly decreases proteoglycan production and increases apoptosis by enhancing nitric acid production.[100, 101] A disturbed AF fiber structure and prolonged biomechanical changes lead to acute tears and fissures in AF tissues, forming a stress point where the structure around AF fissures, including fibers and NP tissue, undertake "push-out" forces that aggravate AF tissue damage and NP herniation, which is closely associated with discogenic pain.[102, 103] AF damage caused by degeneration and biomechanical changes (e.g., overloading) are crucial factors for ECM remodeling and cellular pathology.[98, 99] Therapeutically, it is ideal to repair annulus fissures early, thus reducing the need for future surgery.[104]

Proinflammatory microenvironment of the injured annulus fibrosus

Mechanical stress also promotes the upregulation of proinflammatory genes in AF cells, including cyclooxygenase-2, IL-6, and IL-8.[105, 106] The secreted chemokines and damaged tissue fragments result in the recruitment of immune cells to the wound area to eliminate tissue debris while forming an inflammatory microenvironment. Inflammatory cells, including macrophages, T lymphocytes, and mast cells, have been recognized in the region of injured AF tissue.[93, 107-109] AF injury with a weak immune cell response results in poor healing outcomes.[110] This phenomenon suggests that recruitment of inflammatory cells with an appropriate inflammatory phenotype and timely reversal to an anti-inflammatory healing state may be necessary to repair AF injury. However, NP herniation has been shown to induce a prolonged immune response associated with the exposure of concealed antigens from NP tissue to the immune system.[111, 112] Herniation-related chronic inflammation is one of the key factors that induce phenotype changes and predisposes the tissue to degeneration and painful conditions.[113, 114] Strategies that modify the inflammatory microenvironment have shown great potential for promoting disc cell survival and favoring tissue regeneration.[115-117]

Endplate and bone tissue

Endplates consist of hyaline cartilage and osseous components (subchondral bone) at the cranial and caudal ends of discs. Endplates can prevent disc extrusion into the porous vertebral body and evenly distribute mechanical loads to the adjacent vertebral body.[118, 119] With aging, the endplate gradually undergoes calcification, which affects the nutrient supply of the IVD. Conversely, as the endplate becomes thinner and bone mineral density is lost, the risk of endplate fracture increases.[118, 120-122] The damaged endplate then extrudes into the adjacent vertebrae, increasing the NP volume and resulting in a 30–50% drop in NP pressure and uneven load distribution to the vertebral body.[123] These pathological and biomechanical alterations lead to endplate-driven degeneration.

In patients with IDD, the Modic change is a common observation on magnetic resonance imaging (MRI), referring to the signal change of the vertebral endplate and subchondral bone, which is related to lumbar disc herniation and LBP.[124-126] Modic changes can be divided into three types based on differences in MRI signals. Type 1 changes refer to hypointensity on T1-weighted imaging (T1WI) and hyperintense on T2-weighted imaging (T2WI), which reveal the fracture or tear of the cartilage endplate, as well as revascularization and fibrous tissue formation in the adjacent cancellous bone marrow cavity. In terms of its pathological significance, the hematopoietic bone marrow is characterized by edema and inflammation. Type 2 changes refer to hyperintensity on T1WI and isointense or slightly hyperintense on T2WI. In this case, the pathological significance is that normal hematopoietic bone marrow is replaced by fatty bone marrow. Type 3 changes refer to hypointensity on both T1WI and T2WI and are considered to represent subchondral bone sclerosis.[127] Disc/endplate damage, occult discitis, and autoimmunity are potential risk factors for Modic changes, among which inflammation plays a vital role during the pathological process.[128, 129] Studies have revealed that Modic type 1 changes are more substantially associated with LBP than other types.[127, 130] This association may be related to inflammatory irritation of the dorsal root ganglion following injury and disc degeneration.[129] A previous study revealed that in patients with IDD and Modic type 1 vertebral endplate changes, immunoreactive nerve ingrowth and increased TNF-α expression can be observed in the vertebral endplate.[129] A recent study has reported that sensory innervation in porous endplates induced by osteoclasts may play an important role in spinal pain.[131]

Nerve ingrowth and vascularization

In adult human discs with no apparent histological degeneration, nerves are restricted to the outer third of the AF, while a few nerves can be observed in endplates with similar densities within various anatomical regions.[132, 133] Damage and degenerative changes induce nerves to grow inward, resulting in an expanded distribution of nociceptive nerve endings and LBP.[132] However, the mechanisms underlying increased nerve ingrowth during disc degeneration need to be clarified.[134] Several studies have shown that nerves are confined to proteoglycan-depleted regions of disrupted tissue, especially within annulus fissures, which may be attributed to the inhibitory effects of aggrecan on nerve ingrowth.[135-137] In addition, osteoclasts play a critical role in the ingrowth of sensory nerve porous endplates, in which Netrin-1 derived from osteoclasts is found to be involved.[131] An increasing number of studies have revealed that nerve growth into the IVD is mediated by nerve growth factors secreted from IVD cells, nerve cells, and inflammatory cells.[138-140] Elevated nerve growth factor expression closely correlates with the inflammatory microenvironment of degenerated IVDs.[138, 139, 141, 142] However, the specific mechanisms of innervation and the generation of discogenic pain are not yet well understood and could provide novel therapeutic strategies for LBP. Furthermore, a previous study revealed that although there are more ingrown nerves in endplates than in annulus fibers, many innervated endplate pathologies are undetectable on MRI.[133] Therefore, further research on new visualization methods is critical to better evaluate nerve ingrowth on a full scale while considering the whole disc, as well as to reveal the relationship between nerve ingrowth and LBP or the degree of IVD.

Abnormal vascularization is another pathological change associated with IDD. IVD is recognized as the largest avascular structure in the human body. In healthy adult disc tissues, a few blood vessels can be found in the outermost lamellar layers of AF, while no obvious vascularization can be identified in cartilage endplates and the NP.[143, 144] However, abnormal vascularization has been frequently identified in damaged or disrupted ECM of cartilage endplates and inner layers of AF.[145] Interestingly, nerve ingrowth is often accompanied by vascularization, which provides oxygen and nutrients to the nerve.[135, 146] Therefore, consistent with nerve ingrowth, vascular ingrowth is more likely to be localized near or within damaged tissue, which is probably due to the disruption of anti-angiogenic factors (e.g., proteoglycans and aggrecans) and the increased secretion of angiogenic growth factors and cytokines (e.g., vascular endothelial growth factor and IL-1β).[135, 146] IL-1β can upregulate the expression of vascular endothelial growth factor, thereby triggering neovascularization in the IVD.[141, 142] Accordingly, it can be stated that inflammation plays a vital role in IVD cell dysfunction, reduction in cell number, ECM metabolic disruption, and nerve and blood vessel growth. Therefore, inhibiting inflammation can serve as an important target for IVD therapy and delay IDD progression at multiple levels.

The harsh microenvironment in the degenerated disc

In IDD tissue, a harsh microenvironment is known to exist, including inflammation, low oxygen concentrations, acidity, and hyperosmolarity, which are detrimental to cell survival.[147] As a typical characteristic of IDD, the inflammatory environment is induced by changes in the NP cell phenotype, inflammatory cell infiltration, and cell senescence.[148-150] Inflammation further promotes the dysfunction and apoptosis of disc cells, aggravates the disruption of ECM metabolism, and accelerates IDD development.[76, 151-153]

The IVD itself is inherently avascular and consequently establishes a hypoxic microenvironment, especially in the NP.[154] In relation to anaerobic glycolysis, IVD cells modulate their metabolic strategies to adapt to the hypoxic low-glucose

environment and maintain their viability, which leads to lactic acid accumulation within IVD tissues.[155] Therefore, the average pH is slightly acidic (7.0–7.2) under physiological conditions. However, in mild degenerative conditions, the pH may drop to 6.5, and even to 5.6, in severely degenerated IVDs, which has a detrimental effect on NP cell viability and ECM homeostasis.[156, 157] Hypoxic conditions facilitate energy metabolism and type II collagen production while reducing the unfavorable damage induced by oxidative stress and cell apoptosis.[158] More interestingly, hypoxia may favor mesenchymal stem cell survival in the hostile IVD microenvironment after implantation;[159] in contrast, it has been reported that prolonged exposure to severe hypoxia under serum-deprivation conditions eventually results in complete cell death.[160]

The NP tissue is rich in GAGs characterized by negatively charged side chains of aggrecan molecules, leading to hyperosmolarity within the NP tissue. NP cells can adapt to high osmolarity by regulating the expression of tonicity enhancer-binding protein.[161] However, with progressive loss of proteoglycans with IDD, the osmolarity declines during the degenerative process.[162] Under relative hypo-osmolarity, the apoptosis of NP cells is significantly increased.[163] Furthermore, high osmolarity is detrimental to the viability and proliferation of exogenous mesenchymal stem cells, such as bone marrow stromal cells and adipose-derived stem cells, while the relative hypo-osmolarity promotes NP-derived stem cell proliferation and chondrogenic differentiation.[164, 165] Therefore, the distinct preferences of stem cells and mature disc cells for osmolarity should be considered when designing cell delivery strategies that facilitate the survival and biofunction of implanted cells.[166]

Animal Models

With the continuous development of IVD pathophysiology and material science, it is imperative to establish appropriate animal models that can accurately simulate the pathological and biological properties of human IVDs. Unfortunately, there is currently no recognized model that meets these requirements. The selection of animals for establishing the IDD model needs to consider the following points:

A. IVD geometry: The shape of the IVD determines the state of deformation of various parts when under stress.[167-169] An unreasonable geometric model would fail to accurately reflect the pressure on each component when the IVD is stressed, which leads to inaccurate findings. One previous study has comprehensively evaluated animal disc geometry, including axial cross-sections, shape and position of the NP, and relative disc height of the species used in the disc research.[170] In terms of the geometric parameters of the disc height, AF width, and NP area, the mouse lumbar, rat lumbar, and mouse tail discs most correlated with the human lumbar IVD geometry.[170]

B. IVD disc mechanics: The force imposed on human lumbar discs comprises the axial pressure caused by the upper body weight and dynamic pressure during activities.[90, 148, 171] Accurate simulation of this pressure mode is critical for evaluating the *in vivo* biomechanical properties of implanted biomaterials. Although bioreactors ideally simulate the pressure environment of human IVDs *ex vivo* in controllable magnitudes, the simulation of human disc dynamic pressure performed with an external device in an animal model is still limited.[172, 173] Therefore, the mechanical characteristics of animal models are particularly important. Most animal models include rodents, rabbits, dogs, sheep, pigs, and cows, which are quadrupeds. The pressure on the IVDs of these animals is mainly caused by the paraspinal muscles and ligaments. Maintaining spine stability may require greater muscle tension and passive tension to maintain a stable horizontal state,[174] compared with erect state. The disc pressure caused by this position may not be less than that in the human body.[175] A comprehensive review has summarized the mechanical properties of human and other animal discs.[35] Disc axial mechanics normalized by disc height and area were similar among species. Nevertheless, the normalized stiffness of calves and pigs is slightly more than that of human discs, while that of mice and rats is significantly less than that of humans.[35]

C. IVD size: The IVD size determines the permeability of the tissue fluid and transport of implanted drugs and nano-microparticles.[176] As the IVD is an organ lacking blood vessels, the nutrition obtained by the cells mainly depends on nutrient infiltration.[177-179] Simulating the osmotic dynamics will reduce deviations. Furthermore, the size of the IVD also determines the surgical approach for biomaterial implantation. Compared with larger discs, hydrogels may better repair AF defects of smaller volumes. A critical factor determining annulus repair outcomes is whether the biomaterial can be well anchored on the local defect. In a small annulus defect, the surface tension of the hydrogel may play a role in the fixation of the material, while better adhesion properties are required to achieve satisfactory reparative effects in larger annulus defects.[180]

D. IVD components: A disc model similar to human IVD components should mainly include cellular and biochemical components. The notochord cells in the human IVD gradually decrease from birth and disappear in adulthood.[181] Human notochord cells can proliferate and differentiate into mature NP cells that secrete the ECM.[182, 183] It is currently believed that the reduction in human notochord cells plays a critical role in IDD with age.[45, 184] Like humans, notochord cells of sheep, goats, horses, and cattle rapidly decrease after birth.[175, 185, 186] However, in most other mammals, notochord cells in the NP tissue persist throughout a considerable portion of their life, including mice, rats, rabbits, and pigs.[45, 187, 188]

Notably, there are two types of dogs. Chondrodystrophoid (CD) dogs, such as Dachshund and Beagle, which demonstrate a shortening of the long bones and decreased notochordal cells after birth. However, notochordal cells persist in non-chondrodystrophoid (NCD) dogs, like hounds, leading to a lower incidence of IVD.[189] Furthermore, the biochemical composition of IVD is another factor that differs between humans and other species. For example, rodents do not express MMP-1, a general and critical matrix regulator that participates in the ECM catabolism of human IVDs.[175]

E. Animal age: IDD is an age-related disease. With the increase in pig age (newly born: 2–3 weeks; mature: 6–9 months; older: 2–3 years), the ECM protein of the AF

gradually decreases, while that of the NP first increases and then decreases.[190] When CD dogs are 3–7 years old, the thoracic and lumbar IVDs present degenerative morphology, while NCD dogs have similar pathophysiological changes of IDD when 6–8 years old.[191] Clarifying the animal age for degenerative morphology or controlling the influence of age in external stimulation-induced disc degeneration (e.g., needle puncture and compression) should be carefully considered for robust experimental designs that enroll animal models of IDD.

F. Animal sex: Although human disc morphology showed no significant differences between males and females, other animals showed a unique relationship between sex and disc degeneration or related LBP.[192, 193] The disc degeneration grade was higher in female Sprague-Dawley rats than in male rats after annular puncture injuries.[194] In a rat model of spontaneous degeneration, females showed a greater incidence of radiologic disc space narrowing and wedging than males.[195] In terms of discogenic pain, female rodents demonstrated increased sensitivity to nerve root injury, and the prevalence of LBP is greater in women than in men.[196-198] However, after annular puncture, paw withdrawal thresholds of female rats were more variable, and normalized paw withdrawal thresholds did not significantly differ between sham and injury groups; however, annular puncture induced significantly decreased paw withdrawal thresholds in male cohorts. Estrogen variation may underlie the controversial results in female models.[199] Therefore, male animals may be more suitable for establishing a reliable discogenic pain model.

Primates may be the most appropriate after considering all these factors. 1) Non-human primates have semi-upright and upright characteristics.[200-202] 2) The shape, size, and geometric structure of the IVD are extremely similar to those of human.[201-203] 3) Non-human primates share disc degeneration biomechanical properties and pathological patterns with human.[202] 4) Age-related disc degeneration of non-human primates simulates the pattern of human disc degeneration. For example, the notochord cells naturally degenerate, simultaneously. The aging spines of rhesus monkeys are afflicted with disc degeneration, osteophytosis, and kyphosis, while these degenerative changes are most severe in the thoracolumbar and lumbosacral zones in human[200, 204-206] However, the large size of primate discs makes the modeling operation more varible and less stable, which may reduce the comparability among studies.[207] Also, ethical and cost restrictions hinder the application of primate models.[208] In fact, besides aging model, local needle puncture model and chemical stimulation with pingyangmycin and bleomycin have been performed to accelerate the progression of primates disc degeneration, while pingyangmycin and bleomycin results in more mild and slowly progressive disc degeneration.[209-218]

Sheep may be another suitable candidate for the following reasons: 1) The absence of notochord cells in adulthood; 2) a disc size similar to that of humans; and 3) mechanical characteristics are similar to those of humans.[170, 185, 219] Currently, there are various approaches to establishing animal IDD models[220-226] (**Additional Table 1**).

Spontaneous

Aging

As mentioned in an earlier section, naturally occurring animal aging predisposes to IDD in certain species, and the pathological performance is substantially similar to that of humans.

CD and NCD breeds can be distinguished based on their physical appearance.[227] Specifically, due to disrupted endochondral ossification, CD dog breeds (e.g., Beagles and Dachshunds) have short bowlegs, and CD dogs are closely linked with severe IDD.[228] In CD dog breeds, IDD (mainly Hansen type I herniation) typically develops in the cervical or thoracolumbar spine at approximately 3–7 years of age.[228] NCD dog breeds (e.g., hound) can also develop IDD (mainly Hansen type II herniation), but in the caudal cervical or lumbosacral spine at about 6–8 years old, primarily attributed to trauma or "wear and tear." The macroscopic, histopathological, and biochemical changes, as well as the diagnostics and treatment of IVD disease, are similar in NCD and CD dogs.[228, 229]

The mouse model is one of the most applied animal models for IDD owing to its availability, economy, ease of operation, similar genomic pattern to humans, and ease of obtaining ethical approval. The mouse spontaneously developed disc degeneration in an age-related manner. IVDs in mice less than 14–18 months of age reportedly show no significant degenerative signs, although disc degeneration was found to start from 3–6 months.[30, 230-232] Moreover, a moderate to severe lumbar disc condition was observed by MRI analysis and histological grade in 22-month-old mice.[230]

Baboons are quadruped for locomotion but spend a considerable proportion of their lifetime in the upright position, which imposes chronic spinal mechanical loading.[233] Their life expectancy is 30–45 years.[201] Reportedly, an aging baboon was found to routinely demonstrate radiographic findings of disc degeneration similar to those in humans, including disc space narrowing, endplate sclerosis, and osteophytosis.[234] Statistically, the average age at which baboons developed radiologic grades 1, 2, and 3 were 17.41, 19.94, 20.05 years.[200]

Gene mutations

Gene engineering is a common tool to investigate the specific roles of certain genes, non-coding RNAs, and proteins in disease development and progression. Mutation of ECM genes, such as collagen and aggrecan, induces degenerative morphology, including NP shrinkage or disappearance and fissures in the AF, which can sometimes lead to herniation of disc material and slight osteophyte formation, along with progressive joint degeneration.[200, 235-249]

Although genetically modified mice with ECM gene mutations have revealed the significance of these genes in maintaining IVD integrity, age-related degeneration is more relevant to the human disorder. DNA damage is a critical feature of senescence.[250] A failure in DNA repair is a common approach for inducing progeroid syndrome. Mice deficient in the DNA repair endonuclease, ERCC1, were developed to study accelerated aging.[251, 252] Ercc1(−/Δ) mice represent an accurate and rapid disc aging model, including premature loss of disc proteoglycan, reduced matrix proteoglycan synthesis, and

enhanced apoptosis and cell senescence.[253]

Secreted protein, acidic and rich in cysteine, also known as osteonectin and BM-40 (40-kDa basement membrane protein), is a matricellular protein essential for tissue remodeling.[254] Secreted protein acidic and rich in cysteine (SPARC)-null mice showed signs of movement-evoked discomfort as early as 3 months of age.[255] More importantly, SPARC-null mice developed region-specific, age-dependent hypersensitivity to cold, icilin, and capsaicin (hind paw only), as well as axial discomfort, motor impairment, and reduced physical function.[256] Therefore, both structural and functional alterations of SPARC-null mice suggest its superior representation of human IDD.

Mechanical alteration

Compared with the general population, drivers, athletes, and workers undertaking heavy labor are more inclined to develop LBP, in which biomechanical "wear and tear" plays a critical role in the development of IDD.[257-259] Excessive mechanical loading leads to dysfunction of the energetic metabolism of IVD cells, disc inflammation, apoptosis, necroptosis, and imbalanced catabolic and anabolic metabolism.[47, 260-270]

Mechanical factors that induce IDD include the gravity generated by the upper body when walking upright and the torsion and shear force in activities, such as bending. Several animal models have been developed to alter disc biomechanics and induce disc degeneration, including spine instability, tail suspension, amputation of the upper limbs, tail bending, spinal shear stress, and microgravity.[31, 271-275] However, most mechanical modifications fail to accurately simulate both static and dynamic biomechanics of the human disc.

Spinal instability

The spinal instability model involves damaging the muscles and ligaments around the spine, causing mechanical instability in the corresponding spine segment. Generally, spinous processes are resected along with the supraspinous and interspinous ligaments[31, 83] (**Figure 3**). On removing these structures, the remaining muscles and ligaments form an uneven tension around the disc segments, resulting in persistent abnormalities in spinal mechanics during daily activities. With progressing days, the physiological curvature of the spine gradually disappears, along with the gradually decreasing NP tissue, increased AF microfissures, and deformed or broken endplates in severe cases.[157, 276] The mouse model with IVD instability showed significant histological degeneration within one week of surgery. Additionally, the IDD grade in the 12th month after establishing the mouse instability model was comparable with that observed in the 18-month age group.[31] Additional ovariectomy aggravates degenerative morphology and promotes vascularization into the discs.[277] Mechanical instability has been shown to promote nerve invasion into IVD tissues, resulting in hypersensitive pain, which is a critical clinical symptom of patients with IDD.[278] Therefore, spinal instability is a reliable strategy for creating degenerated mechanical performance. Additionally, although laminectomy has been adopted to establish the *ex vivo* porcine or sheep lumbar disc instability models,[279, 280] *in vivo* spine instability model for large animals is still lacking, and which kind of spine instability model better resembles the biomechanical properties of human degenerative discs is still a maze.[280] Moreover, the mechanical alteration is limited to operated segments, which cannot compete with the systematic disc degeneration of spontaneous models. Furthermore, the tissue damage is markedly severe, and several spinous processes are destroyed, leading to neuralgia after tissue injury rather than discogenic pain in IDD.

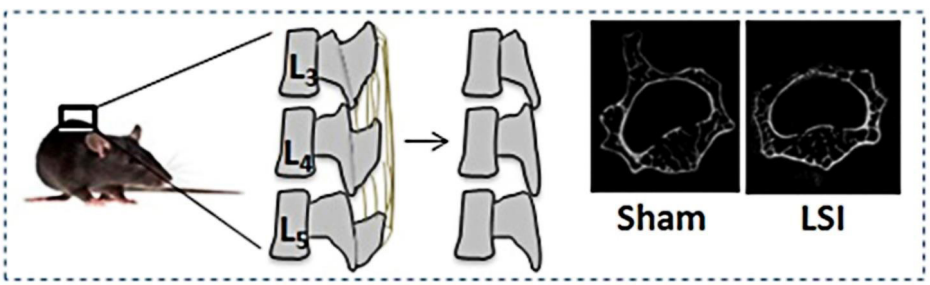

Figure 3. Lumbar spine instability mouse model (LSI). Mouse L3–5 spinous processes were resected along with the supraspinous and interspinous ligaments to induce instability of lumbar spine. Reprinted by permission from Macmillan Publishers Ltd.: Bian et al.[83] Copyright 2016.

Static/dynamic compression

Different static/dynamic compression models are shown in **Figure 4**.

Suspension and microgravity

Suspension simulates an enhanced tensile force on the spine. On hanging by the tail, the IVD experiences a low compressive force similar to weightlessness during space flight.[272, 285] In turn, low hydrostatic pressure is produced. Furthermore, tail suspension creates an extensive tensile force on IVD, especially the annulus (e.g., bending stretches the posterior annulus, and twisting induces tension in the whole annulus).[272] Tail suspension is economical and well-established, with a string and pulley system to maintain the hind limbs off the ground (**Figure 4A**). Reportedly, proteoglycan levels decrease by 35% after rat tail suspension for 4 weeks.[272, 274] Catabolic genes (*MMP3* and *Admts5*) were significantly upregulated in NP and AF tissues after 6 weeks, but degenerative histological changes were not apparent.[286] In mouse tail suspension, the lumbar IVD height index and matrix protein expression levels were

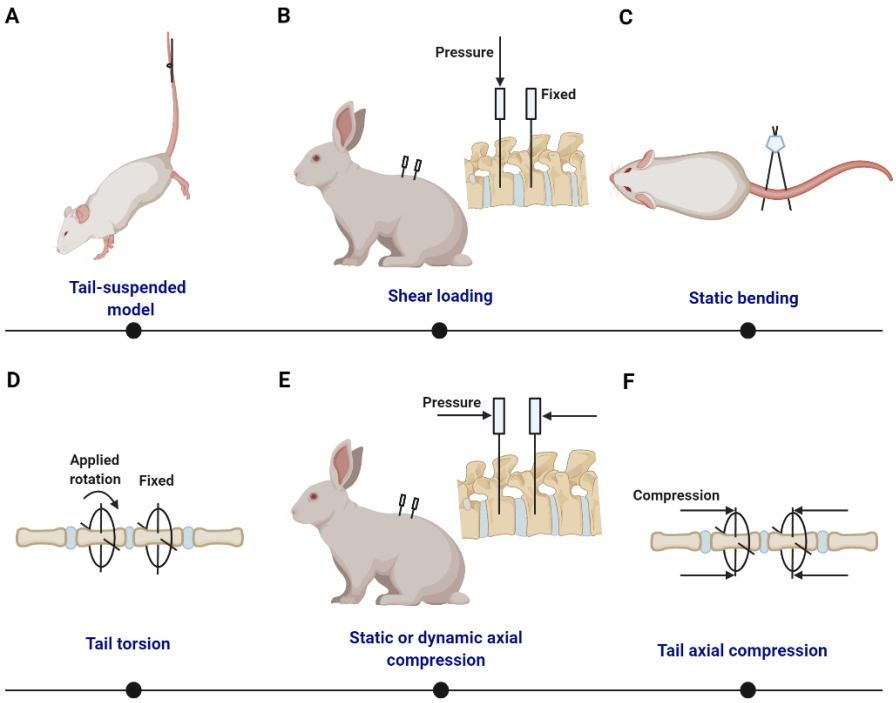

Figure 4. Summary of static/dynamic compression models with external apparatus. (A) Tail-suspended rat with its hind limbs off the floor.[272] (B) Shear loading is generated from forces of different magnitudes on the adjecant vertebrae.[281, 282] (C) Static disc bending model based on pins and an alignment jig.[283] (D) Ilizarov-type apparatus is used to produce tail torsion. (E) Surgically implanted transfixing pins and percutaneous posts allow the application of static or dynamic axial compression and distraction loading at a single level of the rabbit lumbar spine.[284] (F) Ilizarov-type apparatus is used to produce tail axial compression.

significantly decreased, with delayed cell cycling, increased proportions of senescent cells, and senescence-associated secretory phenotype, suggesting an age-related pathological alteration.[152]

Shear stress

Rotation, or body twisting, induces torsion or shear stress in various parts of the IVD. Generally, peripheral surfaces are subjected to the greatest stress, consequently developing maximum strains.[28, 287] A stainless steel shear loading device has been developed to apply a static shear load of up to 4 N to intervertebral joints via attachment to the indicated vertebral bones of the rat in the dorsoventral direction[281] (**Figure 4B**). With an adjustable spring force, the shear force imposed on the disc can be easily controlled at approximately 4 ± 1 N. After shear loading, the posterior annulus initially curves into the corresponding portion of the NP. Impressively, over 2 weeks, the NP tissue completely disappeared, and continued loss of the typical lamellar architecture of the inner and middle annulus resulted in a more severely disorganized tissue after surgery. Another similar external loading device was performed on rabbits to exert an adjustable shear force to around 50 N, and induced significant disc height narrowing as well as degenerative morphology after 1–2 months.[282]

Bending

Spine bending is a general posture change that imposes excessive deformation and compression on the concave AF and NP; for example, when a human picks up or participates in specific activities, such as farming or lifting. Rat tail bending is mainly performed owing to availability and stability. Tail bending achieved by external devices results in different mechanical and cellular alterations on the concave and convex sides (**Figure 4C**). With excessive compression, aggrecan expression decreased in the concave annulus when compared with the convex annulus in both the rat bending model.[283] More cell death was observed in the concave annulus (compression) than in the convex annulus (tension).[288] Although tissue denaturation is more evident on the concave side during spine bending, NP herniation typically occurs on the convex side. Therefore, the tissue regeneration strategy should focus on the unfavorable tensile stress on the convex annulus.

Torsion

Torsion is often accompanied by shear stress. Ilizarov-type fixators are similar to the components, organization, and manufacturing processes of the Ilizarov-type apparatus that induces static axial compression (**Figure 4D**). By altering the angle between the carbon fiber rings, rotation of various angles can be generated. By employing motor, cyclic rotations were performed at different frequencies. Maintaining a ±30° orientation significantly promoted the expression of proinflammatory cytokines (IL-1β and TNF-α) and catabolic genes.[289]

Based on our understanding, when processing an Ilizarov-type apparatus to generate static compression, the dislocation of carbon fiber rings, in either the sagittal or coronal plane, is inevitable during initial manufacture or later animal activities.

Therefore, an unpredictable amount of torsion is inevitable when using the Ilizarov-type apparatus.

Axial compression

Axial compression represents pressure along the spine while standing. For inducing compressive IVD stimulation, a dynamic-loading rabbit model has been established to perform controlled and dynamic axial loading on rabbit lumbar discs. Surgically implanted transfixing pins and percutaneous posts allow the application of controlled axial compression and distraction loading at a single level of the New Zealand white rabbit lumbar spine[284] (**Figure 4E**). Also, the Ilizarov-type apparatus was employed, an external fixation device that enables mechanical force application across the IVD[290] (**Figure 4F**). This device not only compresses but also immobilizes the IVD. Compressive loads on the IVD result in axial compression of the AF and bulging of the NP, which radially compresses the AF. Immobilization resulted in decreased disc thickness, axial compliance, and angular laxity, while compression induced these changes earlier and to a more severe extent.[32, 291] Recently, a novel approach in which sutures were employed to induce compression was developed. The skin was cut along parallel lines, and 2 mm of skin was freed from the tail. Then, 4-0 silk thread was used to suture the skin and subcutaneous tissue via a simple end-to-end suture to create suture-induced compression (**Figure 5**).[292] This model is characterized by dynamic compression generated by tail movement and avoids immobilization-induced disc degeneration, which may cause bias in readout parameters. A compression dog model was established with the pairs of screws planted in lumbar discs symmetrically, then springs attached to these screws exert static compression force on adjacent discs.[293] This model showed early sign of IDD with reduced cellular density and decreased proteoglycan.

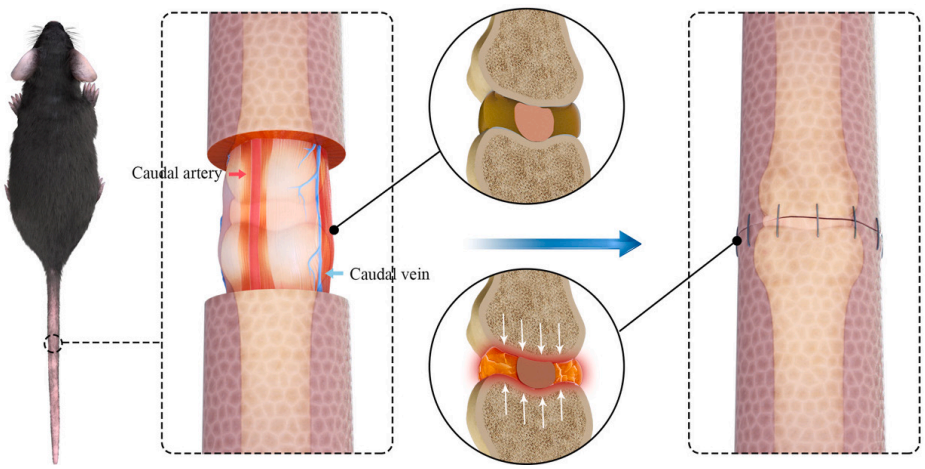

Figure 5. Compressive suture-induced rat IDD model. Circumcising the skin around index discs with a width of 2 mm and anastomosing the skin impose axial compression on the tail. Reprinted from Liu et al.[292] Copyright © 2021 with permission from Elsevier. IDD: intervertebral disc degeneration.

Disc lesions/herniation

The acupuncture model is the most commonly used method for constructing a herniated disc model.[294-308] Following damage to AF integrity, the NP tissue prolapsed during exercise, resulting in morphological changes in IDD and symptoms of nerve root compression. In addition to destroying the integrity of the AF, acupuncture altered the mechanical state of the IVD, resulting in abnormal torsional and compressive biomechanics, leading to mechanical-related degeneration.[103] The most significant bias for needle puncture results from the relative needle size, depth, segments, and surgical approaches. A puncture that does not penetrate the whole layers of AF mimics the initiation of disc degeneration with AF fissures, with no apparent NP damage.[309-311] In other models, a straight penetration through the AF to the disc center or the contralateral skin can be observed, which leads to NP herniation and degeneration.[312-315] Various needle sizes (18–30G) have been used to induce IDD. The needle gauage and corresponding inner/outer diameter are summarized in **Additional Table 2**. Several studies have performed comparative investigations to determine the optimal needle size. van Heeswijk et al.[316] applied 18G (38% of ovine lumbar disc height) and 25G (15% of lumbar disc height) on the posterolateral annuli of healthy ovines to assess the impact of needle size on the herniation path. The results showed no association between 25G puncture and disc disruption and herniation, while nuclear material migrated through the 18G needle puncture. Accordingly, a larger needle size leads to more significant disc degeneration.[317-321] However, no consensus has been reached regarding the optimal parameters for certain species, leading to incomparable results in different studies. These parameters are summarized in **Additional Table 3**.[322-349]

In 2008, a systematic review summarized animal studies that treated discs with a needle puncture or sham injection, using the ratio of needle diameter to disc height (diameter:height) as an important parameter to indicate the relative size of the needle or lesion.[350] This review concluded that significant disc degeneration, in terms of histological disruption, radiological changes, or mechanical alteration, was not observed with a diameter:height ratio less than 40%. This conclusion is well supported by numerous studies[103, 351-353] (**Additional Table 3**), although a few studies have revealed alterations in radiography, MRI, and disc biochemicals in diameter:height

ratios less than 40%, especially for lumbar disc injury of larger animals (e.g., pigs).[209, 315, 354-357] The ongoing degeneration of lesions (diameter:height less than 40%) may be attributed to the stronger adjacent muscle strength of lumbar discs, causing excessive mechanical loading on injured discs. Additionally, 30G needle (34% of rat tail disc height) was reported to decrease T2-weight intensity in MRI images without inducing histological changes.[358] Furthermore, Keorochana et al.[359] reported that a 22G (76% of rat tail disc height) puncture induced significant histological impairment, increasing the histological grade from 2 to 6 weeks, while the grading and proteoglycan stain grading decreased after 8 weeks; this indicated spontaneous repair after injury that should not be underestimated. In contrast, punctures using 18–21G (135–87% of rat tail disc height), 27G (54% of rat lumbar disc height) needles induced a progressive disc degeneration process, with no spontaneous recovery observed after 8–12 weeks.[320, 360-366] Although diameter:height ratios below 40% results were variable, and some significant effects were observed, disc changes were universal for diameter:height ratios exceeding 40%. Therefore, a diameter of > 40% may be a reliable and safe parameter for establishing a degeneration model of disc lesions.

In addition, approaches to needle puncture significantly influence outcomes. An open puncture was performed using a 2-cm longitudinal skin incision to expose the AF before the annulus puncture. A percutaneous puncture was performed using a radiograph-assisted IVD targeting puncture. Accordingly, the percutaneous injection induced a less severe rat NP degeneration, with no obvious NP herniation, compared with an open injection; this could be attributed to a larger tissue defect around the puncture site that facilitates the extrusion of the disc material.[367] Similarly, rabbits with a percutaneous puncture experienced less tissue injury and showed delayed and fewer degenerative outcomes when compared with the disc exposure approach.[368, 369] In addition, this approach determines potential herniation sites. Most studies have utilized anterior/anterolateral approaches for lumbar disc injury (**Additional Table 3**). In these studies, the herniated disc tissue barely influenced the dorsal root ganglion, which is not typical in clinical cases. Due to the thinner AF layers in the dorsal area, the posterior approach induced more severe disc degeneration and more obvious discogenic pain than other approaches.[370, 371]

For medium- and large-sized animals, such as dogs and rabbits, laminectomy or facet joint amputation is also needed, apart from disrupting the AF integrity.[33, 372] As the muscle and tendon tension for large animals is supposedly extensive to support the stability and motion of the vertical spine, removing the adjacent vertebral attachments, like ligaments or facet joints, causes disc instability, increasing the range of motion such as a posterior extension or lateral flexion, which accelerates the NP degeneration and damage of the AF, leading to NP prolapse.

Another method that modulates the amount of herniated NP was developed by amputating the rat tail to collect the NP.[373] Then, the NP tissue was quantified, and a specific amount of tissue was placed on the selected nerve roots. Although this is considered a promising strategy to generate painful radiculopathy, potential dislocation of implanted NP tissue may lead to unexpected radiculopathy in other segments. Additionally, ethical considerations regarding tail amputation may limit its application in several institutions.

Chemical stimulation

In addition to physical damage, chemical agents that impair the IVD matrix or cellular integrity have been employed to develop IDD. Injection of degradative enzymes, including chymopapain and chondroitinase ABC (ChABC), is a traditional approach for digesting proteoglycan or breaking GAG chains. Chymopapain causes the destruction of proteoglycan and GAG, which help maintain the hydration of NP tissues, leading to decreased intradiscal hydrostatic pressure and altered biomechanical stability.[374] On administering an intradiscal injection of chymopapain to Macaca fasciculata, pain-related brain areas, the secondary somatosensory cortex and insular cortex, were provoked 1 and 3 days after chymopapain treatment, suggesting a reliable acute discogenic LBP model.[375] As a proteolytic enzyme, chymopapain has been approved to treat herniated discs by degrading aggrecan and decreasing the herniated tissue volume, thus reducing pressure on the spinal cord or nerve root.[376, 377] However, it was withdrawn owing to serious complications, including anaphylaxis, paraplegia, and subarachnoid hemorrhage.[378]

ChABC is another digestive enzyme that cleaves the protein core of proteoglycans with GAG side chains. Proteoglycans determine the hydration level of the IVD tissue as well as mediate interactions between collagen and other connective tissues.[379] Injecting ChABC into the lumbar IVD of goats decreased disc height, reduced T2 and T1p, aggravated collagen disruption, downregulated matrix content, and altered disc dynamic viscoelastic mechanics.[380-382] Interestingly, although ChABC digestion decreased GAG content, the released GAG fragments, such as hyaluronic acid fragments, have been reported to promote an anabolic effect on surrounding cells.[383] Meanwhile, using ChABC during cartilage development increased the tensile properties of this tissue.[384, 385] Thus, ChABC is beneficial for matrix-rich tissue regeneration. Moreover, ChABC increased the elastic toughness and total shear energy of the high-density collagen (HDC) gel-AF interface by 88% and 46%, respectively, and enhanced the adhesion of the HDC gel to the AF without significantly decreasing native AF cell viability.[386] However, spontaneous repair may occur after digestive enzymes are degraded, indicating that the degenerative process may be short.

Diabetic mellitus is reportedly associated with IDD.[387, 388] In a mouse model, diabetes was found to induce pathological changes in the structure and composition of IVDs and vertebrae.[389] Advanced glycation end-products (AGEs), a heterogeneous group of molecules, are major biochemical benchmarks in diabetes mellitus.[390] Chronically elevated blood glucose levels lead to AGE formation in patients with diabetes, with AGE localization in IVDs.[391] Accumulation of AGEs in IVD results in disruption of IVD cell metabolism, senescence, death, and matrix destruction.[392-395] Intradiscal injection of AGEs (200 μg/mL, 2 μL) into rat tails resulted in significantly low disc

height and decreased T2-weight intensity, increased apoptosis, and a disturbed IVD structure after 4 and 8 weeks.[396, 397] Furthermore, chronic exposure to dietary AGEs in mice resulted in age-accelerated IVD degeneration and vertebral alterations involving ectopic calcification.[393]

Complete Freund's adjuvant (CFA) is a water in oil mixture of Mycobacterium tuberculosis that promotes inflammatory reaction at the local injection site. A rat disc degeneration model was developed to serve as a discogenic pain model by injecting CFA into discs.[398] By provoking an inflammatory reaction, CFA injection resulted in significant dehydration of NP and blurred boundaries between the NP and AF.[399] Moreover, CFA injection leads to a sustained increase in pain-related neurotransmitters and receptor expression, resulting in prolonged central sensitization for 8–10 weeks.[398-400]

Fibronectin is elevated and frequently presents as fragments, corresponding to the degenerative process of IDD. In IDD, most fragments were large (around 240 kDa), with relatively few fragments presenting molecular weights less than 40 kDa.[401] Fibronectin fragments inhibit matrix synthesis and upregulate the synthesis of some metalloproteases, leading to decreased tissue integrity.[402, 403] These fibronectin fragments serve as damage-associated molecular patterns to activate toll-like receptors and promote the proinflammatory phenotype to induce disc degeneration.[404] Injection of 30 kDa N-terminal fibronectin fragments into the central region can induce a progressive, degenerative process resembling degenerative disc disease over 16 weeks, supported by histological changes where the NP region appeared to shrink rapidly, replaced by fibrous tissue.[405, 406]

The inflammatory microenvironment is a primary characteristic of disc degeneration. Proinflammatory cytokines secreted by disc cells and infiltrated immune cells, such as IL-1β, TNF-α, IL-6, and IL-12, impair matrix synthesis, cell survival, and disc integrity.[407, 408] Local administration of IL-1β, the predominant cytokine involved in the pathological process of IDD, accelerated the disc degeneration process, demonstrating rapid NP herniation, a robust immune response, and neuropathic pain in less than 3 weeks of the intradiscal injection.[409]

Autoimmunity against proteoglycan and aggrecan can induce spondylitis and erosive polyarthritis in BALB/c mice.[153, 410-412] Systemic immunity to proteoglycan and aggrecan resulted in early mononuclear cell infiltration in the ligamentous tissue and entheses adjacent to the annulus. Later, structural disruption and bone erosion were observed in association with mononuclear cell infiltration.[413, 414] However, this systemic immunity could induce other joint diseases and enthesitis, which may cause unexpected bias in the readout parameters.[153]

Others

Fusion

Spinal fusion immobilizes the adjacent IVD at the index level, which is often applied to immobilize spines and decompress the impaired discs after removing herniated disc tissues. However, spinal fusion usually alters the biomechanics of adjacent discs. For example, the adjacent segment (L3–4) after spinal fusion (L4-S1) in patients revealed significantly increased intradiscal pressure by 0.29 (0.13, 0.47) MPa.[415] During surgery, manual contouring of the spinal rods is often required for proper rod alignment within the pedicle screw heads, while dedicated reduction devices correct residual misalignments.[416] However, pulling forces up to 1.0 kN were required to correct the induced misalignments. Accordingly, the adjacent facet, discs, and vertebrae experienced abnormally asymmetrical high forces, leading to progressive disc degeneration and vertebral disease.[417] Patients who underwent anterior cervical instrumented fusion experienced severe adjacent-level ossification and showed significantly increased osteophyte growth and decreased disc height with a minimum 2-year follow-up.[418] Therefore, an animal model of lumbar fusion was established to simulate the adjacent disc dysfunction.[419, 420] For example, the rabbit model underwent spinal fusion at the proximal (L4–5) and caudal (L7-S1) levels. After 3 months, IVDs adjacent to the fusion showed a loss of parallel collagen bundle arrangement within the annular lamellae. Furthermore, the disc structure was wholly replaced by disorganized fibrous tissue, with annular tears observed after 9 months.[419, 421, 422]

Loss of nutrient supply

In the NP and AF, nutrient supply is primarily achieved by solute transport from the endplate structure, which largely relies on the blood supply of adjacent vertebrae.[145, 423] IVD allograft transplantation requires revascularization of the endplate and AF to reestablish the nutrient supply, while insufficient nutrient diffusion could lead to transplantation failure.[424] Endplate perforation on pig lumbar discs was performed, which led to a reactive response in the early phase, including infiltration of inflammatory cells, fibroblast-like cell dominance, and reactive bone formation around the drill canal.[425-427] However, endplate perforation also leads to the disruption of NP and/or AF tissues by drill puncture, and numerous blood vessels were found to grow into NP tissues through the drill hole.[426] Therefore, endplate perforation may not be an ideal model to mimic nutrient restriction. Ossification of the endplate is a crucial factor that leads to restricted nutrient diffusion. Destruction of the blood supply to adjacent vertebrae is another approach to induce nutrient restriction. After injection of ethanol and cement into the vertebral body, bone sclerosis was found to develop in the endplate, and NP cells gradually changed from predominantly vacuolar cells to chondrogenic cells and eventually fibrocartilaginous cells, presenting NP fibrosis and AF rupture.[428, 429] Although a nutrient restriction model has been established, the interruption by either perforation, ethanol, or cement injection does not represent age-related nutrient insufficiency in disc tissues and appears irreversible.[222] Therefore, appropriate regeneration strategies may not be suitable for investigation in these models.

Nerve and vessel ingrowth

The outer AF structure is disrupted during IDD, probably allowing the inappropriate entry of nerves and blood vessels, ultimately inducing pain.[430, 431] In addition to structural destruction, increased levels of inflammatory mediators, neurotrophins, and angiogenic factors induce nerve

ingrowth.[139, 432] Furthermore, matrix disorganization, for example, aggrecan, inhibits nerve fiber growth.[137, 433, 434] Melrose et al.[435] developed an AF defect sheep model, demonstrating increased blood vessel and nerve ingrowth and infiltration of cells through the original defect 3–12 months post-surgery, primarily associated with proteoglycan depletion. Bioactive molecules also contribute to nerve ingrowth. Puncture-induced mouse AF defects resulted in increased nerve growth factor expression, elevated from 2 weeks and maintained at 12 weeks post-surgery.[436] Interestingly, to control the leakage of nucleus content, Xin et al.[336] established a nerve ingrowth model that induced annular injury using a 16G needle puncture, followed by sealing with poly (lactic-co-glycolic acid)/fibrin gel, promoting detrimental nerve and blood vessel growth into deeper regions of the injured disc.

Intervertebral Disc Biomaterials

Annulus fibrosus regeneration

During IDD, reduced intradiscal hydrostatic pressure poses an excessive loading burden on AF tissues, including elevated compression, torsion, and shear force.[90, 437] These aberrant biomechanical characteristics lead to irreversible structural damage such as fissures or small tears that may progress over time to larger defects, allowing nuclear content leakage to develop disc herniation.[438, 439] Surgical interventions mainly focus on the removal of herniated tissues and decompression of intradiscal pressure.[440, 441] However, untreated AF defects may cause unwanted reherniation and imbalanced mechanical properties.[104] Moreover, patients with annular defects of at least 6 mm in width experience reherniation and necessitate reoperation at more than twice the rate of those with smaller annular defects.[442] Therefore, the current biomaterial strategies have been developed to prevent AF destruction and regenerate tissues to maintain lamellar integrity and alignment at certain levels.[25, 443] The AF defect model induced by needle puncture or incision is mainly employed to evaluate the regenerative effects of these biomaterials.

Biomaterials designed for AF regeneration should consider the following criteria: (1) repair of axial, torsional, and viscoelastic motion segment responses (e.g., regenerated AF can withstand multidirectional and multitype motion with minimal risk of re-disruption); (2) repair of mechanical strength and the corresponding herniation risk (e.g., reconstruction of AF can repair abnormal mechanics and maintain tissue integrity under anisotropic force); (3) durability of the repair strategy (e.g., AF repair materials can seal local defects for an extended period, allowing native tissue regeneration).

Mesh

Typically, a physical block of AF fissures is a traditional approach to maintain the outer lamellar integrity and prevent progressive nuclear content herniation. Numerous closure and repair systems have been used in clinical trials.

The Barricaid® annular closure device consists of a woven polyethylene terephthalate, flexible fabric component attached to a titanium alloy (Ti-6Al-4 V ELI) intravertebral bone anchor, designed to treat large AF defects (4–6 mm tall and 6–10 mm wide).[444] This device received U.S. Food and Drug Administration (FDA) premarket approval in 2019, and its repair effects have been evaluated in several clinical trials and comparative clinical studies.[445-447] A systematic review of four controlled studies (801 patients with large AF defects) has reported that the risks of symptomatic reherniation and reoperation were approximately 50% lower in patients who received additional treatment with the Barricaid® device after a 2-year follow-up period.[447] However, the Barricaid® device is unsuitable for treating AF defects less than 6 mm in width, as the reherniation risk in these patients is relatively low, and this device does not encourage tissue regeneration to prevent progressive AF tearing.[442] Although the 2-year follow-up data showed favorable outcomes, long-term comparative data are warranted to comprehensively evaluate the clinical applications. A 5-year follow-up study was recently completed,[448] but data remain unpublished.

The Anulex-Xclose™ device comprises tension band(s), each with two tissue anchors placed on either side of the annular defect on the AF surface, allowing repair of the defect opening in a single band or multiple band pattern.[449] This device received FDA clearance in 2009.[447] A 2-year follow-up clinical trial has reported no significant benefit in reducing reherniation, although no increased adverse effects were reported with the use of the Xclose™ device.[450]

These suture repair systems require additional damage to AF tissues or adjacent vertebrae to fix the systems on the outer layer of the AF rings. Moreover, they do not integrate with AF lamella and fail to promote disc ECM regeneration and cellular biofunction, which could explain the limited success.

Hydrogels

Although some closure devices have focused on reducing the reherniation rate post-surgery, most patients still complained of residual leg pain (around 70%).[451] The could be attributed to the fractured AF lamellae structure, which fails to provide a physical barrier against nerve ingrowth.[430, 431] Therefore, it remains crucial to develop materials that can integrate with the AF tissue and restore the native ECM architecture to an intact state.

Adhesive hydrogels have gained popularity in IVD tissue regeneration, depending on their processability, injectability, water retention, and cell-laden capability.[40] Hydrogels injected or placed in lamella surface defects are exposed to asymmetric axial and sagittal forces that expel the implanted hydrogel from the lesion.[452, 453] Therefore, the adhesive property is a critical characteristic that helps hydrogels maintain their location and integrate with surrounding tissues, which should be seriously considered for establishing reparative AF biomaterials. However, minimal attention has been paid to properties that influence the adhesion and interface between the index tissue and adhesive hydrogel system when fabricating AF hydrogels.[180] When considering the ideal integration of implanted hydrogels, the optimized adhesion to the tissue of interest plays a critical role. Three mechanisms of interactive adhesion should be emphasized for proper selection when developing AF hydrogels. (1) Physical interaction: This occurs when the interface of tissue and adhesive hydrogels forms a

key-lock structure, and a topological match is achieved, which usually requires rough topography on both surfaces.[454] (2) Electrostatic interaction: atoms distributed on the surface of both interfaces show different eletronegativities, and therefore generate an electrostatic state where one surface performs positive charge and the other performs negative charge. This electrical attraction contributes to the interaction between charged surfaces.[455] (3) Chemical interaction: an intrinsic concentration difference of chemicals or polymers between the adhesive hydrogels and the corresponding tissue surface forces the initiation of chemical diffusion, thus leading to hydrogel integration;[456, 457] non-covalent binding, including hydrogen bonding or van der Waals forces, is another common chemical interaction that anchors hydrogels on tissue surfaces or lesions, also referred to as physisorption, which generates covalent bonds that form strong linkages among chemical functional groups and results in various types of covalent bonds (including imine bonds, amide bonds, urea bonds, and N–N bonds resulting in hydrazine derivatives, bonds arising from Michael addition, and disulfide bridges arising from thiol oxidation).[454, 458-460] Strong adhesive properties, mostly dependent on selected components, are essential for AF hydrogels to remain adherent to defects. Natural, synthetic, or complex polymers containing both of these two component types have been fabricated into adhesive hydrogels. However, the lack of a standardized protocol for adhesive measurement renders comparison among AF hydrogels from different studies nearly impossible.

Although several adhesive hydrogels have been developed to permeate AF lesions, few have undergone rigorous mechanical testing to assess the biomechanical compatibility between the hydrogel and native AF tissues.[28] Discs sealed using genipin-crosslinked fibrin hydrogel matched the torque range and stiffness of intact discs, with restored the stress-relaxation parameters, including the effective hydraulic permeability.[461, 462] Another study revealed that genipin-crosslinked fibrin hydrogel fully restored compressive stiffness to intact levels, validating organ culture findings, with only partial restoration of tensile and torsional stiffness obtained.[452] The addition of polymer materials is a feasible approach to enhance mechanical performance, while biocompatibility should be considered. Moreover, a genipin-crosslinked decellularized AF hydrogel showed a compressive modulus similar to that of native AF tissues and alleviated the continuous loss of the NP tissue during IDD progression.[463] The additive poly (D,L-lactide-co-glycolide) improved mechanical outcomes of genipin-crosslinked fibrin hydrogel, including adhesive strength (~5 to 35 kPa), shear moduli (~10 to 110 kPa), and compressive moduli (~25 to 150 kPa), overlapping with native AF properties; however, tensile moduli (~300 kPa) were still five times lower than the native AF circumferential tensile moduli (~30 MPa).[464] The combination of hydrogels and other scaffolds is another feasible strategy. Biocomposite laminates composed of long collagen fibers in unidirectional and angle-plied ±30° orientations, embedded in alginate hydrogel, can duplicate the entire stress-strain mechanical behavior of the AF lamellae in the longitudinal and circumferential directions, allowing comparison between *in vitro* results and human AF literature data.[465] To our knowledge, no existing material completely possesses all biomechanical parameters of native AF. Determining which mechanical property should be considered most critical for material behavior outcomes of *in vivo* regeneration remains controversial. Moreover, a comprehensive review has summarized parameters of human IVD motion segment stiffness, apparent modulus values, and strain measurements, which should be matched for better material selection and performance outcomes.[28]

Scaffolds

Hydrogel-based matrices usually lead to unorganized tissue regeneration.[452] An organized structure that mimics the aligned distribution of AF lamellae plays an important role in delivering guidance cues for biomaterial integration with surrounding tissues.[90, 466-468] It is critical to regenerate the organized AF structure to appropriately distribute the push-out force transduced from the inner NP to prevent reherniation. Scaffolds that can be conveniently modified to establish ideal microstructures have been developed to achieve structural reconstruction and mechanical repair.

Various techniques have been developed to fabricate AF scaffolds, including silk fiber winding, freezing, and collagen gel contraction.[469-472] In an attempt to simulate the collagen fiber alignment and related multilamellar AF structural hierarchy, a silk winding machine was used to wrap silk fibers around the central hydrogel, such that the fibers lay parallel to each other at an angle of approximately 30° to the vertical axis in a single layer, oriented at alternating angles in successive layers. This three-dimensional (3D) silk fibroin scaffold allowed cells to align along the fibers and produced an oriented cartilaginous matrix.[470] A directional freezing technique, with a pre-designed polydimethylsiloxane mold, was adopted to prepare lamellar scaffolds encircled in alternate directions to mimic a disc-like angle-ply construction. This scaffold not only promoted stem cell proliferation, oriented matrix deposition, and differentiation to an AF-specific phenotype but also matched the compressive modulus of native AF tissues.[471]

Electrospinning is a controllable technique for generating ideal structural characteristics according to the reparative needs.[466, 473, 474] The polymer solution present in a syringe is attracted by the voltage between the syringe and collector, shrinking along its trajectory to form a mass of fibers on the metallic collector.[475, 476] By controlling the molecular weight, concentration, and viscosity of the solution, as well as the flow rate, voltage, distance between the needle and collector, and environmental conditions, the electrospun fibers can be modified into microfibers or nanofibers.[473] The sequential rotation of the collector should be aligned with fiber distribution, and its morphology should be carefully designed.[477, 478] Electrospun poly L-lactic acid fibrous scaffolds mimic key structural features (fiber size and alignment) of native AF tissue, promoting differentiation of AF-derived stem cells to a specific AF cell phenotype, which provides a solid basis for designing novel strategies for improved AF repair and regeneration using the physical cues of scaffolds.[479] Aligned nanoyarn scaffolds generated from gelatin/poly(L-lactide-co-caprolactone) solution showed tensile properties similar to the native AF tissue and substantially promoted

the expression of AF-associated ECM (type I collagen) when compared with hybrid scaffolds with randomly organized nanofibrous.[480] Compared with the disorganized and scarcer fibrous tissue in a randomly organized control fibrous scaffold, electrospun-aligned polycaprolactone formed a biomimetic multilayer fibrous scaffold integrated with the surrounding tissue and homogeneously aligned collagen fiber organization within each lamella after implantation into ovine box AF defects.[467]

Decellularization tissue matrix (DTM) removes the material's immunogenicity and maintains the matrix composition, microscopic nanostructure, and biological properties of the native tissue to the greatest extent.[481, 482] DTM materials can promote cell proliferation, differentiation, and migration through various mechanisms, including micro-nanostructure, cytokines, matrix-bound nanovesicles, and peptides produced during preparation.[483] For example, decellularized tissue sheets were gently dried with tissue paper to identify a clearly defined collagen fiber-preferred/aligned direction and then cut out into squares. The fiber-aligned direction of each square was then oriented ±30° (verified via a protractor) relative to a stationary grid containing a common horizontal axis. The established angle-ply multi-laminate AF repair patch demonstrated structural and mechanical properties comparable with those of native human AF tissue.[484] The combination of a decellularized matrix with synthetic polymers promoted both mechanical and biological repair. Decellularized AF was conjugated with poly(ether carbonate urethane) urea using coaxial electrospinning technology and revealed appropriate mechanical properties and significant promotion of ECM secretion.[485] Additional *in vivo* data regarding the degradation, adhesive properties, and the time and extent of its integration with surrounding tissues are required to further evaluate whether the implanted AF would allow for timely annulus regeneration before degradation.

The microarchitecture pore size influences implanted cell morphology, cellular adhesion, and distribution of cellular skeleton, which predominantly affects cellular interaction, migration, growth, stem cell differentiation, and inflammatory phenotype.[486-488] Larger pore sizes, providing a large survival room, good nutrient supply, and metabolite discharge, encourage cell proliferation;[489-492] smaller pore sizes better mimic intimate cellular interactions and 3D cell aggregation, which favor chondrogenesis and matrix secretion.[493-496] For example, an AF biomimetic structure with a pore size of 343.0 ± 88.25 μm could provide an ideal scaffold for adipose-derived stem cell proliferation.[491] Polylactic-co-glycolic acid (PLGA) scaffolds were fabricated by solvent casting/salt-leaching with pore sizes of 90–180, 180–250, 250–355, and 355–425 μm; among these, pore sizes of 90–250 μm showed better effects on ECM production.[496] Inflammatory cells, including macrophages, monocytes, and adaptive cells, reportedly infiltrate into the IVD through AF defects, among which macrophages play a critical role in initiating local inflammation.[497-499] Macrophages should be appropriately modified to avoid excessive proinflammatory phenotypes that interfere with the regenerative outcomes of implanted biomaterials.[116] The properties of porous scaffolds significantly influence macrophage activation. Specifically, compared with 34 μm pore size, the 160 μm ± 12% pore size can better promote macrophages toward an anti-inflammatory phenotype (M2-type).[500, 501] If the pore size was increased from 0.3 to 1.5 mm, the release of proinflammatory cytokines from macrophages was significantly decreased when cells were implanted on either alginate, glass, or polystyrene.[502] Smaller pores allow for greater interaction between cells and the pore wall, encouraging macrophages to recognize antigenic epitopes, limiting M2-type polarization, while larger pores would reduce the interaction and favor the M2 phenotype. However, excessive pores may cause scaffold collapse and premature degradation.[500] Pore shape determines cellular morphology, which significantly alters M1 and M2 gene expression profiles.[503] Specifically, box-shaped scaffolds elongate cell phenotypes to trigger murine polarization into M2-like macrophages, while restricted cellular elongation leads to significant M1-like polarization.[503-505] Therefore, both pore size and shape should be cautiously designed to modify cell fate and favor tissue integration and inflammatory response after a scaffold has been implanted at the repair site.

Scaffolds mainly fabricated for void filling on AF defects rarely achieve *in vivo* regeneration; this could be attributed to their instability after implantation into the defect area, considering the relatively lower adhesive strength when compared with hydrogels and delayed integration with surrounding tissues. Moreover, an additional process may be needed during surgery, as scaffolds need to be polished to match the size and shape of the AF defect. Moreover, scaffolds usually require an additional patch to anchor them at the site of implantation.[467] A combination of scaffold and hydrogel may be a feasible approach to enhance the adhesive properties of materials, facilitate nutrition/cell infiltration, and achieve the ideal mechanical repair.

Nucleus pulposus regeneration

IDD is closely related to NP cell degeneration and a decrease in the ECM, which leads to structural changes and functional defects of the spine.[506] The unfavorable microenvironment in the degenerated IVD can cause autophagy, mitochondrial dysfunction, and even programmed or non-programmed death in NP cells.[260, 507] Dysfunction of NP cells results in an inability to effectively maintain the content and structure of the ECM. Decreased NP anabolism directly leads to the loss of ECM integrity, including reduced proteoglycan and collagen and the substitution of GAGs.[508] Typically, the ECM of NP has a high charge and proteoglycan concentration. A well-functioning proteoglycan should possess an abundance of sulfated GAG chains and hyaluronic acid, which can form highly hydrophilic aggregates with aggrecan.[42] However, during IDD, proteoglycans in the ECM of the NP are gradually replaced by truncated proteoglycan molecules (formed by the aggregation of fewer and short chondroitin sulfate chains).[508, 509] Accumulation of the truncated proteoglycan form weakens its ability to bind to hyaluronic acid and impact its distribution, leading to ECM fragmentation.[510] Given the two major pathophysiological processes (cell degeneration and imbalanced ECM metabolism), many tissue engineering materials have successfully restored NP tissue hydration and

alleviated the ongoing IDD by repairing cell functions and introducing natural proteoglycan and/or artificial replacement components. Similar to the evaluation of AF regeneration, the currently applied biomaterials for NP regeneration are primarily assessed at single or specific IVD levels. Therefore, animal models based on disc lesions are the most frequently applied models.

Nucleus pulposus device for clinical trials

Many NP engineering materials have been employed in clinical trials. For these materials, the design concept involves *in situ* hydration. The objective is to simulate the hydration properties of the NP tissue to restore its water content, which facilitates disc distraction and allows the disc to cushion the load during weight-bearing activities, as well as restores the disc height for spinal motion. The prosthetic disc nucleus, PDN® (Raymedica, Inc., Minneapolis, MN, USA), a material comprised of a woven polyethylene jacket encasing a copolymer hydrogel composed of hydrophobic polyacrylonitrile and hydrophilic polyacrylamide, reportedly allows the hydrogel to absorb surrounding fluid, with the jacket constraining its swelling.[511] DiscMaxx HydroGel™ (Replication Medical, Inc., Monmouth Junction, NJ, USA), also known as Gelstix™, is composed of hydrolyzed polyacrylonitrile that absorbs the surrounding fluid to restore NP hydration and biomechanical properties.[512, 513] BioDisc™, composed of albumin and glutaraldehyde, is injectable through a dual syringe delivery system, with polymerization occurring during the delivery process.[514] NuCore® injectable nucleus (Spine Wave, Shelton, CT, USA), comprising a sequential block copolymer of silk and elastin components, is first mixed with a crosslinker and immediately injected into the NP through the AF defect, allowing polymerization at the surrounding tissue. In particular, this technique seals the AF defect while filling the NP void and prevents gel extrusion.[515] Novocart® Disc (TETEC, Reutlingen, Germany) is composed of two main components: (1) a suspension with 3.6 to 4.4 million autologous IVD cells contained in a solution of modified human albumin, human serum, culture media components, chondroitin sulfate, and hyaluronic acid; (2) a bis thio-polyethylene glycol solution. The mentioned NP devices for clinical trials have achieved their design purpose of maintaining NP hydration and restoring disc height and mobility.[511, 515, 516] Moreover, Novocart® Disc improves the bioactivity of the NP tissue and increases ECM deposits by introducing autologous cells, exerting anti-inflammatory, anti-angiogenic, and anti-osteogenic properties.[517, 518]

However, for swelling materials such as PDN® and Gelstix™, it is difficult to ensure that the swollen device ideally matches the NP lesion. An oversized device may impose extensive pressure on the endplates or adjacent facets, contributing to the ongoing degeneration.[25, 513] However, without a restraining device, fragments of Gelstix™ hydrogels were found to dislocate and compress the spinal root.[513] Therefore, the safety and efficacy of existing commercial devices should be further assessed with more extensive trials and a larger sample size.

Hydrogels

Several bioactive components have been fabricated to produce hydrogels for NP regeneration, including natural materials (collagen, hyaluronic acid, fibrin, gelatin, alginate, and chitosan),[116, 519-523] synthetic materials such as poly(ethylene glycol) diglycidyl ethers, polyvinyl pyrrolidone, poly(ethylene glycol) dimethacrylate, poly(ethylene argininylaspartate diglyceride),[524-526] and biosynthetic materials that combine the bioactive properties of natural components with the characteristics of synthetic polymers, including cross-linking, strength, and easy modification.[527] Owing to the native gel-like structure of NP tissues, hydrogels are the most commonly fabricated bioactive materials for NP regeneration. Hydrogels have become popular materials in the field of IVD tissue regeneration, dependent on their processability, injectability, water retention, and cell-laden capability.[40, 528] A fine needle puncture can be used to inject the material into the NP tissue. Compared with cutting a window on AF and placing the graft into the intradiscal area, the injectable material causes little damage to the AF tissue. Therefore, it can be ideally employed for treating early NP degeneration.

The injectable material can be transformed from liquid to gel or solid-like material after injection into the NP tissue via chemical cross-linking, temperature, and pH control. For example, a fully synthetic, thermoresponsive poly(glycerol monomethacrylate)-poly(2-hydroxypropyl methacrylate) diblock copolymer worm gel, mimicking the structure of hydrophilic GAGs, can form highly anisotropic worms at 21°C to create an ECM network that can differentiate stem cells into the NP phenotype, despite the addition of growth factors (TGF-β3 or GDF-6).[529] Cross-linking agents can inhibit protein degradation and improve the mechanical properties of the material, to meet the requirements of IVD repair.[530] Genipin, derived from geniposide following hydrolysis by β-glucosidase, is a commonly used natural biological cross-linking agent.[530, 531] The addition of genipin to the decellularized matrix hydrogel or a collagen/hyaluronic acid hydrogel can quickly promote the transformation of the material from a liquid to a gel state, significantly increasing the mechanical properties of the material.[463, 532-534] Furthermore, genipin cross-linking can reduce the enzymatic degradation rate of the material, thereby ensuring sufficient time for regeneration of surrounding tissues and significantly increasing the water content and disc height.[535] Interestingly, the genipin concentration controls the release of cytokines such as TGF-β3.[531] Hydrogels directly loaded with cytokines usually experience burst release kinetics driven by the largest gradients during the initial stage.[536] Genipin cross-linking efficiently reduced the porosity and mesh size to limit the release of encapsulated cytokines. Gelation occurred in approximately 20 minutes without an initiator; laminin-111 functionalized poly(ethylene glycol) hydrogel achieved ideal gelation within 20 minutes with the temperature adjusted to 37°C and pH adjusted to 7.4. This hydrogel maintained the cellular viability of NP cells in the IVD explants.[537] Chitosan/hyaluronic acid hydrogels conjugated with kartogenin, a chondrogenic and chondroprotective reagent, can achieve continuous kartogenin release for days, promoting cell proliferation and ECM deposition (type II collagen, aggrecan).[538] Hydrogels that mimic the natural NP microenvironment for exogenous and resident cells allow

convenient intradiscal delivery and serve as an ideal carrier for bioactive reagents and cell delivery.

Cell delivery microspheres

The application of microspheres in *in vitro* cell expansion, with or without external stimulation, and as an efficient delivery system periodically releasing drugs or bioactive reagents have been well-established.[539] Microspheres with a large specific surface area facilitate nutrient infiltration and release of internal reagents. Many commercial microspheres are available to facilitate biomaterial fabrication, while alginate, chitosan, silk, and gelatin are selective alternatives for developing microspheres.[540-544]

Numerous biomaterials based on microspheres have been developed as injectable materials for NP regeneration.[545-548] For example, NP cells encapsulated in decellularized small intestinal submucosal matrix microspheres proliferated and produced ECM components to modify microspheres. Then, following decellularization, the microsphere containing NP ECM was injected into the degenerated rabbit IVDs. Consequently, the T2WI imaging intensity revealed that the IVD water content increased along with the increased disc height.[549] Adipose-derived stem cell-seeded PLGA microspheres supplemented with dexamethasone and TGF-β3 promoted disc regeneration with evident ECM production, as well as restored NP hydration and disc mobility.[550] Similarly, biodegradable PLGA microspheres can achieve sustained release of recombinant human GDF-5 for more than 40 days, effectively maintaining recombinant human GDF in the IVD. The slow-release of the active molecule significantly promoted expression levels of type II collagen and aggrecan and restored the height of the degenerated IVD.[361]

Microfluidic technology allows for simultaneous loading of reagents and cells and enables convenient delivery via a minimally invasive approach.[551, 552] An injectable "peptide-cell-hydrogel" microsphere was constructed using a microfluidic technique with the covalent coupling of active peptide APETx2 and further loading of NP cells, which inhibited local inflammatory cytokine storms, regulating the metabolic balance of the ECM.[76] The established microsphere system can potentially provide gradients for electrospinning and 3D printing to develop biomaterials with required properties and may even serve as units for fabricating organoids.[539]

Nano particles

Nanoparticle materials serve as carriers for active biomolecules and therapeutic agents, maintaining molecular activity while achieving controlled drug release, with superior potential for IDD treatment.[553, 554] Commercial nanoparticle carriers (MaxSuppressor *In Vivo* RNALANCEr II Kit and Lipid Extruder, BIOO Scientific, Austin, TX, USA) equipped with micro-RNA-141 were injected into the mouse tail IVD and alleviated NP degeneration caused by the puncture.[555] Albumin/heparin nanoparticles, as a carrier of stromal cell-derived factor-1α, can effectively maintain the activity of stromal cell-derived factor-1α, significantly promote the expression of aggrecan, type II collagen, and other matrix proteins, and improve the integrity of the NP structure.[24] Intradiscal injection of chitosan/poly-(γ-glutamic acid) nanoparticles with an anti-inflammatory drug (diclofenac) not only reduces the release of inflammatory cytokines from IVD cells but also promotes native matrix production.[23] Heparin/poly(L-lysine) nanoparticles embedded with dexamethasone and growth factor showed continuous release of dexamethasone and TGF-β3/basic fibroblast growth factor to achieve minimal implantation-associated inflammation and promoted stem cell differentiation toward the NP cell phenotype and matrix deposition.[550, 556] Moreover, targeting strategies can often be achieved by adequately designed nanosized delivery systems through the appropriate selection of nanoparticle types and surface molecules for particular cell targeting.[557-559]

Although several nanoparticle-mediated bioactive reagent delivery systems have been developed, maintaining a prolonged local drug presence may be challenging. The monocyte-macrophage system is efficient in removing exogenous particles, especially particles < 10 μm, and nanoparticles (10–200 nm) are also taken up via endocytosis by various cells.[560, 561] The amount and approach of uptake depend on the cell type and nanoparticle characteristics (e.g., size and surface).[562, 563] Moreover, the infiltrated vessels during disc degeneration also contribute to the removal of nanoparticles.[561] Chitosan nanoparticles showed shorter retention than their microsphere counterparts.[564] Nanoparticles embedded in microspheres or hydrogels may withdraw their limited release profiles while maintaining the advantages of both nanoparticles and microspheres or hydrogels.[565, 566]

Combined regeneration

Various studies have attempted to replace damaged IVDs with integrated disc materials. Instead of simply regenerating the degenerated or injured AF or NP tissues, AF and NP combined strategies allow for the replacement of damaged tissue with an intact and complete functional unit; this could theoretically reduce the progressive degeneration of adjacent facet joints and prevent stenosis and spondylosis. Moreover, AF or NP individual strategies cannot replace the whole IVD, which means that the remaining tissue may still undergo age-related degeneration. IVD replacement with bioactive components with/without cellular delivery reduces the reoccurrence potential of degeneration.

The main challenges in establishing and delivering an IVD implant are as follows: (1) the implanted IVD must be functional to maintain the mobility of segments and allow for proper spinal flexion, torsion, and extension;[567] (2) the implanted IVD must integrate with adjacent vertebrae mechanically or biologically to remain at the implanted location;[568-570] and (3) the implanted IVD must withstand the complex mechanical loading of the disc space.[571]

IVD transplantation from healthy donors has been performed to entirely restore the diseased IVD. Initial attempts to perform IVD transfer in dogs and rhesus monkeys rarely presented satisfactory outcomes, which might be attributed to the poor natural remodeling potential.[572, 573] Later, fresh-frozen disc allografts requiring dimethyl sulfoxide, which is typically used to maintain cellular viability and metabolic activity during the

cell freezing process, appeared to promote bony remodeling with adjacent vertebral bone.[574, 575] Five patients with cervical disc herniation underwent transplantation of fresh-frozen composite disc allografts after disc excision. Within 3 months, the graft endplates showed good integration with adjacent vertebral bones, and the motion and stability of the spinal unit were preserved after 5 years of follow-up, despite signs of mild age-related degeneration.[575] Moreover, four cases confirmed the safety and rationality of disk allografting after a follow-up of 10 years.[576] IVD transplantation requires size matching to ensure graft retention and prevent disc migration. Considerable efforts are required to perform careful pre-surgery preparation to ensure size matching and donor sources.

Notably, several artificial discs have gained FDA approval for lumbar total disc replacement, including ProDisc-L and activL.[577, 578] Maverick™, has completed the investigational device exemption and is awaiting FDA approval.[579, 580] Favorable outcomes have been witnessed with the clinical application of commercial artificial discs and are summarized in a comprehensive review.[581] A lumbar disc device, named ActivL®, was developed with an inferior and superior cobalt-chromium plate anchored in the endplate, presenting an ultra-high molecular weight polyethylene insert that may translate 2 mm in the anterior-posterior direction on the inferior endplate.[578, 582] The 5-year results of a randomized controlled trial with 324 enrolled patients reported that the ActivL® group presented a significantly better range of motion for flexion-extension rotation, flexion-extension translation, and disc angle than the groups treated with the previous generations (either Pro Disc-L® or Charité®).[583]

However, complications related to the technique, specific device, and approach may lead to transplant failure. Technique-related complications, including facet joint degeneration, endplate mispositioning, and vertebral body split fractures, can attribute to the general features of artificial discs that fail to match expected disc sizes, alter the biomechanical properties, and disturb adjacent vertebral discs for anchoring.[584, 585] Specific devices, such as Maverick™, induced severe persistent pain 1 year after initial implantation, with metallosis around articulation surfaces of the disc prosthesis, which was attributed to the persistent release of metal ions such as chromium and cobalt.[586-588] Metal-on-metal devices may lead to metallic debris and ion release, causing immunoreactions against implanted devices and connective tissue diseases.[588, 589] Approach complications result from damage to adjacent tissues during surgery, including retrograde ejaculation, ureteral injury, and vascular injury.[590, 591] Injury to the superior hypogastric plexus and anterior vessels have been reported on employing an approach similar to anterior lumbar interbody fusion, leading to retrograde ejaculation and increased risk of postoperative hematoma.[592, 593] XL TDR (NuVasive, Inc., San Diego, CA, USA) is a lumbar disc replacement instrument that allows a lateral approach, effectively resulting in pain relief and improved quality of life at mid- to long-term follow-up; this could be attributed to the superiority of the lateral approach over the anterior approach in reducing vessel injury.[594, 595]

Based on existing complications, several studies have attempted to achieve total disc engineering with or without cellular delivery. Layers of electrospun poly(e-caprolactone) and interspersed poly(ethylene oxide) were combined with cell-seeded hydrogels to form disc-like angle-ply structures. This structure was used to replace the rat disc by employing a stable fixation system. Accordingly, good integration was achieved, as endogenous cells populated the full thickness of the implant and produced a collagenous network.[596] Decellularization is a promising approach to remove cells while preserving the ECM structure and components. A decellularized whole IVD xenograft was fabricated with proper detergents, ultrasonication, freeze-thaw cycles, and nucleases. Although the native angle-ply collagen microarchitecture and collagen contents were preserved, the linear region moduli, peak stress, and equilibrium moduli were significantly reduced.[597, 598] The contracted-collagen (AF)/alginate (NP) technique was applied to fabricate a tissue-engineered total disc implant that can adequately withstand mechanical loads, producing an integrated and mechanically functional ECM similar to the native IVD in rat and canine spines;[472, 599] the implant-endplate interface demonstrated progressive integration with only small discontinuities at boundaries between the endplate and engineered tissue.[472] Although many bioactive disc replacement devices have been developed and used for *in vivo* regeneration, long-term reparative strategies are still required to gain a comprehensive understanding of nutrient reestablishment and potential degeneration of the implanted disc.

Acellular and cellular repair strategies

Numerous studies have attempted to modify the local microenvironment and promote native cell function using bioactive hydrogels. Acellular regeneration of the annulus impairs native cellular infiltration and subsequent remodeling of matrix tissues. Collagen gel is a well-known material used in the field of acellular repair. HDC gel has been fabricated to repair annular defects in rat or sheep models generated by annular puncture and NP discectomy.[600, 601] The HDC gel was maintained in the defects for up to 18 weeks, preserving approximately 70% of the NP tissue.[600] Moreover, collagen gel appeared to enhance intrinsic healing by attracting host fibroblast cells and forming aligned, fibrous tissue.[600, 601] However, the defect size and shape could influence the reparative effects of the HDC gel, especially in large animal models. A rectangular defect may better facilitate gel adhesion than a round defect, which is attributed to increased tension.[601-604] Fibrinogen is another material that possesses excellent tissue adhesion, which remains in the injected area with or without membrane anchoring.[605] An *ex vivo* test in bovine discs has reported that fibrinogen crosslinked with genipin restored IVD height and compressive properties, as well as partially restored other biomechanical behaviors of IVD motion segments under a range of physiological loads, without herniation.[452] However, *in vivo* long-term tests showed equivalent outcomes between fibrinogen and control groups, which may be attributed to the unexpected disruption of the endplate during surgery, limited cell infiltration, and no aligned fiber lamellae formation.[605]

Identifying signals toward which AF cells possess sensitivity could aid in designing biomaterials that facilitate cellular

recruitment strategies. IDD-associated inflammation promotes the expression of C-C chemokine ligand receptors (CCRs), such as CCR1, CCR2, and CCR5, in native AF and NP cells. CCRs can bind CCLs to stimulate cell migration and matrix production.[606-608] However, *in vivo* data revealed that CCL5 might not recruit AF cells to repair the defect area after disc puncture treated with fibrin gel delivery.[609] In contrast, CCLs have been used to recruit stem cells for tissue regeneration.[610, 611] A sequential chemokine delivery system that releases CCL-5, TGF-β1, and GDF-5 sequentially uses CCL-5 to recruit stem/progenitor cells and TGF-β1 and GDF-5 to induce the synthesis of a type II collagen- and aggrecan-rich ECM, resulting in promising disc regeneration.[612] As CCRs undergo degeneration-related upregulation for promoting cellular assembly, the application of CCLs may be a promising strategy for designing acellular regeneration, while their *in vivo* recruiting effects on native AF and NP cells needs further evaluation. Moreover, there are other concerns regarding the use of CCLs. Certain CCLs, especially CCL4, present liver toxicity and have been used to establish a liver fibrosis model.[613, 614] CCLs possess oncologic potential, including cell proliferation, drug resistance, migration, invasion, and organ-specific metastasis of tumor cells.[615-617] As a proinflammatory cytokine, CCL also showed chemo-attraction toward macrophages, which may aggravate disc inflammation.[618, 619]

Supplementary bioactive molecules are an efficient approach to enhance native cell recruitment. Cytokines, TGF-β3, BMP-2, BMP-3, insulin-like growth factor 1, and osteogenic protein-1, showed positive regulatory effects on the amelioration of disc anabolism.[620-624] Sustained TGF-β1 release induced an anabolic stimulus in AF cells while mimicking the 3D ECM environment of the AF tissue.[625] Other reagents also modify the function of AF cells to enhance tissue self-repair. However, it should be noted that TGF-β1 and BMPs in regenerative therapy can lead to the generation of osteophytes at the repair site, resulting in an exacerbated spinal pathology.[626, 627] Hyaluronan oligosaccharides upregulated AF proMMP-2 and MMP-9 and downregulated MMP-13, ADAMTS1, ADAMTS4, ADAMTS5, aggrecan, and type II collagen; simultaneously, hyaluronan oligosaccharides promoted the upregulation of MMP-1, MMP-13, and ADAMTS1 and the anabolic matrix repair genes aggrecan, type I collagen, and type II collagen in the NP.[625, 628] These modulations are expected to promote clearance of granulation/scar tissues from AF defects, as well as matrix replenishment. The *in vivo* test revealed that AF defect sites contained enlarged annular lamellae in response to the hyaluronan oligosaccharides, consistent with an active repair response.

Delivery of exogenous cells is an attractive approach to effectively control the number, type, quality, and genetic or chemical modification of delivered cells. Comprehensive reviews have discussed cell-based strategies for IVD repair.[25,26,629] Although several cell delivery systems have achieved ideal regenerative outcomes for IVD repair, no significant difference has been observed between the cell-loaded and no-cell-loaded systems; this could be attributed to inappropriate selection of loading substances and limited nutrition at the repair site. Following IDD development, an unfavorable microenvironment, including oxidative stress and the release of inflammatory factors, aggravates cell death and matrix decline, causing excessive cellular autophagy, apoptosis, and necrosis of stem/progenitor cells, thereby limiting the repair efficiency.[630,631] Accordingly, modifying the local microenvironment is required to promote the reparative potential of implanted cells *in vivo*. Additionally, primary stem cell sources for clinical treatment are autologous sources, such as bone marrow stromal cells or adipose stem cells extracted from the patient's bone marrow or adipose tissue.[632] However, these sources may encounter limited donor tissues, with high economic cost and time for *in vitro* culture, potential cellular infection by pathogens, and additional invasive operations in donors.[633, 634] The donor age and disease status, *in vitro* cell preservation, and cell processing during surgery may affect clinical outcomes after auto-transplantation. Moreover, xenogeneic or allogeneic stem cells may result in unexpected host-versus-graft reactions.[635] In addition, reparative biomaterial systems with cellular delivery may delay their clinical translation.

Systemic regeneration

Systemic administration of therapeutic biomaterials that targeting IVD, including oral, intravenous and intraperitoneal administration, potentially achieve the regeneration of general IDD related to aging. A new functionalized nanofullerene conjugated with a peptide that binds specifically to a formyl peptide receptor-1 expressed on activated macrophages was developed and denoted FPR-1 targeted C60 nanoparticle (FT-C60). By preferentially binding to formyl peptide receptor-1, FT-C60 significantly attenuated the mRNA expression of proinflammatory cytokines, which are critical components for inflammation and discogenic pain. Furthermore, FT-C60 alleviated pain in a mouse model of lumbar radiculopathy established by puncture-induced nucleus protrusion toward the L5 nerve root following abdominal administration. The systemic application of FT-C60 showed targeting properties to the local injury site.[636]

Systemic administration of nanoparticles, such as alginate oligosaccharides, can be employed as a feasible strategy to reduce clinical complications (infection, prolonged pain) after lumbar fusion surgery.[637]

PLGA nanoparticles are widely applied carriers for delivering reagents. A previous study has evaluated the safety of a PLGA nanoparticle delivery system by assessing superoxide dismutase and catalase in healthy dogs. A typical complement activation-related pseudoallergy was observed, widely known to be associated with nanoparticle-based drug delivery, including a combination of bradycardia, hypotension, hypersalivation, pale gums, and involuntary urination, within 7 days, while no long-term clinical signs and pathologies were recorded.[638]

However, systemic regeneration for IDD is still debating, based on the fact that IVD is an avascular organ with less chance of local assembling of systemic administrated biomaterials.[639] To solve the problem, robust IVD tissue-specific markers, proper vascularization and well designed targeting biomaterials should be determined and established. Then, the systemic and early intervention of IDD may be achieved with no need of invasive operations.

Characteristics of Intervertebral Disc Biomaterials

Clinical manifestations

LBP is often described as pain, muscle tension, or stiffness in the body region below the costal margin and above the inferior gluteal fold, with or without limb pain.[640-642] Generally, diseases affecting the anatomical structure around the lumbar spine, including vertebrae, ligaments, muscles, facet joints, and IVD, can lead to LBP, among which IDD is the leading cause contributing to 40% of LBP cases.[2, 258] Pain originating from degenerated IVD is referred to as discogenic pain.[643]

Evaluation of pain, which is often neglected, is necessary to comprehensively demonstrate the regenerative effects of IVD biomaterials. A systematic review has summarized different pain types, including neuropathic/nociceptive pain, acute/chronic pain, evoked/spontaneous pain, and hyperalgesia/allodynia.[644] Numerous behavioral assays have been performed on rodent models to evaluate pain associated with LVD degeneration (**Additional Tables 4** and **5**). As the plantar surface of the rodent hind paw is primarily innervated by the tibial nerve, which is composed of spinal nerve roots from L4-S2, pain sensitivity detected from the hind paw can represent a measurement of LBP.645 In addition, LBP related disc discomfort indicated by movement-evoked hypersensity and spontaneous painful bahavior is also an important sign of LBP. Therefore, the evaluation of rodent pain sensitivity is mainly composed of stimuli-evoked hyperalgesia on mainly on hind paw, movement-evoked hyperalgesia and spontaneous tests.

Stimuli-evoked hyperalgesia evaluation

Evoked tests involve external stimuli to initiate pain and evaluate responses to controlled stimulation, including mechanical and thermal stimulation (**Additional Table 4**). Mechanical pain is usually based on the von Frey assay, which applies mechanical force by calibrated microfilaments.[646-648] When force is applied to the hind paws, a positive response is defined as the brisk withdrawal of the probed foot. The up and down" method provides a solution to calculate the 50% mechanical withdrawal threshold by repeatedly adjusting the mechanical degree of the probing filaments.[649, 650] An algometer used to measure tenderness is a reliable approach for evaluating mechanical hyperalgesia. This device is valuable and can be applied to various locations, including the tail, hind paw, and spine. Indeed, it has been employed to assess pressure pain thresholds in clinical settings.[651, 652] Thus, algometer data from animal models are comparable with clinical situations. Thermal pain, either with hot or cold stimulation, can be measured to determine pain sensitivity.[30, 314, 653-662] On applying heat or cold, the time when rodents first display avoidance reactions such as foot withdrawal, paw lifting, or jumping is recorded as paw withdrawal latency. Interestingly, mice with progressive disc degeneration present normal sensitivity to mechanical stimuli applied to the hind paw, with hypersensitivity to cold stimuli applied to the hind paw.[30, 255, 256, 663]

Movement-evoked hyperalgesia evaluation

In disc degeneration, the tolerance to axial stretch is assumed to be decreased, indicating a bending hyperalgesia in human.[30, 256] Grip Force assay is based on a Grip Strength Meter (Stoelting Co., Wood Dale, IL, USA) that can record the stretching force performed on the metal bar.[30] Initially, it was designed to determine the neuromuscular function of animals.[664-666] This assay involves stretching a mouse tail back with the mouse forelimb grasping the wire gauzes and recording the maximal force when the mouse releases the gauze. Decreased maximal force is an indication of impaired tolerance to axial stretch and discomfort[30, 667] (**Additional Table 5**). Notably, the tolerance is not attenuated in all degenerative model. For example, a spontaneous degenerative model, SPARC-null mice, showed significantly dimished grip force, while needle puncture-induced degeneration model revealed no obvious alteration.[30, 256, 657] The efficacy of grip force in other degeneration model shall be further evaluated.

Tail suspension is another assay to measure axial discomfort.[255] Specifically, mice are individually suspended by the tail underneath a platform with adhesive tape. The duration of time spent in a) immobility (not moving but stretched out), b) rearing (trying to reach the underside of the platform), c) full extension (actively reaching for the floor), and d) self-supported (holding either the base of its tail or the tape), is analyzed by a digital software over the entire testing period around 180 seconds. Deceased immobility is indicative of axial discomfort.[663] This assay is often used as a traditional measure of depression in mice.[668] It has been proven to reliably measure signs of axial pain in mice.[256, 663]

Besides, FlexMaze is designed to measure lateral flexion–induced discomfort. It force the mice to undergo lateral flexion in order to explore the maze. Then, the total distance and velocity covered by the mice indicate the movement-evoked hyperalgesia with other variables controlled.[256]

Spontaneous behaviors

The measurement of spontaneous pain does not require external stimulation. Instead, certain inconspicuous behaviors can be recorded to reveal signs of pain. Unilateral injury or related pain models have shown weight-bearing differences in paws, which can be detected by an expert investigator.[669] Furthermore, if the animal experiences discomfort, the explored area is reduced. Therefore, an open-field test was used to record the exploratory behavior for assessing spontaneous pain.[670, 671] When rodents experience pain, they demonstrate high-frequency ultrasonic vocalization, like screaming in humans.[672] Ultrasonic vocalization is often accompanied by audible vocalization, which challenges the usefulness of measuring ultrasonic vocalization.[673] Finally, analysis based on animal expression and altered movements is another strategy to assess spontaneous pain. The Mouse Grimace Scale was initially established to evaluate spontaneous pain based on mouse facial expression utilizing five features (orbital tightening, nose bulge, cheek bulge, ear position, and whisker change).[674] Similarly, the Rat Grimace Scale, based on four units: orbital tightening, nose/cheek flattening, ear changes, and whisker change, was employed to analyze pain according to rat expression[675] (**Figure 6**). The reliability of these scales has been verified in numerous spontaneous pain models by experienced observers.[674, 675] However, this approach may

Figure 6. Scales for spontaneous pain evaluation based on rodent facial expressions. Copyright ©2011 Sotocinal et al.[675] Reprinted from BioMed Central Ltd.

not be highly reliable, as judgments regarding spontaneous expression and movement are subjective and affected by the observers' proficiency.[676] Moreover, baseline scores significantly differed between men and women, whereas live scores were significantly lower than retrospective scores from images.[677]

Biocompatibility and degradation

Biocompatibility is a characteristic of materials that determines cellular, tissue, and organ responses to the respective materials.[678] Biocompatibility is mainly determined by the nature and application of the material. Material properties, including shape, size, surface roughness, residual toxic low-molecular substances during material polymerization or preparation, material processing pollution, and material degradation products, are associated with biocompatibility.[679,680] On considering a material for application in the biomedical field, biocompatibility is an important indicator that needs to be considered and evaluated.

Material components possess critical characteristics that may lead to cellular toxicity and host immunological responses. For example, in the DTM, residual cellular components after decellularization include high mobility group box 1 (HMGB1), DNA, and gal antigen epitopes. HMGB1, an intracellular protein that binds DNA, is one of the most common damage-associated molecular patterns following cell rupture.[681] The current decellularization protocols cannot comprehensively eliminate HMGB1, and the residual content depends on the tissue source, decellularization strategies, and application of cross-linking agents.[682] HMGB1 induces inflammation by promoting the release of inflammatory factors such as CCL2 and CCL4 and activating proinflammatory signaling pathways, such as the toll-like receptor pathway.[683] Apart from the irritating inflammatory response, HMGB1 is reportedly chemotactic and promotes the proliferation of bone marrow mesenchymal stem cells and keratinocytes.[684, 685] Therefore, damage-associated molecular patterns not only activate resident inflammation but also induce cell aggregation and proliferation, consequently affecting the graft-versus-host reaction and overall repair.

Reportedly, α-(1,3) epitopes of α-1, 3-galactosyl transferase are abundant on the cellular membrane in almost all species, except humans.[686] However, large amounts of the oligosaccharide galactose-alpha-1,3-galactose (α-Gal)

antibodies exist in the human circulatory system.[687] Therefore, the immune response triggered by α-Gal epitopes is a major concern after transplantation of tissue-derived biomaterials. Porcine AF tissue was treated by freeze-thawing in liquid nitrogen, incubated in a hypotonic buffer at 37°C for 24 hours, and decellularized in 0.1% sodium dodecyl sulfate, 0.1% ethylenediamine tetraacetic acid, and 10 KIU/mL aprotinin, resulting in the removal of nearly 80% of α-Gal epitopes, with good immuno-compatibility and a decrease in mononuclear cells after implantation on AF defects at 14 days.[688] Galactosidase removes 60–75% of α-Gal epitope residues following tendon decellularization, resulting in excellent histocompatibility after subcutaneous implantation of decellularized tendon.[689, 690]

Un-α-Gal antibody refers to antibodies that target epitopes other than α-Gal. In humans, they may bind with non-homologous proteins in the ECM polypeptide sequences. If these antibodies bind to the xenograft, graft rejection is induced by activating the complete cascade.[685] For example, allograft transplantation of the heart and kidney with knocked out α-Gal epitopes resulted in xenograft rejection induced by un-α-Gal antibodies at 6 months and 1 month, respectively.[691] The remaining major histocompatibility complex antigen after decellularization presents another group of un-α-Gal antigen epitopes.[686] Major histocompatibility complex staining is essential for evaluating the decellularization efficacy when fabricating materials with low immunogenicity.[692] The presence of residual major histocompatibility complex I/II antigens in implanted materials can lead to macrophage infiltration.[693, 694] Furthermore, an excessive humoral reaction induced by the un-α-Gal antigen epitope in DTM may block adhesion sites and inhibit adhesion and host cell infiltration.[687] Hence, the presence of un-α-Gal antibodies may induce graft rejection or hinder the interaction between cells and DTM, leading to failed repair.[695]

Following decellularization, DNA fragments released from cells tend to adhere to the surface of decellularized matrix owing to its adhesiveness. Resident or infiltrating macrophages derived from monocytes recognize DNA fragments and phagocytose them.[689] This procedure is a primary step in innate immunity for the removal of damaged cells and tissues. Excessive DNA residues result in a relative lack of DNase in macrophages, leading to the accumulation of DNA in cells, which may activate the nuclear factor-κB pathway, resulting in inflammatory cell aggregation and aggravating local inflammation.[696, 697] Notably, if the tissue was contaminated during processing, the residual DNA may be derived from viruses or prions, which can cause severe consequences by infecting host cells after transplantation.

Products released during material degradation should promote local tissue regeneration and must nontoxic. Several polymers utilized in IVD regeneration are reportedly degradable. By hydrolytic scission of the ester bonds, polylactic acid results in monomeric lactic acid, which can worsen the low pH of the disc microenvironment.[698] The persistently acidic microenvironment leads to increased cell glycolysis and overexpression of the acid-sensing ion channel family.[64, 155, 699, 700] Sequential energetic exhaustion and calcium overload induction by acid-sensing ion channel results in cellular dysfunction and death.[155, 699] Multiple studies have unraveled a shift from M1-type to M2-type within 1 to 2 weeks of implanting biological scaffolds composed of mammalian ECM.[687, 701, 702] ECM degradation appears to be necessary for the transition from M1 to M2 phenotypes, suggesting that decomposition products may be essential for this transition. Hydrogels composed of ECM biological scaffolds can promote the transformation to the M2-type when compared with materials lacking ECM.[504] Several studies have reported that DTM scaffolds demonstrate an adequate effect of promoting the polarization of infiltrating macrophages toward the M2-type.[504, 505, 527]

One barrier that hinders the development of biomaterials with idea-degrading properties is the discrepancy between *in vitro* and *in vivo* degradation profiles. A typical approach to establish an *in vitro* degradation profile can be evaluated by immersing biomaterials in phosphate-buffered saline with or without enzymes or detergents.[703, 704] Nevertheless, the *in vitro* condition is completely differs from *in vivo* situation. After implantation, biomaterials interact with surrounding tissue fluid, and infiltrated cells play critical roles in modifying biomaterials and mediating their degradation. Considerable attention has been paid to optimizing the regulatory effects of biomaterials on cells and tissues. Furthermore, data on how cellular responses and tissue reactions influence the degradation and other modification processes of biomaterials are lacking.[705, 706] The host response to biomaterials involves sophisticated biochemical changes that modulate biomaterial erosion. A typical response to biomaterials is the formation of a fibrous capsule that may interfere with tissue fluid changes and influence the degradation rate.[707] Therefore, the *in vivo* evaluation of degradation is relatively more valuable when considering biomaterials for tissue regeneration. As the subcutaneous immunological response is considered timely and intensive, biomaterials are subcutaneously implanted to evaluate their biocompatibility and degradation.[708-711] After certain days or weeks, histological images are obtained to evaluate the amount of residual biomaterials.[704] However, compared with a non-vascularized structure such as IVD, skin tissues possess an abundance of vessels and lymph nodes to provide effortless and rapid tissue fluid changes, which may exaggerate the degradation rate of materials used for IVD regeneration.[712, 713] Moreover, a subcutaneously intensive immunological response leads to the formation of a fibrous capsule after material implantation and may impede material degradation.[714, 715] Other studies have attempted to evaluate degradation by histological analysis of tissues with implanted biomaterials. Hematoxylin-eosin staining showed retention of implanted decellularized spinal cord ECM in spinal cord lesions after 8 weeks.[716] Another study recorded time-dependent changes in hydrogel thickness in the rat abdominal wall using histological images.[717] Intradiscal implantation is necessary for accurately measuring the degradation properties of these materials.

However, the analysis based on histological images is semi-quantitative and largely depends on the obtained section, which can sometimes greatly influence tissue and implanted material morphology. A fluorescent dye may be a feasible approach to track hydrogel retention time at repair sites. RGD-biotin

encapsulated with the fluorescent dye cyanine 5.5 was used to track the location of the hydrogel implanted in the kidney injury site.[718] By employing epitope as a labeling agent, the degradation of elastin-like polypeptide gels can be monitored through enzyme-linked immunosorbent assay, estimating the amount of leached-out antibodies.[719] With a real-time imaging system, the degradation of the hydrogel can be easily recorded and analyzed.[718] However, the fluorescence from conventional fluorophores quickly decays and requires ultraviolet or visible light as the excitation source, which fails to sufficiently penetrate deep biological tissues.[720, 721] Lanthanide-doped upconverting nanoparticles may be a feasible alternative, as they can convert near-infrared (NIR) to ultraviolet or visible-NIR light via a sequential multiphoton absorption process referred to as upconversion. As NIR light can penetrate up to a few centimeters inside tissues, upconverting nanoparticles allow the tracking of gel degradation with photoluminescence spectroscopy and NIR imaging after implantation in discs.[722]

Imaging

Imaging technologies are useful for clinical IDD diagnosis and surgical planning.[723] For preclinical research, imaging technologies are reliable methods for identifying animal disc degeneration and the degree of degeneration.

Radiographic technology, based on X-ray or computed tomography discography, clearly illustrates the vertebrae but does not depict soft tissues clearly, requiring contrast to detect intradiscal abnormalities. With a clear illustration of the vertebrae, an image intensity adjustment technique was developed to precisely evaluate the relative disc height.[724] Vertebral body height and disc height were measured along different axes (denoted as A, B, C…, I) using an image analysis program. IVD height was expressed as the disc height index.[312, 313, 725] The disc height index is a calculated relative index comparable among different studies, regardless of the differences in background and intensity (**Figure 7**).

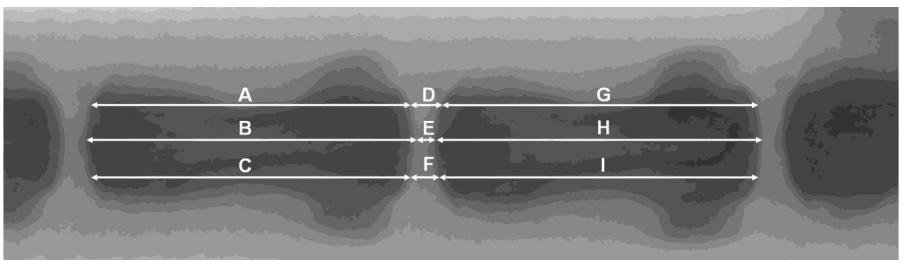

Figure 7. Measurements and calculations of vertebral body height and IVD height based on radiographs. The IVD height should be quantified using a relative value, %DHI, which measures changes in the DHI of punctured discs. DHI = 2 × (D + E + F) / (A + B + C + G + H + I); %DHI = post-punctured DHI / pre-punctured DHI × 100. DHI: disc height index; IVD: intervertebral disc.[313]

MRI is a typical diagnostic method and a reliable surgical indication for IDD.[726] Currently, conventional T1WI-, T2WI-, and proton density-weighted vessel wall MRI have been successfully employed in the clinical work-up of patients with LBP and suspected (advanced) IDD.[727] Proteoglycans are critical IVD components to maintain tissue fluid, and their downregulation occurs concurrently with the loss of hydration, particularly that of the NP.[728] The Pfirrmann grading system based on the mid-sagittal plane of T2WI is widely applied for IDD grading.[729] Pfirrmann provides a grade from I to V, according to structural morphology (homogeneity within NP, signal intensity, disc height) illustrated on T2WI[729] (**Additional Table 6**). The Pfirrmann grading system requires subjective evaluation of T2WI and requires independent and skilled observers to perform the grading process.[730, 731] Water content alteration and ECM degradation usually occur before the appearance of detectable morphological MRI findings.[728, 732] Therefore, changes in T2WI and Pfirrmann grading are usually apparent in advanced IDD.[733, 734] Additionally, T2WI- and proton density-weighted vessel wall MRI provides limited information regarding the mechanical functioning of the disc or the cause of degeneration and pain.[735-737] Moreover, the Pfirrmann grading system combined with IVD micro-nano structural changes more comprehensively reflects the extent of disc degeneration, including GAG assay, histological analysis, evaluation of bony endplates by scanning electron microscopy, atomic force microscopy imaging, and nano-mechanical testing.[738]

Advanced MRI techniques sensitive to proton-matrix interaction (proteoglycans-bound water), matrix-organization, and water diffusion, rather than water content only, could provide more meaningful findings to identify early IDD.[739-741] Quantitative T2* axial maps based on quantitative T2* MRI provide information regarding the interaction of water within the macromolecular network.[742] The combination of surface volumes and quantitative T2* axial maps provides insight into the initial degeneration stages.[743] T1rho is an MRI relaxation time parameter and a promising MRI contrast for imaging proteoglycan-rich nucleus regions, demonstrating a superior correlation with proteoglycans than T2.[744, 745] Interestingly, T1rho values in the NP were found to be strongly associated with GAG content and mechanical properties, including swelling pressure.[746] Diffusion-tensor imaging is another MRI contrast that enables quantification of the water apparent diffusion constant (ADC), which indicates the integrity of IVD tissues.[747,748] ADC values from diffusion-tensor imaging of IVD can distinguish time-dependent fluid changes and regional fluid-flow directional shifts.[748-750] Additionally, ADC identified by diffusion-weighted imaging was found to be effective in diagnosing early IDD with tiny variations.[751] A comparative study showed that the T1rho nucleus value was superior to

T2 and ADC, correlating with GAG content, histological degeneration, and disc mechanical properties.[752] Chemical exchange saturation transfer is a method to directly detect exchangeable solute protons in tissues by constant irradiation and saturation of their chemically shifted magnetization, based on the MRI protocol of a T2W sequence.[753] GAGs chemical exchange saturation transfer, using the Spin-Lock technique (chemical exchange saturation transfer) and WASABI (WaterSaturation and B1) methods for B0 and B1 field inhomogeneity correction, generating a color-coded GAGs chemical exchange saturation transfer map with high GAG content in blue and low GAG content in red in the lumbar spine, correlating with either LBP or radiculopathy.[754]

Apart from the indication of disc degeneration, videography also enables non-invasive monitoring of implanted components. A study has attempted to monitor mesenchymal stem cell survival after implantation into an IVD with surgically induced degeneration. Compared with MRI, the positron emission tomography reporter probe, 9-(4-[18F]-fluoro-3-hydroxymethylbutyl)-guanine, was more sensitive and identified the longest survival data at 3 weeks after implantation.[755] However, the cost-benefit ratio of positron emission tomography is relatively low. Cells labeled with ferumoxides (Endorem®) or protamine sulfate (USPIONs) appear as hypointense regions on MR images and demonstrate significant signal intensity loss and contrast on T2*-weighted images; thus, they can be distinguished from the surroundings.[756, 757] Radiopaque zirconia nanoparticles enable long-term non-invasive assessment of the implanted hydrogel, as well as scaffold performance and distribution, without impairing the viability and biofunction of encapsulated cells.[758, 759]

Histology

Histological evaluation is the most convincing for disc degeneration, assessing factors such as the annulus integrity, endplate disruption, fiber alignment, nucleus arrangement, and tissue components. In addition, histological images can reliably indicate the penetration of nerves, vessels, and inflammatory cells. However, the subjective observations performed by individual researchers were incomparable between studies and species. Therefore, although several grading scales have been developed, no consensus has been reached. Herein, we list the most commonly used grading scales.

Nomura et al.[760] developed a grading system based on the classification of AF established by Nishimura and Mochida.[761] The grading system contained grades of only NP and AF tissues (**Additional Table 7**). This method is relatively precise and straightforward. However, the classification is limited to two primary IVD components and neglects the degenerative morphology of the endplate and adjacent vertebral body.[334, 362]

Masuda et al.[725] developed a more detailed grading scale that separates the grades of NP cellular components and the matrix and emphasizes the border between the NP and AF[317, 725, 762, 763] (**Additional Table 8**).

Han et al.[313] upgraded the grading scale of Masuda et al. by grading cellular components of the AF tissue (**Additional Table 9**). Clear interpretation and easy grading systems have been reported by several studies for histological evaluation.[764-766]

Thompson et al.[767] provided a comprehensive grading system widely employed for histological grading of human discs, distributing equal weights to the nucleus, annulus, endplates, and vertebral body (**Additional Table 10**). Both intra-observer and inter-observer agreement values in the initial Thompson grading scheme were 85%,[80] and these levels were maintained when the scheme was applied across species.[79, 80]

The grading scales described by Boos et al.[768] are more detailed, containing 23 items, including the evaluation of the IVD and vertebral endplate region. It allows for a comprehensive evaluation of these criteria across the entire IVD, with no provision for separate evaluation of the AF or NP regions. All grades are clearly claimed and explained (**Additional Table 11**). Interrater reliability estimates for the assessment of histologic features generally showed good to excellent rater agreement. The agreement of each detailed content exceeded 80%. As a comprehensive grading system and detailed explanation are provided, several studies evaluating disc degeneration have utilized this grading system.[769] However, it is not highly practical, and considerable effort is required to evaluate histological images. Boyd et al.[232] extracted 11 criteria from those described by Boos et al.[768] and formed a new grading system[232, 770] (**Additional Table 12**). Each criterion was graded from 0–4. However, the definition of each grade is missing, which may restrict the reliability and repeatability.

Although many grading scales have been established, these scales have been cited recently. Nevertheless, the established grading system barely considers nerve ingrowth into the disc, which signifies the ongoing degenerative process and persistent discogenic pain.[136, 278, 771] We recommend that the grading system should meet the following characteristics: 1) Comprehensiveness: the grading system should evaluate the degenerative degree of all substructures of IVDs and symptom-related structures, such as innervation; 2) Simplicity: easy and quick evaluation that requires less effort will contribute to the consistency of results, and help save manpower and material resources; 3) Repeatability: the agreement rate should be evaluated by independent and proficient or less proficient observers to ensure the repeatability of a certain grading system among researches and species; 4) Universality: the grading system should be suitable for different species to facilitate the comparison of biomaterials used in various species. Although the Boos et al.[768] grading scale is currently the most comprehensive and detailed system for histological evaluation with good repeatability, grading systems with less comprehensiveness, such as Han et al.[313] and Masuda et al.[725] are still widely employed.[762, 764-766] Adequate simplification and inclusion of innervation for the Boos et al.[768] grading scale are required to facilitate reliable histological evaluation and a robust experimental design.

Adhesive

The adhesive property is a critical characteristic for biomaterials to be maintained at the implantation site and integrate with adjacent tissues, especially for AF regeneration. However, studies that fabricate AF biomaterials often pay less attention

to adhesive evaluation,[463, 772] which may partially be attributed to a lack of guidance documents providing a systematic framework for screening the biomechanical performance of newly established AF materials. A comprehensive review has summarized approaches for adhesive properties.[180] Here, we updated the methods and provided detailed protocols to facilitate the experimental design and selection of relevant testing configurations[117, 773-776] (**Additional Table 13**).

Mechanical evaluation

The spine is a critical weight-bearing organ that can withstand gravity generated by the upper body. Therefore, biomaterials designed for IVD regeneration must satisfy mechanical demands to support tissue regeneration and spine motion. NP materials that cannot withstand hydrostatic pressure within the disc are likely to cause excessive stress on the surrounding AF and endplate, leading to progressive disc degeneration.[513] Furthermore, mechanical restoration is a tremendous challenge for AF reparative materials, as AF suffers from an asymmetric "push-out" force transduced from the NP tissue and an axial force from endplates. Therefore, additional studies should be performed to satisfy the mechanical requirements of AF regeneration. In addition, standards of robust experimental design and comparative mechanical outcomes should be met among studies. Many reviews have compared the mechanical properties among different species, and suggested the parameters for IVD regeneration.[203, 777] Here, we adapted a paradigm, including series of screening tests, has been illustrated to rapidly evaluate if the materials meet required mechanical properties[28, 778-780] (**Additional Table 14**). Correspondingly, the recommended parameters for mechanical properties after biomaterials implantation have been summarized as a benchmark for disc regeneration[28] (**Additional Table 15**), which has been acknowledged in many research studies.[28, 453, 462, 475] Whereas, many factors, including the testing environment, machine No. and loading rate etc. can cause bias to the obtained mechanical results. The same specimen tested in three institutions (two in UK, one in USA) with different testing machines by the same protocol came out with ~35% difference in compressive stiffness, after normalizing for disc geometry and adjusting for system compliance.[781] Therefore, as it is difficult to unify the testing environment and machine in different researches, a unified control group, such as health bovine/sheep lumbar discs, should be selected to enable the comparison of the mechanical reparative efficiency among different biomaterials.

A real-time monitoring system containing two fluorophore particle probes (blue or NIR emitting) can remotely, with minimal invasiveness, measure the stain exhibited by load-supporting gels. The compressive deformation ratio of gels is equal to the photoluminescence intensity from the blue-emitting probe, while the deformation ratio with a transition from compression to tension is linear to the normalized ratio of the photoluminescence intensity for the blue and NIR probes.[782] This system may be an important tool for remotely monitoring the compression and tension alterations in the implanted gel in a real-time manner.

Conclusion & Perspectives

Although several animal models have been established, there is a lack of consensus regarding the selection of specific models for evaluating therapeutic strategies. The spontaneous degenerative model from non-human primates, especially the aging model, is probably the most satisfying model that resembles both the components and mechanical characteristics of human disc degeneration.[200, 206] However, this model is hindered by ethical restrictions, time consumption, and financial burden. Instead, sheep may be a reliable species for developing animal models that simulate the natural disappearance of notochord cells in adulthood, with similar disc size and mechanical characteristics to humans.[170, 185, 219] Furthermore, established methods for pain detection in large animals remain unavailable and need to be developed to assess the pain-relieving effects of implanted biomaterials.

Currently, the most commonly used degenerative models are induced by acute injuries, such as needle puncture and mechanical alteration established by external apparatus.[32, 136, 290, 435, 783] In contrast, the age-related degenerative process is a long-term condition with gradual changes in the mechanical properties of the disc and microenvironment.[506, 784] The occurrence of replication-related senescent cells also plays a critical role in the disc degeneration process by producing senescence-associated secretory phenotypes.[152, 785, 786] However, the acute injury-induced disc degenerative model cannot replicate this situation. Therefore, animal models developed by mechanical alteration in an elderly animal may be a situational simulation of the most common clinical cases (approximately 40%), with excessive or acute labor increasing intradiscal pressure on age-related degenerative discs, resulting in disc herniation and nerve root irritation.[787, 788]

Most repair materials that achieved ideal reparative effects were applied at the initial stage of the degenerative model.[463, 467, 758, 759, 789] The time required for biomaterial implantation approximates the time required to establish a degenerative model. Therefore, in these cases, disc degeneration is prevented but not reversed; this does not match the clinical situation, where disc degeneration is usually established before patients visit the clinic. Therefore, searching for better treatment options is more practical than focusing on the prevention of IDD.[546] Furthermore, when evaluating the reparative effects, many studies have failed to address pain relief, which is the main reason why patients approach a physician. Future studies should evaluate the pain sensitivity of degenerative models before and after treatment to assess the pain-relieving effects of biomaterials.

The surgical approach is another challenge that needs to be highlighted. Due to the lordotic alignment of disc spaces, AF fissures often occur at the posterolateral site during the range of motion. The fissure is near the spinal cord and dorsal root ganglion, which largely influences the surgical approach to implant repair materials.[370] However, annulus defects of lumbar discs are often developed by anterior puncture or incision, and the injury and herniation sites are not likely to irritate the dorsal root ganglion, which is not relevant to the clinical case in terms of disc degeneration and herniation.[337, 601, 790]

Scaffolds and AF defects must be reshaped and polished to allow for sturdy implantation. Therefore, additional surgery is required, and an enlarged AF damage may occur during surgery. Scaffolds or hydrogels that lack suitable adhesive properties are unstable, and dislocation of these materials will cause further damage to surrounding tissues along with nerve irritation. Moreover, hydrogels fabricated for AF regeneration do not provide cues for organized tissue repair, and the resulting tissue usually lacks an ideal organization matching the original tissue; this may alter the mechanical features of AF and increase the rate of reherniation.[452, 531, 791]

All human discs undergo age-related degeneration to different extents.[792, 793] Disc herniation often occurs in lumbar discs of certain levels (L2–4) but usually not in all discs.[793] Does herniation in adjacent discs only occur when herniated segments are treated? Studies have shown that spinal fusion aggravates the degeneration of adjacent discs.[8, 794, 795] The number of levels that should be treated remains a debatable question among surgeons. Most biomaterials designed for disc regeneration are meant to be employed on local discs but do not focus on overall disc protection. To achieve overall repair, systemic administration with disc targeting properties seems to be more feasible than a comprehensive surgical approach or multi-level injection. Systemic administration of biomaterials, such as nanoparticles with functional domains that can target degenerative disc cell markers or ECM components, may fail to produce an adequate response owing to the limited blood supply of the IVD.[796-799] However, increased vascularization of degenerative discs may facilitate the penetration of systemically administered biomaterials, which helps avoid biomaterial assembly in relatively healthy discs.

Author contributions

YP, ZS and XC designed the review; YP definited the intellectual content; YP, XQ, HS, ST and WY performed literature research; YP, XQ, HS, ST, HL, XL, LZ, XC, FP and SC acquired data; YP, XQ, HS and ST analyzed data lite; YP, XQ and WYprepared and finished the manuscript; HL, XL, LZ, XC, FP, SC and HDH edited the manuscript; WY, HL, XL, LZ, XC, FP, SC and HDH reviewed the manuscript; ZS and XC supervised manuscript drafting and determined the final draft. All authors reviewed and approved the final version of manuscript.

Financial support

This work was supported by the Major Research Plan of National Natural Science Foundation of China (No. 91649204), the National Key Research and Development Program of China (No. 2016YFC1100100), the National Natural Science Foundation of China (No. 81974352), the Scientific Research Training Program for Young Talents from Union Hospital, Tongji Medical College, Huazhong University of Science and Technology, National Natural Science Foundation of China (No. 82002333), and Zhejiang Provincial Natural Science Foundation of China (No. LQ21H060004). These fundings were not involved in the collection, analysis, or interpretation of data in the study.

Acknowledgement

We thank the considerate suggestions provided by Prof. Qian Wang from University of South Carolina, Prof. Bin Li from Soochow University, Prof. Zhidao Xia from Swansea University, Prof. Xiaodong Guo and Prof. Weihua Xu from Wuhan Union Hospital.

Conflicts of interest statement

The authors declare no conflict of interest.

Editor note: Xu Cao and Zengwu Shao are Editorial Board members of *Biomaterials Translational.*

The article was subject to the journal's standard procedures, with peer review handled independently of this Editorial Board Member and their research groups.

Additional files

Additional Table 1: Animal models used to study disc degeneration.
Additional Table 2: Needle gauge and corresponding size.
Additional Table 3: Parameters for needle puncture-induced intervertebral disc degeneration models.
Additional Table 4: Stimuli-evoked hypersensitivity measurement in rodent model.
Additional Table 5: Movement-evoked hypersensitivity measurement in rodent model.
Additional Table 6: Pfirrmann et al.'s classification of disc degeneration.
Additional Table 7: Nomura et al.'s histological grading system.
Additional Table 8: Masuda et al.'s histological grading scale.
Additional Table 9: Han et al.'s histological grading scale.
Additional Table 10: Thompson et al.'s description of morphologic grades.
Additional Table 11: Boos et al.'s variables of macroscopic and histological assessment.
Additional Table 12: Boyd et al.'s grading for intervertebral disc and endplate regions.
Additional Table 13: Methods for the evaluation of adhesive properties.
Additional Table 14: A paradigm for testing intervertebral disc mechanical properties.
Additional Table 15: Recommended parameters for disc regeneration.

1. Cieza, A.; Causey, K.; Kamenov, K.; Hanson, S. W.; Chatterji, S.; Vos, T. Global estimates of the need for rehabilitation based on the Global Burden of Disease study 2019: a systematic analysis for the Global Burden of Disease Study 2019. *Lancet.* **2021**, *396*, 2006-2017.
2. Cheung, K. M.; Samartzis, D.; Karppinen, J.; Luk, K. D. Are "patterns" of lumbar disc degeneration associated with low back pain?: new insights based on skipped level disc pathology. *Spine (Phila Pa 1976).* **2012**, *37*, E430-438.
3. Hunter, D. J.; Bierma-Zeinstra, S. Osteoarthritis. *Lancet.* **2019**, *393*, 1745-1759.
4. Guevar, J.; Olby, N. Minimally invasive microsurgical decompression of an intervertebral disc protrusion in a dog. *Vet Surg.* **2020**, 49 Suppl 1, O86-O92.
5. Geisler, F. H.; McAfee, P. C.; Banco, R. J.; Blumenthal, S. L.; Guyer, R. D.; Holt, R. T.; Majd, M. E. Prospective, randomized, multicenter FDA IDE study of CHARITÉ artificial disc versus lumbar fusion: effect at 5-year follow-up of prior surgery and prior discectomy on clinical outcomes following lumbar arthroplasty. *SAS J.* **2009**, *3*, 17-25.
6. Zou, S.; Gao, J.; Xu, B.; Lu, X.; Han, Y.; Meng, H. Anterior cervical discectomy and fusion (ACDF) versus cervical disc arthroplasty (CDA) for two contiguous levels cervical disc degenerative disease: a meta-analysis of randomized controlled trials. *Eur Spine J.* **2017**, *26*, 985-997.
7. Parker, S. L.; Mendenhall, S. K.; Godil, S. S.; Sivasubramanian, P.; Cahill, K.; Ziewacz, J.; McGirt, M. J. Incidence of low back pain after lumbar discectomy for herniated disc and its effect on patient-reported outcomes. *Clin Orthop Relat Res.* **2015**, *473*, 1988-1999.
8. Hilibrand, A. S.; Robbins, M. Adjacent segment degeneration and adjacent segment disease: the consequences of spinal fusion? *Spine J.* **2004**, *4*, 190s-194s.
9. Mukherjee, D.; Nissen, S. E.; Topol, E. J. Risk of cardiovascular events associated with selective COX-2 inhibitors. *JAMA.* **2001**, *286*, 954-959.
10. Rosenzweig, D. H.; Fairag, R.; Mathieu, A. P.; Li, L.; Eglin, D.; D'Este, M.; Steffen, T.; Weber, M. H.; Ouellet, J. A.; Haglund, L. Thermoreversible hyaluronan-hydrogel and autologous nucleus pulposus cell delivery regenerates human intervertebral discs in an ex

vivo, physiological organ culture model. *Eur Cell Mater.* **2018**, *36*, 200-217.
11. Noriega, D. C.; Ardura, F.; Hernández-Ramajo, R.; Martín-Ferrero, M.; Sánchez-Lite, I.; Toribio, B.; Alberca, M.; García, V.; Moraleda, J. M.; Sánchez, A.; García-Sancho, J. Intervertebral disc repair by allogeneic mesenchymal bone marrow cells: a randomized controlled trial. *Transplantation.* **2017**, *101*, 1945-1951.
12. Orozco, L.; Soler, R.; Morera, C.; Alberca, M.; Sánchez, A.; García-Sancho, J. Intervertebral disc repair by autologous mesenchymal bone marrow cells: a pilot study. *Transplantation.* **2011**, *92*, 822-828.
13. Pettine, K.; Suzuki, R.; Sand, T.; Murphy, M. Treatment of discogenic back pain with autologous bone marrow concentrate injection with minimum two year follow-up. *Int Orthop.* **2016**, *40*, 135-140.
14. Pettine, K. A.; Suzuki, R. K.; Sand, T. T.; Murphy, M. B. Autologous bone marrow concentrate intradiscal injection for the treatment of degenerative disc disease with three-year follow-up. *Int Orthop.* **2017**, *41*, 2097-2103.
15. Elabd, C.; Centeno, C. J.; Schultz, J. R.; Lutz, G.; Ichim, T.; Silva, F. J. Intra-discal injection of autologous, hypoxic cultured bone marrow-derived mesenchymal stem cells in five patients with chronic lower back pain: a long-term safety and feasibility study. *J Transl Med.* **2016**, *14*, 253.
16. Centeno, C.; Markle, J.; Dodson, E.; Stemper, I.; Williams, C. J.; Hyzy, M.; Ichim, T.; Freeman, M. Treatment of lumbar degenerative disc disease-associated radicular pain with culture-expanded autologous mesenchymal stem cells: a pilot study on safety and efficacy. *J Transl Med.* **2017**, *15*, 197.
17. Laslett, M.; Oberg, B.; Aprill, C. N.; McDonald, B. Centralization as a predictor of provocation discography results in chronic low back pain, and the influence of disability and distress on diagnostic power. *Spine J.* **2005**, *5*, 370-380.
18. Pettine, K. A.; Murphy, M. B.; Suzuki, R. K.; Sand, T. T. Percutaneous injection of autologous bone marrow concentrate cells significantly reduces lumbar discogenic pain through 12 months. *Stem Cells.* **2015**, *33*, 146-156.
19. Fayad, F.; Lefevre-Colau, M. M.; Rannou, F.; Quintero, N.; Nys, A.; Macé, Y.; Poiraudeau, S.; Drapé, J. L.; Revel, M. Relation of inflammatory modic changes to intradiscal steroid injection outcome in chronic low back pain. *Eur Spine J.* **2007**, *16*, 925-931.
20. Bedard, N. A.; Pugely, A. J.; Elkins, J. M.; Duchman, K. R.; Westermann, R. W.; Liu, S. S.; Gao, Y.; Callaghan, J. J. The John N. Insall award: do Intraarticular injections increase the risk of infection after TKA? *Clin Orthop Relat Res.* **2017**, *475*, 45-52.
21. Chambers, A. W.; Lacy, K. W.; Liow, M. H. L.; Manalo, J. P. M.; Freiberg, A. A.; Kwon, Y. M. Multiple hip intra-articular steroid injections increase risk of periprosthetic joint infection compared with single injections. *J Arthroplasty.* **2017**, *32*, 1980-1983.
22. Pal, B.; Morris, J. Perceived risks of joint infection following intra-articular corticosteroid injections: a survey of rheumatologists. *Clin Rheumatol.* **1999**, *18*, 264-265.
23. Teixeira, G. Q.; Leite Pereira, C.; Castro, F.; Ferreira, J. R.; Gomez-Lazaro, M.; Aguiar, P.; Barbosa, M. A.; Neidlinger-Wilke, C.; Goncalves, R. M. Anti-inflammatory chitosan/poly-γ-glutamic acid nanoparticles control inflammation while remodeling extracellular matrix in degenerated intervertebral disc. *Acta Biomater.* **2016**, *42*, 168-179.
24. Zhang, H.; Yu, S.; Zhao, X.; Mao, Z.; Gao, C. Stromal cell-derived factor-1α-encapsulated albumin/heparin nanoparticles for induced stem cell migration and intervertebral disc regeneration in vivo. *Acta Biomater.* **2018**, *72*, 217-227.
25. Bowles, R. D.; Setton, L. A. Biomaterials for intervertebral disc regeneration and repair. *Biomaterials.* **2017**, *129*, 54-67.
26. Harmon, M. D.; Ramos, D. M.; Nithyadevi, D.; Bordett, R.; Rudraiah, S.; Nukavarapu, S. P.; Moss, I. L.; Kumbar, S. G. Growing a backbone - functional biomaterials and structures for intervertebral disc (IVD) repair and regeneration: challenges, innovations, and future directions. *Biomater Sci.* **2020**, *8*, 1216-1239.
27. Virk, S.; Chen, T.; Meyers, K. N.; Lafage, V.; Schwab, F.; Maher, S. A. Comparison of biomechanical studies of disc repair devices based on a systematic review. *Spine J.* **2020**, *20*, 1344-1355.
28. Long, R. G.; Torre, O. M.; Hom, W. W.; Assael, D. J.; Iatridis, J. C. Design requirements for annulus fibrosus repair: review of forces, displacements, and material properties of the intervertebral disk and a summary of candidate hydrogels for repair. *J Biomech Eng.* **2016**, *138*, 021007.
29. Krock, E.; Millecamps, M.; Anderson, K. M.; Srivastava, A.; Reihsen, T. E.; Hari, P.; Sun, Y. R.; Jang, S. H.; Wilcox, G. L.; Belani, K. G.; Beebe, D. S.; Ouellet, J.; Pinto, M. R.; Kehl, L. J.; Haglund, L.; Stone, L. S. Interleukin-8 as a therapeutic target for chronic low back pain: Upregulation in human cerebrospinal fluid and pre-clinical validation with chronic reparixin in the SPARC-null mouse model. *EBioMedicine.* **2019**, *43*, 487-500.
30. Millecamps, M.; Czerminski, J. T.; Mathieu, A. P.; Stone, L. S. Behavioral signs of axial low back pain and motor impairment correlate with the severity of intervertebral disc degeneration in a mouse model. *Spine J.* **2015**, *15*, 2524-2537.
31. Bian, Q.; Ma, L.; Jain, A.; Crane, J. L.; Kebaish, K.; Wan, M.; Zhang, Z.; Edward Guo, X.; Sponseller, P. D.; Séguin, C. A.; Riley, L. H.; Wang, Y.; Cao, X. Mechanosignaling activation of TGFβ maintains intervertebral disc homeostasis. *Bone Res.* **2017**, *5*, 17008.
32. Huang, D.; Peng, Y.; Ma, K.; Qing, X.; Deng, X.; Li, Z.; Shao, Z. Puerarin relieved compression-induced apoptosis and mitochondrial dysfunction in human nucleus pulposus mesenchymal stem cells via the PI3K/Akt pathway. *Stem Cells Int.* **2020**, *2020*, 7126914.
33. Sekiguchi, M.; Konno, S.; Kikuchi, S. The effects of a 5-HT2A receptor antagonist on blood flow in lumbar disc herniation: application of nucleus pulposus in a canine model. *Eur Spine J.* **2008**, *17*, 307-313.
34. Bailey, J. F.; Fields, A. J.; Liebenberg, E.; Mattison, J. A.; Lotz, J. C.; Kramer, P. A. Comparison of vertebral and intervertebral disc lesions in aging humans and rhesus monkeys. *Osteoarthritis Cartilage.* **2014**, *22*, 980-985.
35. Beckstein, J. C.; Sen, S.; Schaer, T. P.; Vresilovic, E. J.; Elliott, D. M. Comparison of animal discs used in disc research to human lumbar disc: axial compression mechanics and glycosaminoglycan content. *Spine (Phila Pa 1976).* **2008**, *33*, E166-173.
36. Weiler, C.; Schietzsch, M.; Kirchner, T.; Nerlich, A. G.; Boos, N.; Wuertz, K. Age-related changes in human cervical, thoracal and lumbar intervertebral disc exhibit a strong intra-individual correlation. *Eur Spine J.* **2012**, 21 Suppl 6, S810-818.
37. Robinson, W. A.; Nassr, A. N.; Sebastian, A. S. Thoracic disc herniation, avoidance, and management of the surgical complications. *Int Orthop.* **2019**, *43*, 817-823.
38. Colombier, P.; Camus, A.; Lescaudron, L.; Clouet, J.; Guicheux, J. Intervertebral disc regeneration: a great challenge for tissue engineers. *Trends Biotechnol.* **2014**, *32*, 433-435.
39. Stergar, J.; Gradisnik, L.; Velnar, T.; Maver, U. Intervertebral disc

tissue engineering: A brief review. *Bosn J Basic Med Sci.* **2019**, *19*, 130-137.

40. Chuah, Y. J.; Peck, Y.; Lau, J. E.; Hee, H. T.; Wang, D. A. Hydrogel based cartilaginous tissue regeneration: recent insights and technologies. *Biomater Sci.* **2017**, *5*, 613-631.
41. Gruber, H. E.; Hoelscher, G. L.; Leslie, K.; Ingram, J. A.; Hanley, E. N., Jr. Three-dimensional culture of human disc cells within agarose or a collagen sponge: assessment of proteoglycan production. *Biomaterials.* **2006**, *27*, 371-376.
42. Silagi, E. S.; Shapiro, I. M.; Risbud, M. V. Glycosaminoglycan synthesis in the nucleus pulposus: Dysregulation and the pathogenesis of disc degeneration. *Matrix Biol.* **2018**, 71-72, 368-379.
43. Erwin, W. M.; Ashman, K.; O'Donnel, P.; Inman, R. D. Nucleus pulposus notochord cells secrete connective tissue growth factor and up-regulate proteoglycan expression by intervertebral disc chondrocytes. *Arthritis Rheum.* **2006**, *54*, 3859-3867.
44. Erwin, W. M.; Islam, D.; Inman, R. D.; Fehlings, M. G.; Tsui, F. W. Notochordal cells protect nucleus pulposus cells from degradation and apoptosis: implications for the mechanisms of intervertebral disc degeneration. *Arthritis Res Ther.* **2011**, *13*, R215.
45. McCann, M. R.; Séguin, C. A. Notochord cells in intervertebral disc development and degeneration. *J Dev Biol.* **2016**, *4*, 3.
46. Hu, B.; Zhang, S.; Liu, W.; Wang, P.; Chen, S.; Lv, X.; Shi, D.; Ma, K.; Wang, B.; Wu, Y.; Shao, Z. Inhibiting heat shock protein 90 protects nucleus pulposus-derived stem/progenitor cells from compression-induced necroptosis and apoptosis. *Front Cell Dev Biol.* **2020**, *8*, 685.
47. Chen, S.; Lv, X.; Hu, B.; Shao, Z.; Wang, B.; Ma, K.; Lin, H.; Cui, M. RIPK1/RIPK3/MLKL-mediated necroptosis contributes to compression-induced rat nucleus pulposus cells death. *Apoptosis.* **2017**, *22*, 626-638.
48. Chen, S.; Liu, S.; Zhao, L.; Lin, H.; Ma, K.; Shao, Z. Heme Oxygenase-1-mediated autophagy protects against oxidative damage in rat nucleus pulposus-derived mesenchymal stem cells. *Oxid Med Cell Longev.* **2020**, *2020*, 9349762.
49. Zhang, Y.; Yang, B.; Wang, J.; Cheng, F.; Shi, K.; Ying, L.; Wang, C.; Xia, K.; Huang, X.; Gong, Z.; Yu, C.; Li, F.; Liang, C.; Chen, Q. Cell senescence: a nonnegligible cell state under survival stress in pathology of intervertebral disc degeneration. *Oxid Med Cell Longev.* **2020**, *2020*, 9503562.
50. Di Micco, R.; Krizhanovsky, V.; Baker, D.; d'Adda di Fagagna, F. Cellular senescence in ageing: from mechanisms to therapeutic opportunities. *Nat Rev Mol Cell Biol.* **2021**, *22*, 75-95.
51. Childs, B. G.; Gluscevic, M.; Baker, D. J.; Laberge, R. M.; Marquess, D.; Dananberg, J.; van Deursen, J. M. Senescent cells: an emerging target for diseases of ageing. *Nat Rev Drug Discov.* **2017**, *16*, 718-735.
52. Wang, F.; Cai, F.; Shi, R.; Wang, X. H.; Wu, X. T. Aging and age related stresses: a senescence mechanism of intervertebral disc degeneration. *Osteoarthritis Cartilage. 2016*, *24*, 398-408.
53. Zou, H.; Stoppani, E.; Volonte, D.; Galbiati, F. Caveolin-1, cellular senescence and age-related diseases. *Mech Ageing Dev.* **2011**, *132*, 533-542.
54. van Deursen, J. M. The role of senescent cells in ageing. *Nature.* **2014**, *509*, 439-446.
55. Chen, X. J.; Kim, S. R.; Jiang, K.; Ferguson, C. M.; Tang, H.; Zhu, X. Y.; Lerman, A.; Eirin, A.; Lerman, L. O. Renovascular disease induces senescence in renal scattered tubular-like cells and impairs their reparative potency. *Hypertension.* **2021**, *77*, 507-518.
56. Dookun, E.; Walaszczyk, A.; Redgrave, R.; Palmowski, P.; Tual-Chalot, S.; Suwana, A.; Chapman, J.; Jirkovsky, E.; Donastorg Sosa, L.; Gill, E.; Yausep, O. E.; Santin, Y.; Mialet-Perez, J.; Andrew Owens, W.; Grieve, D.; Spyridopoulos, I.; Taggart, M.; Arthur, H. M.; Passos, J. F.; Richardson, G. D. Clearance of senescent cells during cardiac ischemia-reperfusion injury improves recovery. *Aging Cell.* **2020**, *19*, e13249.
57. Dookun, E.; Passos, J. F.; Arthur, H. M.; Richardson, G. D. Therapeutic Potential of Senolytics in Cardiovascular Disease. *Cardiovasc Drugs Ther.* **2020**. doi: 10.1007/s10557-020-07075-w.
58. Walaszczyk, A.; Dookun, E.; Redgrave, R.; Tual-Chalot, S.; Victorelli, S.; Spyridopoulos, I.; Owens, A.; Arthur, H. M.; Passos, J. F.; Richardson, G. D. Pharmacological clearance of senescent cells improves survival and recovery in aged mice following acute myocardial infarction. *Aging Cell.* **2019**, *18*, e12945.
59. Ogrodnik, M.; Evans, S. A.; Fielder, E.; Victorelli, S.; Kruger, P.; Salmonowicz, H.; Weigand, B. M.; Patel, A. D.; Pirtskhalava, T.; Inman, C. L.; Johnson, K. O.; Dickinson, S. L.; Rocha, A.; Schafer, M. J.; Zhu, Y.; Allison, D. B.; von Zglinicki, T.; LeBrasseur, N. K.; Tchkonia, T.; Neretti, N.; Passos, J. F.; Kirkland, J. L.; Jurk, D. Whole-body senescent cell clearance alleviates age-related brain inflammation and cognitive impairment in mice. *Aging Cell.* **2021**, *20*, e13296.
60. Johmura, Y.; Yamanaka, T.; Omori, S.; Wang, T. W.; Sugiura, Y.; Matsumoto, M.; Suzuki, N.; Kumamoto, S.; Yamaguchi, K.; Hatakeyama, S.; Takami, T.; Yamaguchi, R.; Shimizu, E.; Ikeda, K.; Okahashi, N.; Mikawa, R.; Suematsu, M.; Arita, M.; Sugimoto, M.; Nakayama, K. I.; Furukawa, Y.; Imoto, S.; Nakanishi, M. Senolysis by glutaminolysis inhibition ameliorates various age-associated disorders. *Science.* **2021**, *371*, 265-270.
61. Hwang, P. Y.; Chen, J.; Jing, L.; Hoffman, B. D.; Setton, L. A. The role of extracellular matrix elasticity and composition in regulating the nucleus pulposus cell phenotype in the intervertebral disc: a narrative review. *J Biomech Eng.* **2014**, *136*, 021010.
62. Gilbert, H. T. J.; Hodson, N.; Baird, P.; Richardson, S. M.; Hoyland, J. A. Acidic pH promotes intervertebral disc degeneration: Acid-sensing ion channel-3 as a potential therapeutic target. *Sci Rep.* **2016**, *6*, 37360.
63. Quero, L.; Klawitter, M.; Schmaus, A.; Rothley, M.; Sleeman, J.; Tiaden, A. N.; Klasen, J.; Boos, N.; Hottiger, M. O.; Wuertz, K.; Richards, P. J. Hyaluronic acid fragments enhance the inflammatory and catabolic response in human intervertebral disc cells through modulation of toll-like receptor 2 signalling pathways. *Arthritis Res Ther.* **2013**, *15*, R94.
64. Zhao, K.; An, R.; Xiang, Q.; Li, G.; Wang, K.; Song, Y.; Liao, Z.; Li, S.; Hua, W.; Feng, X.; Wu, X.; Zhang, Y.; Das, A.; Yang, C. Acid-sensing ion channels regulate nucleus pulposus cell inflammation and pyroptosis via the NLRP3 inflammasome in intervertebral disc degeneration. *Cell Prolif.* **2021**, *54*, e12941.
65. Bachmeier, B. E.; Nerlich, A.; Mittermaier, N.; Weiler, C.; Lumenta, C.; Wuertz, K.; Boos, N. Matrix metalloproteinase expression levels suggest distinct enzyme roles during lumbar disc herniation and degeneration. *Eur Spine J.* **2009**, *18*, 1573-1586.
66. Gruber, H. E.; Hoelscher, G. L.; Ingram, J. A.; Bethea, S.; Hanley, E. N., Jr. Growth and differentiation factor-5 (GDF-5) in the human intervertebral annulus cells and its modulation by IL-1ß and TNF-α in vitro. *Exp Mol Pathol.* **2014**, *96*, 225-229.
67. Weiler, C.; Nerlich, A. G.; Zipperer, J.; Bachmeier, B. E.; Boos, N. 2002 SSE Award Competition in Basic Science: expression of major matrix metalloproteinases is associated with intervertebral disc degradation and resorption. *Eur Spine J.* **2002**, *11*, 308-320.
68. Risbud, M. V.; Shapiro, I. M. Role of cytokines in intervertebral disc degeneration: pain and disc content. *Nat Rev Rheumatol.* **2014**, *10*, 44-56.

69. Willems, N.; Tellegen, A. R.; Bergknut, N.; Creemers, L. B.; Wolfswinkel, J.; Freudigmann, C.; Benz, K.; Grinwis, G. C.; Tryfonidou, M. A.; Meij, B. P. Inflammatory profiles in canine intervertebral disc degeneration. *BMC Vet Res.* **2016**, *12*, 10.
70. Zhang, Y.; Liu, L.; Wang, S.; Zhao, Y.; Liu, Y.; Li, J.; Nie, L.; Cheng, L. Production of CCL20 on nucleus pulposus cells recruits IL-17-producing cells to degenerated IVD tissues in rat models. *J Mol Histol.* **2016**, *47*, 81-89.
71. Wang, J.; Chen, H.; Cao, P.; Wu, X.; Zang, F.; Shi, L.; Liang, L.; Yuan, W. Inflammatory cytokines induce caveolin-1/β-catenin signalling in rat nucleus pulposus cell apoptosis through the p38 MAPK pathway. *Cell Prolif.* **2016**, *49*, 362-372.
72. Guo, H. Y.; Guo, M. K.; Wan, Z. Y.; Song, F.; Wang, H. Q. Emerging evidence on noncoding-RNA regulatory machinery in intervertebral disc degeneration: a narrative review. *Arthritis Res Ther.* **2020**, *22*, 270.
73. Hernandez, P. A.; Jacobsen, T. D.; Chahine, N. O. Actomyosin contractility confers mechanoprotection against TNFα-induced disruption of the intervertebral disc. *Sci Adv.* **2020**, *6*, eaba2368.
74. Qi, W.; Ren, D.; Wang, P.; Song, Z.; Wu, H.; Yao, S.; Geng, L.; Su, Y.; Bai, X. Upregulation of Sirt1 by tyrosol suppresses apoptosis and inflammation and modulates extracellular matrix remodeling in interleukin-1β-stimulated human nucleus pulposus cells through activation of PI3K/Akt pathway. *Int Immunopharmacol.* **2020**, *88*, 106904.
75. Molinos, M.; Almeida, C. R.; Caldeira, J.; Cunha, C.; Gonçalves, R. M.; Barbosa, M. A. Inflammation in intervertebral disc degeneration and regeneration. *J R Soc Interface.* **2015**, *12*, 20141191.
76. Bian, J.; Cai, F.; Chen, H.; Tang, Z.; Xi, K.; Tang, J.; Wu, L.; Xu, Y.; Deng, L.; Gu, Y.; Cui, W.; Chen, L. Modulation of local overactive inflammation via injectable hydrogel microspheres. *Nano Lett.* **2021**, *21*, 2690-2698.
77. Liu, L.; He, J.; Liu, C.; Yang, M.; Fu, J.; Yi, J.; Ai, X.; Liu, M.; Zhuang, Y.; Zhang, Y.; Huang, B.; Li, C.; Zhou, Y.; Feng, C. Cartilage intermediate layer protein affects the progression of intervertebral disc degeneration by regulating the extracellular microenvironment (review). *Int J Mol Med.* **2021**, *47*, 475-484.
78. Tsingas, M.; Ottone, O. K.; Haseeb, A.; Barve, R. A.; Shapiro, I. M.; Lefebvre, V.; Risbud, M. V. Sox9 deletion causes severe intervertebral disc degeneration characterized by apoptosis, matrix remodeling, and compartment-specific transcriptomic changes. *Matrix Biol.* **2020**, *94*, 110-133.
79. McCann, M. R.; Patel, P.; Pest, M. A.; Ratneswaran, A.; Lalli, G.; Beaucage, K. L.; Backler, G. B.; Kamphuis, M. P.; Esmail, Z.; Lee, J.; Barbalinardo, M.; Mort, J. S.; Holdsworth, D. W.; Beier, F.; Dixon, S. J.; Séguin, C. A. Repeated exposure to high-frequency low-amplitude vibration induces degeneration of murine intervertebral discs and knee joints. *Arthritis Rheumatol.* **2015**, *67*, 2164-2175.
80. Bergknut, N.; Grinwis, G.; Pickee, E.; Auriemma, E.; Lagerstedt, A. S.; Hagman, R.; Hazewinkel, H. A.; Meij, B. P. Reliability of macroscopic grading of intervertebral disk degeneration in dogs by use of the Thompson system and comparison with low-field magnetic resonance imaging findings. *Am J Vet Res.* **2011**, *72*, 899-904.
81. Chen, S.; Liu, S.; Ma, K.; Zhao, L.; Lin, H.; Shao, Z. TGF-β signaling in intervertebral disc health and disease. *Osteoarthritis Cartilage.* **2019**, *27*, 1109-1117.
82. Wang, S. Z.; Chang, Q.; Lu, J.; Wang, C. Growth factors and platelet-rich plasma: promising biological strategies for early intervertebral disc degeneration. *Int Orthop.* **2015**, *39*, 927-934.
83. Bian, Q.; Jain, A.; Xu, X.; Kebaish, K.; Crane, J. L.; Zhang, Z.; Wan, M.; Ma, L.; Riley, L. H.; Sponseller, P. D.; Guo, X. E.; Lu, W. W.; Wang, Y.; Cao, X. Excessive activation of TGFβ by spinal instability causes vertebral endplate sclerosis. *Sci Rep.* **2016**, *6*, 27093.
84. Zieba, J.; Forlenza, K. N.; Khatra, J. S.; Sarukhanov, A.; Duran, I.; Rigueur, D.; Lyons, K. M.; Cohn, D. H.; Merrill, A. E.; Krakow, D. TGFβ and BMP dependent cell fate changes due to loss of filamin B produces disc degeneration and progressive vertebral fusions. *PLoS Genet.* **2016**, *12*, e1005936.
85. Hu, Y.; Tang, J. S.; Hou, S. X.; Shi, X. X.; Qin, J.; Zhang, T. S.; Wang, X. J. Neuroprotective effects of curcumin alleviate lumbar intervertebral disc degeneration through regulating the expression of iNOS, COX-2, TGF-β1/2, MMP-9 and BDNF in a rat model. *Mol Med Rep.* **2017**, *16*, 6864-6869.
86. Li, H.; Li, W.; Liang, B.; Wei, J.; Yin, D.; Fan, Q. Role of AP-2α/TGF-β1/Smad3 axis in rats with intervertebral disc degeneration. *Life Sci.* **2020**, *263*, 118567.
87. Finnson, K. W.; Parker, W. L.; ten Dijke, P.; Thorikay, M.; Philip, A. ALK1 opposes ALK5/Smad3 signaling and expression of extracellular matrix components in human chondrocytes. *J Bone Miner Res.* **2008**, *23*, 896-906.
88. Than, K. D.; Rahman, S. U.; Vanaman, M. J.; Wang, A. C.; Lin, C. Y.; Zhang, H.; La Marca, F.; Park, P. Bone morphogenetic proteins and degenerative disk disease. *Neurosurgery.* **2012**, *70*, 996-1002; discussion 1002.
89. Enochson, L.; Stenberg, J.; Brittberg, M.; Lindahl, A. GDF5 reduces MMP13 expression in human chondrocytes via DKK1 mediated canonical Wnt signaling inhibition. *Osteoarthritis Cartilage.* **2014**, *22*, 566-577.
90. Ghezelbash, F.; Eskandari, A. H.; Shirazi-Adl, A.; Kazempour, M.; Tavakoli, J.; Baghani, M.; Costi, J. J. Modeling of human intervertebral disc annulus fibrosus with complex multi-fiber networks. *Acta Biomater.* **2021**, *123*, 208-221.
91. Hayes, A. J.; Benjamin, M.; Ralphs, J. R. Extracellular matrix in development of the intervertebral disc. *Matrix Biol.* **2001**, *20*, 107-121.
92. Tavakoli, J.; Diwan, A. D.; Tipper, J. L. Advanced strategies for the regeneration of lumbar disc annulus fibrosus. *Int J Mol Sci.* **2020**, *21*, 4889.
93. Torre, O. M.; Mroz, V.; Bartelstein, M. K.; Huang, A. H.; Iatridis, J. C. Annulus fibrosus cell phenotypes in homeostasis and injury: implications for regenerative strategies. *Ann N Y Acad Sci.* **2019**, *1442*, 61-78.
94. Bruehlmann, S. B.; Rattner, J. B.; Matyas, J. R.; Duncan, N. A. Regional variations in the cellular matrix of the annulus fibrosus of the intervertebral disc. *J Anat.* **2002**, *201*, 159-171.
95. Tavakoli, J.; Elliott, D. M.; Costi, J. J. Structure and mechanical function of the inter-lamellar matrix of the annulus fibrosus in the disc. *J Orthop Res.* **2016**, *34*, 1307-1315.
96. Fernandez-Moure, J.; Moore, C. A.; Kim, K.; Karim, A.; Smith, K.; Barbosa, Z.; Van Eps, J.; Rameshwar, P.; Weiner, B. Novel therapeutic strategies for degenerative disc disease: Review of cell biology and intervertebral disc cell therapy. *SAGE open medicine.* **2018**, *6*, 2050312118761674.
97. Pritzker, K. P. Aging and degeneration in the lumbar intervertebral disc. *Orthop Clin North Am.* **1977**, *8*, 66-77.
98. Bron, J. L.; Helder, M. N.; Meisel, H. J.; Van Royen, B. J.; Smit, T. H. Repair, regenerative and supportive therapies of the annulus fibrosus: achievements and challenges. *Eur Spine J.* **2009**, *18*, 301-313.

99. Chu, G.; Shi, C.; Wang, H.; Zhang, W.; Yang, H.; Li, B. Strategies for annulus fibrosus regeneration: from biological therapies to tissue engineering. *Front Bioeng Biotechnol.* **2018**, *6*, 90.
100. Chu, G.; Shi, C.; Lin, J.; Wang, S.; Wang, H.; Liu, T.; Yang, H.; Li, B. Biomechanics in annulus fibrosus degeneration and regeneration. *Adv Exp Med Biol.* **2018**, *1078*, 409-420.
101. Vergroesen, P. P.; Kingma, I.; Emanuel, K. S.; Hoogendoorn, R. J.; Welting, T. J.; van Royen, B. J.; van Dieën, J. H.; Smit, T. H. Mechanics and biology in intervertebral disc degeneration: a vicious circle. *Osteoarthritis Cartilage.* **2015**, *23*, 1057-1070.
102. Zhou, Z.; Cui, S.; Du, J.; Richards, R. G.; Alini, M.; Grad, S.; Li, Z. One strike loading organ culture model to investigate the post-traumatic disc degenerative condition. *J Orthop Translat.* **2021**, *26*, 141-150.
103. Michalek, A. J.; Funabashi, K. L.; Iatridis, J. C. Needle puncture injury of the rat intervertebral disc affects torsional and compressive biomechanics differently. *Eur Spine J.* **2010**, *19*, 2110-2116.
104. Guterl, C. C.; See, E. Y.; Blanquer, S. B.; Pandit, A.; Ferguson, S. J.; Benneker, L. M.; Grijpma, D. W.; Sakai, D.; Eglin, D.; Alini, M.; Iatridis, J. C.; Grad, S. Challenges and strategies in the repair of ruptured annulus fibrosus. *Eur Cell Mater.* **2013**, *25*, 1-21.
105. Miyamoto, H.; Doita, M.; Nishida, K.; Yamamoto, T.; Sumi, M.; Kurosaka, M. Effects of cyclic mechanical stress on the production of inflammatory agents by nucleus pulposus and anulus fibrosus derived cells in vitro. *Spine (Phila Pa 1976).* **2006**, *31*, 4-9.
106. Pratsinis, H.; Papadopoulou, A.; Neidlinger-Wilke, C.; Brayda-Bruno, M.; Wilke, H. J.; Kletsas, D. Cyclic tensile stress of human annulus fibrosus cells induces MAPK activation: involvement in proinflammatory gene expression. *Osteoarthritis Cartilage.* **2016**, *24*, 679-687.
107. Kanerva, A.; Kommonen, B.; Grönblad, M.; Tolonen, J.; Habtemariam, A.; Virri, J.; Karaharju, E. Inflammatory cells in experimental intervertebral disc injury. *Spine (Phila Pa 1976).* **1997**, *22*, 2711-2715.
108. Wiet, M. G.; Piscioneri, A.; Khan, S. N.; Ballinger, M. N.; Hoyland, J. A.; Purmessur, D. Mast Cell-Intervertebral disc cell interactions regulate inflammation, catabolism and angiogenesis in discogenic back pain. *Sci Rep.* **2017**, *7*, 12492.
109. Sainoh, T.; Orita, S.; Miyagi, M.; Sakuma, Y.; Yamauchi, K.; Suzuki, M.; Kubota, G.; Oikawa, Y.; Inage, K.; Sato, J.; Fujimoto, K.; Shiga, Y.; Inoue, G.; Aoki, Y.; Takahashi, K.; Ohtori, S. Interleukin-6 and interleukin-6 receptor expression, localization, and involvement in pain-sensing neuron activation in a mouse intervertebral disc injury model. *J Orthop Res.* **2015**, *33*, 1508-1514.
110. Osti, O. L.; Vernon-Roberts, B.; Fraser, R. D. 1990 Volvo Award in experimental studies. Anulus tears and intervertebral disc degeneration. An experimental study using an animal model. *Spine (Phila Pa 1976).* **1990**, *15*, 762-767.
111. You, C.; Zhu, K.; Liu, X.; Xi, C.; Zhang, Z.; Xu, G.; Yan, J. Tumor necrosis factor-α-dependent infiltration of macrophages into the dorsal root ganglion in a rat disc herniation model. *Spine (Phila Pa 1976).* **2013**, *38*, 2003-2007.
112. Rand, N. S.; Dawson, J. M.; Juliao, S. F.; Spengler, D. M.; Floman, Y. In vivo macrophage recruitment by murine intervertebral disc cells. *J Spinal Disord.* **2001**, *14*, 339-342.
113. Nakazawa, K. R.; Walter, B. A.; Laudier, D. M.; Krishnamoorthy, D.; Mosley, G. E.; Spiller, K. L.; Iatridis, J. C. Accumulation and localization of macrophage phenotypes with human intervertebral disc degeneration. *Spine J.* **2018**, *18*, 343-356.
114. Park, J. J.; Moon, H. J.; Park, J. H.; Kwon, T. H.; Park, Y. K.; Kim, J. H. Induction of proinflammatory cytokine production in intervertebral disc cells by macrophage-like THP-1 cells requires mitogen-activated protein kinase activity. *J Neurosurg Spine.* **2016**, *24*, 167-175.
115. Bai, J.; Zhang, Y.; Fan, Q.; Xu, J.; Shan, H.; Gao, X.; Ma, Q.; Sheng, L.; Zheng, X.; Cheng, W.; Li, D.; Zhang, M.; Hao, Y.; Feng, L.; Chen, Q.; Zhou, X.; Wang, C. Reactive oxygen species-scavenging scaffold with rapamycin for treatment of intervertebral disk degeneration. *Adv Healthc Mater.* **2020**, *9*, e1901186.
116. Takeoka, Y.; Yurube, T.; Morimoto, K.; Kunii, S.; Kanda, Y.; Tsujimoto, R.; Kawakami, Y.; Fukase, N.; Takemori, T.; Omae, K.; Kakiuchi, Y.; Miyazaki, S.; Kakutani, K.; Takada, T.; Nishida, K.; Fukushima, M.; Kuroda, R. Reduced nucleotomy-induced intervertebral disc disruption through spontaneous spheroid formation by the low adhesive scaffold collagen (LASCol). *Biomaterials.* **2020**, *235*, 119781.
117. Lin, H. A.; Varma, D. M.; Hom, W. W.; Cruz, M. A.; Nasser, P. R.; Phelps, R. G.; Iatridis, J. C.; Nicoll, S. B. Injectable cellulose-based hydrogels as nucleus pulposus replacements: Assessment of in vitro structural stability, ex vivo herniation risk, and in vivo biocompatibility. *J Mech Behav Biomed Mater.* **2019**, *96*, 204-213.
118. Moore, R. J. The vertebral endplate: disc degeneration, disc regeneration. *Eur Spine J.* **2006**, *15 Suppl 3*, S333-337.
119. Lakshmanan, P.; Purushothaman, B.; Dvorak, V.; Schratt, W.; Thambiraj, S.; Boszczyk, M. Sagittal endplate morphology of the lower lumbar spine. *Eur Spine J.* **2012**, *21 Suppl 2*, S160-164.
120. Che-Nordin, N.; Deng, M.; Griffith, J. F.; Leung, J. C. S.; Kwok, A. W. L.; Zhu, Y. Q.; So, R. H. Y.; Kwok, T. C. Y.; Leung, P. C.; Wáng, Y. X. J. Prevalent osteoporotic vertebral fractures more likely involve the upper endplate than the lower endplate and even more so in males. *Ann Transl Med.* **2018**, *6*, 442.
121. Nagaraja, S.; Awada, H. K.; Dreher, M. L.; Bouck, J. T.; Gupta, S. Effects of vertebroplasty on endplate subsidence in elderly female spines. *J Neurosurg Spine.* **2015**, *22*, 273-282.
122. Ferguson, S. J.; Steffen, T. Biomechanics of the aging spine. *Eur Spine J.* **2003**, *12 Suppl 2*, S97-S103.
123. Adams, M. A.; Dolan, P. Intervertebral disc degeneration: evidence for two distinct phenotypes. *J Anat.* **2012**, *221*, 497-506.
124. Braithwaite, I.; White, J.; Saifuddin, A.; Renton, P.; Taylor, B. A. Vertebral end-plate (Modic) changes on lumbar spine MRI: correlation with pain reproduction at lumbar discography. *Eur Spine J.* **1998**, *7*, 363-368.
125. Kuisma, M.; Karppinen, J.; Niinimäki, J.; Ojala, R.; Haapea, M.; Heliövaara, M.; Korpelainen, R.; Taimela, S.; Natri, A.; Tervonen, O. Modic changes in endplates of lumbar vertebral bodies: prevalence and association with low back and sciatic pain among middle-aged male workers. *Spine (Phila Pa 1976).* **2007**, *32*, 1116-1122.
126. Albert, H. B.; Manniche, C. Modic changes following lumbar disc herniation. *Eur Spine J.* **2007**, *16*, 977-982.
127. Rahme, R.; Moussa, R. The modic vertebral endplate and marrow changes: pathologic significance and relation to low back pain and segmental instability of the lumbar spine. *AJNR Am J Neuroradiol.* **2008**, *29*, 838-842.
128. Dudli, S.; Fields, A. J.; Samartzis, D.; Karppinen, J.; Lotz, J. C. Pathobiology of modic changes. *Eur Spine J.* **2016**, *25*, 3723-3734.
129. Crockett, M. T.; Kelly, B. S.; van Baarsel, S.; Kavanagh, E. C. Modic type 1 vertebral endplate changes: injury, inflammation, or infection? *AJR Am J Roentgenol.* **2017**, *209*, 167-170.
130. Hanımoğlu, H.; Çevik, S.; Yılmaz, H.; Kaplan, A.; Çalış, F.; Katar, S.;

Evran, Ş.; Akkaya, E.; Karaca, O. Effects of modic type 1 changes in the vertebrae on low back pain. *World Neurosurg.* **2019**, *121*, e426-e432.
131. Ni, S.; Ling, Z.; Wang, X.; Cao, Y.; Wu, T.; Deng, R.; Crane, J. L.; Skolasky, R.; Demehri, S.; Zhen, G.; Jain, A.; Wu, P.; Pan, D.; Hu, B.; Lyu, X.; Li, Y.; Chen, H.; Qi, H.; Guan, Y.; Dong, X.; Wan, M.; Zou, X.; Lu, H.; Hu, J.; Cao, X. Sensory innervation in porous endplates by Netrin-1 from osteoclasts mediates PGE2-induced spinal hypersensitivity in mice. *Nat Commun.* **2019**, *10*, 5643.
132. Freemont, A. J.; Peacock, T. E.; Goupille, P.; Hoyland, J. A.; O'Brien, J.; Jayson, M. I. Nerve ingrowth into diseased intervertebral disc in chronic back pain. *Lancet.* **1997**, *350*, 178-181.
133. Fields, A. J.; Liebenberg, E. C.; Lotz, J. C. Innervation of pathologies in the lumbar vertebral end plate and intervertebral disc. *Spine J.* **2014**, *14*, 513-521.
134. Ohtori, S.; Miyagi, M.; Inoue, G. Sensory nerve ingrowth, cytokines, and instability of discogenic low back pain: A review. *Spine Surg Relat Res.* **2018**, *2*, 11-17.
135. Lama, P.; Le Maitre, C. L.; Harding, I. J.; Dolan, P.; Adams, M. A. Nerves and blood vessels in degenerated intervertebral discs are confined to physically disrupted tissue. *J Anat.* **2018**, *233*, 86-97.
136. Zhang, S.; Hu, B.; Liu, W.; Wang, P.; Lv, X.; Chen, S.; Shao, Z. The role of structure and function changes of sensory nervous system in intervertebral disc-related low back pain. *Osteoarthritis Cartilage.* **2021**, *29*, 17-27.
137. Johnson, W. E.; Caterson, B.; Eisenstein, S. M.; Hynds, D. L.; Snow, D. M.; Roberts, S. Human intervertebral disc aggrecan inhibits nerve growth in vitro. *Arthritis Rheum.* **2002**, *46*, 2658-2664.
138. Lee, J. M.; Song, J. Y.; Baek, M.; Jung, H. Y.; Kang, H.; Han, I. B.; Kwon, Y. D.; Shin, D. E. Interleukin-1β induces angiogenesis and innervation in human intervertebral disc degeneration. *J Orthop Res.* **2011**, *29*, 265-269.
139. Binch, A. L.; Cole, A. A.; Breakwell, L. M.; Michael, A. L.; Chiverton, N.; Cross, A. K.; Le Maitre, C. L. Expression and regulation of neurotrophic and angiogenic factors during human intervertebral disc degeneration. *Arthritis Res Ther.* **2014**, *16*, 416.
140. Obata, K.; Tsujino, H.; Yamanaka, H.; Yi, D.; Fukuoka, T.; Hashimoto, N.; Yonenobu, K.; Yoshikawa, H.; Noguchi, K. Expression of neurotrophic factors in the dorsal root ganglion in a rat model of lumbar disc herniation. *Pain.* **2002**, *99*, 121-132.
141. Henry, N.; Clouet, J.; Le Bideau, J.; Le Visage, C.; Guicheux, J. Innovative strategies for intervertebral disc regenerative medicine: From cell therapies to multiscale delivery systems. *Biotechnol Adv.* **2018**, *36*, 281-294.
142. Alkhatib, B.; Rosenzweig, D. H.; Krock, E.; Roughley, P. J.; Beckman, L.; Steffen, T.; Weber, M. H.; Ouellet, J. A.; Haglund, L. Acute mechanical injury of the human intervertebral disc: link to degeneration and pain. *Eur Cell Mater.* **2014**, *28*, 98-110; discussion 110-111.
143. Fournier, D. E.; Kiser, P. K.; Shoemaker, J. K.; Battié, M. C.; Séguin, C. A. Vascularization of the human intervertebral disc: A scoping review. *JOR Spine.* **2020**, *3*, e1123.
144. Hassler, O. The human intervertebral disc. A micro-angiographical study on its vascular supply at various ages. *Acta Orthop Scand.* **1969**, *40*, 765-772.
145. Hee, H. T.; Chuah, Y. J.; Tan, B. H.; Setiobudi, T.; Wong, H. K. Vascularization and morphological changes of the endplate after axial compression and distraction of the intervertebral disc. *Spine (Phila Pa 1976).* **2011**, *36*, 505-511.
146. Binch, A. L.; Cole, A. A.; Breakwell, L. M.; Michael, A. L.; Chiverton, N.; Creemers, L. B.; Cross, A. K.; Le Maitre, C. L. Nerves are more abundant than blood vessels in the degenerate human intervertebral disc. *Arthritis Res Ther.* **2015**, *17*, 370.
147. Lyu, F. J.; Cheung, K. M.; Zheng, Z.; Wang, H.; Sakai, D.; Leung, V. Y. IVD progenitor cells: a new horizon for understanding disc homeostasis and repair. *Nat Rev Rheumatol.* **2019**, *15*, 102-112.
148. Wang, B.; Ke, W.; Wang, K.; Li, G.; Ma, L.; Lu, S.; Xiang, Q.; Liao, Z.; Luo, R.; Song, Y.; Hua, W.; Wu, X.; Zhang, Y.; Zeng, X.; Yang, C. Mechanosensitive ion channel piezo1 activated by matrix stiffness regulates oxidative stress-induced senescence and apoptosis in human intervertebral disc degeneration. *Oxid Med Cell Longev.* **2021**, *2021*, 8884922.
149. Lin, J.; Du, J.; Wu, X.; Xu, C.; Liu, J.; Jiang, L.; Cheng, X.; Ge, G.; Chen, L.; Pang, Q.; Geng, D.; Mao, H. SIRT3 mitigates intervertebral disc degeneration by delaying oxidative stress-induced senescence of nucleus pulposus cells. *J Cell Physiol.* **2021**. doi: 10.1002/jcp.30319.
150. Tang, N.; Dong, Y.; Chen, C.; Zhao, H. Anisodamine maintains the stability of intervertebral disc tissue by inhibiting the senescence of nucleus pulposus cells and degradation of extracellular matrix via interleukin-6/janus kinases/signal transducer and activator of transcription 3 pathway. *Front Pharmacol.* **2020**, *11*, 519172.
151. Lotz, J. C.; Haughton, V.; Boden, S. D.; An, H. S.; Kang, J. D.; Masuda, K.; Freemont, A.; Berven, S.; Sengupta, D. K.; Tanenbaum, L.; Maurer, P.; Ranganathan, A.; Alavi, A.; Marinelli, N. L. New treatments and imaging strategies in degenerative disease of the intervertebral disks. *Radiology.* **2012**, *264*, 6-19.
152. Che, H.; Li, J.; Li, Y.; Ma, C.; Liu, H.; Qin, J.; Dong, J.; Zhang, Z.; Xian, C. J.; Miao, D.; Wang, L.; Ren, Y. p16 deficiency attenuates intervertebral disc degeneration by adjusting oxidative stress and nucleus pulposus cell cycle. *Elife.* **2020**, *9*, e52570.
153. Bárdos, T.; Szabó, Z.; Czipri, M.; Vermes, C.; Tunyogi-Csapó, M.; Urban, R. M.; Mikecz, K.; Glant, T. T. A longitudinal study on an autoimmune murine model of ankylosing spondylitis. *Ann Rheum Dis.* **2005**, *64*, 981-987.
154. Mohanty, S.; Dahia, C. L. Defects in intervertebral disc and spine during development, degeneration, and pain: New research directions for disc regeneration and therapy. *Wiley Interdiscip Rev Dev Biol.* **2019**, *8*, e343.
155. Hartman, R.; Patil, P.; Tisherman, R.; St Croix, C.; Niedernhofer, L. J.; Robbins, P. D.; Ambrosio, F.; Van Houten, B.; Sowa, G.; Vo, N. Age-dependent changes in intervertebral disc cell mitochondria and bioenergetics. *Eur Cell Mater.* **2018**, *36*, 171-183.
156. Vadalà, G.; Ambrosio, L.; Russo, F.; Papalia, R.; Denaro, V. Interaction between mesenchymal stem cells and intervertebral disc microenvironment: from cell therapy to tissue engineering. *Stem Cells Int.* **2019**, *2019*, 2376172.
157. Vo, N. V.; Hartman, R. A.; Patil, P. R.; Risbud, M. V.; Kletsas, D.; Iatridis, J. C.; Hoyland, J. A.; Le Maitre, C. L.; Sowa, G. A.; Kang, J. D. Molecular mechanisms of biological aging in intervertebral discs. *J Orthop Res.* **2016**, *34*, 1289-1306.
158. Risbud, M. V.; Schipani, E.; Shapiro, I. M. Hypoxic regulation of nucleus pulposus cell survival: from niche to notch. *Am J Pathol.* **2010**, *176*, 1577-1583.
159. Peck, S. H.; Bendigo, J. R.; Tobias, J. W.; Dodge, G. R.; Malhotra, N. R.; Mauck, R. L.; Smith, L. J. Hypoxic preconditioning enhances bone marrow-derived mesenchymal stem cell survival in a low oxygen and nutrient-limited 3D microenvironment. *Cartilage.* **2019**. doi: 10.1177/1947603519841675.

160. Potier, E.; Ferreira, E.; Meunier, A.; Sedel, L.; Logeart-Avramoglou, D.; Petite, H. Prolonged hypoxia concomitant with serum deprivation induces massive human mesenchymal stem cell death. *Tissue Eng.* **2007**, *13*, 1325-1331.
161. Tsai, T. T.; Danielson, K. G.; Guttapalli, A.; Oguz, E.; Albert, T. J.; Shapiro, I. M.; Risbud, M. V. TonEBP/OREBP is a regulator of nucleus pulposus cell function and survival in the intervertebral disc. *J Biol Chem.* **2006**, *281*, 25416-25424.
162. van Dijk, B.; Potier, E.; Ito, K. Culturing bovine nucleus pulposus explants by balancing medium osmolarity. *Tissue Eng Part C Methods.* **2011**, *17*, 1089-1096.
163. Li, P.; Gan, Y.; Wang, H.; Xu, Y.; Li, S.; Song, L.; Zhang, C.; Ou, Y.; Wang, L.; Zhou, Q. Role of the ERK1/2 pathway in osmolarity effects on nucleus pulposus cell apoptosis in a disc perfusion culture. *J Orthop Res.* **2017**, *35*, 86-92.
164. Wuertz, K.; Godburn, K.; Neidlinger-Wilke, C.; Urban, J.; Iatridis, J. C. Behavior of mesenchymal stem cells in the chemical microenvironment of the intervertebral disc. *Spine (Phila Pa 1976).* **2008**, *33*, 1843-1849.
165. Liang, C.; Li, H.; Tao, Y.; Zhou, X.; Li, F.; Chen, G.; Chen, Q. Responses of human adipose-derived mesenchymal stem cells to chemical microenvironment of the intervertebral disc. *J Transl Med.* **2012**, *10*, 49.
166. Li, H.; Wang, J.; Li, F.; Chen, G.; Chen, Q. The influence of hyperosmolarity in the intervertebral disc on the proliferation and chondrogenic differentiation of nucleus pulposus-derived mesenchymal stem cells. *Cells Tissues Organs.* **2018**, *205*, 178-188.
167. Sandor, Z.; Rathonyi, G. K.; Dinya, E. Assessment of lumbar lordosis distribution with a novel mathematical approach and its adaptation for lumbar intervertebral disc degeneration. *Comput Math Methods Med.* **2020**, *2020*, 7312125.
168. Zhou, C.; Willing, R. Alterations in the geometry, fiber orientation, and mechanical behavior of the lumbar intervertebral disc by nucleus swelling. *J Biomech Eng.* **2020**, *142*, 084502.
169. Weber, C. I.; Hwang, C. T.; van Dillen, L. R.; Tang, S. Y. Effects of standing on lumbar spine alignment and intervertebral disc geometry in young, healthy individuals determined by positional magnetic resonance imaging. *Clin Biomech (Bristol, Avon).* **2019**, *65*, 128-134.
170. O'Connell, G. D.; Vresilovic, E. J.; Elliott, D. M. Comparison of animals used in disc research to human lumbar disc geometry. *Spine (Phila Pa 1976).* **2007**, *32*, 328-333.
171. Kandil, K.; Zaïri, F.; Messager, T.; Zaïri, F. A microstructure-based modeling approach to assess aging-sensitive mechanics of human intervertebral disc. *Comput Methods Programs Biomed.* **2021**, *200*, 105890.
172. Rosenzweig, D. H.; Gawri, R.; Moir, J.; Beckman, L.; Eglin, D.; Steffen, T.; Roughley, P. J.; Ouellet, J. A.; Haglund, L. Dynamic loading, matrix maintenance and cell injection therapy of human intervertebral discs cultured in a bioreactor. *Eur Cell Mater.* **2016**, *31*, 26-39.
173. Hartman, R. A.; Yurube, T.; Ngo, K.; Merzlak, N. E.; Debski, R. E.; Brown, B. N.; Kang, J. D.; Sowa, G. A. Biological responses to flexion/extension in spinal segments ex-vivo. *J Orthop Res.* **2015**, *33*, 1255-1264.
174. Wilke, H. J.; Rohlmann, A.; Neller, S.; Graichen, F.; Claes, L.; Bergmann, G. ISSLS prize winner: A novel approach to determine trunk muscle forces during flexion and extension: a comparison of data from an in vitro experiment and in vivo measurements. *Spine (Phila Pa 1976).* **2003**, *28*, 2585-2593.
175. Alini, M.; Eisenstein, S. M.; Ito, K.; Little, C.; Kettler, A. A.; Masuda, K.; Melrose, J.; Ralphs, J.; Stokes, I.; Wilke, H. J. Are animal models useful for studying human disc disorders/degeneration? *Eur Spine J.* **2008**, *17*, 2-19.
176. Motaghinasab, S.; Shirazi-Adl, A.; Urban, J. P.; Parnianpour, M. Computational pharmacokinetics of solute penetration into human intervertebral discs - effects of endplate permeability, solute molecular weight and disc size. *J Biomech.* **2012**, *45*, 2195-2202.
177. Jackson, A. R.; Yuan, T. Y.; Huang, C. Y.; Brown, M. D.; Gu, W. Y. Nutrient transport in human annulus fibrosus is affected by compressive strain and anisotropy. *Ann Biomed Eng.* **2012**, *40*, 2551-2558.
178. Malandrino, A.; Noailly, J.; Lacroix, D. The effect of sustained compression on oxygen metabolic transport in the intervertebral disc decreases with degenerative changes. *PLoS Comput Biol.* **2011**, *7*, e1002112.
179. Soukane, D. M.; Shirazi-Adl, A.; Urban, J. P. Computation of coupled diffusion of oxygen, glucose and lactic acid in an intervertebral disc. *J Biomech.* **2007**, *40*, 2645-2654.
180. DiStefano, T. J.; Shmukler, J. O.; Danias, G.; Iatridis, J. C. The functional role of interface tissue engineering in annulus fibrosus repair: bridging mechanisms of hydrogel integration with regenerative outcomes. *ACS Biomater Sci Eng.* **2020**, *6*, 6556-6586.
181. Kim, K. W.; Lim, T. H.; Kim, J. G.; Jeong, S. T.; Masuda, K.; An, H. S. The origin of chondrocytes in the nucleus pulposus and histologic findings associated with the transition of a notochordal nucleus pulposus to a fibrocartilaginous nucleus pulposus in intact rabbit intervertebral discs. *Spine (Phila Pa 1976).* **2003**, *28*, 982-990.
182. Zhao, X.; Liu, H.; Feng, G.; Deng, L.; Li, X.; Liang, T. Notochord cells enhance proliferation and phenotype-keeping of intervertebral disc chondroid cells. *Zhongguo Xiu Fu Chong Jian Wai Ke Za Zhi.* **2008**, *22*, 939-943.
183. Sun, Z.; Liu, B.; Liu, Z. H.; Song, W.; Wang, D.; Chen, B. Y.; Fan, J.; Xu, Z.; Geng, D.; Luo, Z. J. Notochordal-cell-derived exosomes induced by compressive load inhibit angiogenesis via the miR-140-5p/Wnt/β-Catenin axis. *Mol Ther Nucleic Acids.* **2020**, *22*, 1092-1106.
184. Yin, X.; Motorwala, A.; Vesvoranan, O.; Levene, H. B.; Gu, W.; Huang, C. Y. Effects of glucose deprivation on ATP and proteoglycan production of intervertebral disc cells under hypoxia. *Sci Rep.* **2020**, *10*, 8899.
185. Tong, W.; Lu, Z.; Qin, L.; Mauck, R. L.; Smith, H. E.; Smith, L. J.; Malhotra, N. R.; Heyworth, M. F.; Caldera, F.; Enomoto-Iwamoto, M.; Zhang, Y. Cell therapy for the degenerating intervertebral disc. *Transl Res.* **2017**, *181*, 49-58.
186. Hansen, H. J. Comparative views of the pathology of disk degeneration in animals. *Lab Invest.* **1959**, *8*, 1242-1265.
187. Souter, W. A.; Taylor, T. K. Sulphated acid mucopolysaccharide metabolism in the rabbit intervertebral disc. *J Bone Joint Surg Br.* **1970**, *52*, 371-384.
188. Scott, N. A.; Harris, P. F.; Bagnall, K. M. A morphological and histological study of the postnatal development of intervertebral discs in the lumbar spine of the rabbit. *J Anat.* **1980**, *130*, 75-81.
189. Daly, C.; Ghosh, P.; Jenkin, G.; Oehme, D.; Goldschlager, T. A review of animal models of intervertebral disc degeneration: pathophysiology, regeneration, and translation to the clinic. *Biomed Res Int.* **2016**, *2016*, 5952165.
190. Cho, H.; Park, S. H.; Lee, S.; Kang, M.; Hasty, K. A.; Kim, S. J. Snapshot of degenerative aging of porcine intervertebral disc: a model to unravel the molecular mechanisms. *Exp Mol Med.* **2011**, *43*, 334-340.
191. Bach, F. C.; Willems, N.; Penning, L. C.; Ito, K.; Meij, B. P.; Tryfonidou, M. A. Potential regenerative treatment strategies for

intervertebral disc degeneration in dogs. *BMC Vet Res.* **2014**, *10*, 3.
192. Li, R.; Wang, Z.; Ma, L.; Yang, D.; Xie, D.; Zhang, B.; Ding, W. Lumbar vertebral endplate defects on magnetic resonance imaging in degenerative spondylolisthesis: novel classification, characteristics, and correlative factor analysis. *World Neurosurg.* **2020**, *141*, e423-e430.
193. Somovilla-Gómez, F.; Lostado-Lorza, R.; Corral-Bobadilla, M.; Escribano-García, R. Improvement in determining the risk of damage to the human lumbar functional spinal unit considering age, height, weight and sex using a combination of FEM and RSM. *Biomech Model Mechanobiol.* **2020**, *19*, 351-387.
194. Mosley, G. E.; Hoy, R. C.; Nasser, P.; Kaseta, T.; Lai, A.; Evashwick-Rogler, T. W.; Lee, M.; Iatridis, J. C. Sex differences in rat intervertebral disc structure and function following annular puncture injury. *Spine (Phila Pa 1976).* **2019**, *44*, 1257-1269.
195. Gruber, H. E.; Gordon, B.; Williams, C.; Norton, H. J.; Hanley, E. N., Jr. Vertebral endplate and disc changes in the aging sand rat lumbar spine: cross-sectional analyses of a large male and female population. *Spine (Phila Pa 1976).* **2007**, *32*, 2529-2536.
196. LaCroix-Fralish, M. L.; Rutkowski, M. D.; Weinstein, J. N.; Mogil, J. S.; Deleo, J. A. The magnitude of mechanical allodynia in a rodent model of lumbar radiculopathy is dependent on strain and sex. *Spine (Phila Pa 1976).* **2005**, *30*, 1821-1827.
197. Fillingim, R. B.; King, C. D.; Ribeiro-Dasilva, M. C.; Rahim-Williams, B.; Riley, J. L., 3rd. Sex, gender, and pain: a review of recent clinical and experimental findings. *J Pain.* **2009**, *10*, 447-485.
198. Gautschi, O. P.; Corniola, M. V.; Smoll, N. R.; Joswig, H.; Schaller, K.; Hildebrandt, G.; Stienen, M. N. Sex differences in subjective and objective measures of pain, functional impairment, and health-related quality of life in patients with lumbar degenerative disc disease. *Pain.* **2016**, *157*, 1065-1071.
199. Yang, S.; Zhang, F.; Ma, J.; Ding, W. Intervertebral disc ageing and degeneration: The antiapoptotic effect of oestrogen. *Ageing Res Rev.* **2020**, *57*, 100978.
200. Lauerman, W. C.; Platenberg, R. C.; Cain, J. E.; Deeney, V. F. Age-related disk degeneration: preliminary report of a naturally occurring baboon model. *J Spinal Disord.* **1992**, *5*, 170-174.
201. Platenberg, R. C.; Hubbard, G. B.; Ehler, W. J.; Hixson, C. J. Spontaneous disc degeneration in the baboon model: magnetic resonance imaging and histopathologic correlation. *J Med Primatol.* **2001**, *30*, 268-272.
202. Nuckley, D. J.; Kramer, P. A.; Del Rosario, A.; Fabro, N.; Baran, S.; Ching, R. P. Intervertebral disc degeneration in a naturally occurring primate model: radiographic and biomechanical evidence. *J Orthop Res.* **2008**, *26*, 1283-1288.
203. Showalter, B. L.; Beckstein, J. C.; Martin, J. T.; Beattie, E. E.; Espinoza Orías, A. A.; Schaer, T. P.; Vresilovic, E. J.; Elliott, D. M. Comparison of animal discs used in disc research to human lumbar disc: torsion mechanics and collagen content. *Spine (Phila Pa 1976).* **2012**, *37*, E900-907.
204. Videman, T.; Battié, M. C.; Gill, K.; Manninen, H.; Gibbons, L. E.; Fisher, L. D. Magnetic resonance imaging findings and their relationships in the thoracic and lumbar spine. Insights into the etiopathogenesis of spinal degeneration. *Spine (Phila Pa 1976).* **1995**, *20*, 928-935.
205. Battié, M. C.; Videman, T. Lumbar disc degeneration: epidemiology and genetics. *J Bone Joint Surg Am.* ***2006***, *88 Suppl 2*, 3-9.
206. Lei, C.; Colangelo, D.; Patil, P.; Li, V.; Ngo, K.; Wang, D.; Dong, Q.; Yousefzadeh, M. J.; Lin, H.; Lee, J.; Kang, J.; Sowa, G.; Wyss-Coray, T.; Niedernhofer, L. J.; Robbins, P. D.; Huffman, D. M.; Vo, N. Influences of circulatory factors on intervertebral disc aging phenotype. *Aging (Albany NY).* **2020**, *12*, 12285-12304.
207. Pfeiffer, M.; Wilke, A.; Goetz, W.; Chaparro, F.; Coetzee, E.; Griss, P. Comparison of two experimental models of intervertebral disc degeneration in mammals. *Orthop Proc.* **2002**, 84-B, 18-d-18.
208. Jin, L.; Balian, G.; Li, X. J. Animal models for disc degeneration-an update. *Histol Histopathol.* **2018**, *33*, 543-554.
209. Xi, Y.; Kong, J.; Liu, Y.; Wang, Z.; Ren, S.; Diao, Z.; Hu, Y. Minimally invasive induction of an early lumbar disc degeneration model in rhesus monkeys. *Spine (Phila Pa 1976).* **2013**, *38*, E579-586.
210. Wei, F.; Zhong, R.; Wang, L.; Zhou, Z.; Pan, X.; Cui, S.; Sun, H.; Zou, X.; Gao, M.; Jiang, B.; Chen, W.; Zhuang, W.; Sun, H.; Liu, S. Pingyangmycin-induced in vivo lumbar disc degeneration model of rhesus monkeys. *Spine (Phila Pa 1976).* **2015**, *40*, E199-210.
211. Wei, F.; Zhong, R.; Zhou, Z.; Wang, L.; Pan, X.; Cui, S.; Zou, X.; Gao, M.; Sun, H.; Chen, W.; Liu, S. In vivo experimental intervertebral disc degeneration induced by bleomycin in the rhesus monkey. *BMC Musculoskelet Disord.* **2014**, *15*, 340.
212. Ando, T.; Kato, F.; Mimatsu, K.; Iwata, H. Effects of chondroitinase ABC on degenerative intervertebral discs. *Clin Orthop Relat Res.* **1995**, 214-221.
213. Yamada, K.; Tanabe, S.; Ueno, H.; Oinuma, A.; Takahashi, T.; Miyauchi, S.; Shigeno, S.; Hirose, T.; Miyahara, K.; Sato, M. Investigation of the short-term effect of chemonucleolysis with chondroitinase ABC. *J Vet Med Sci.* **2001**, *63*, 521-525.
214. Lu, D. S.; Luk, K. D.; Lu, W. W.; Cheung, K. M.; Leong, J. C. Spinal flexibility increase after chymopapain injection is dose dependent: a possible alternative to anterior release in scoliosis. *Spine (Phila Pa 1976).* **2004**, *29*, 123-128.
215. Melrose, J.; Taylor, T. K.; Ghosh, P.; Holbert, C.; Macpherson, C.; Bellenger, C. R. Intervertebral disc reconstitution after chemonucleolysis with chymopapain is dependent on dosage. *Spine (Phila Pa 1976).* **1996**, *21*, 9-17.
216. Melrose, J.; Hall, A.; Macpherson, C.; Bellenger, C. R.; Ghosh, P. Evaluation of digestive proteinases from the Antarctic krill Euphasia superba as potential chemonucleolytic agents. In vitro and in vivo studies. *Arch Orthop Trauma Surg.* **1995**, *114*, 145-152.
217. Suguro, T.; Oegema, T. R., Jr.; Bradford, D. S. Ultrastructural study of the short-term effects of chymopapain on the intervertebral disc. *J Orthop Res.* **1986**, *4*, 281-287.
218. Jiang, H.; Wang, J.; Xu, B.; Yang, Q.; Liu, Y. Study on the expression of nerve growth associated protein-43 in rat model of intervertebral disc degeneration. *J Musculoskelet Neuronal Interact.* **2017**, *17*, 104-107.
219. Wilke, H. J.; Kettler, A.; Claes, L. E. Are sheep spines a valid biomechanical model for human spines? *Spine (Phila Pa 1976).* **1997**, *22*, 2365-2374.
220. Turgut, M.; Başaloğlu, H. K.; Yenisey, C.; Ozsunar, Y. Surgical pinealectomy accelerates intervertebral disc degeneration process in chicken. *Eur Spine J.* **2006**, *15*, 605-612.
221. Machida, M.; Murai, I.; Miyashita, Y.; Dubousset, J.; Yamada, T.; Kimura, J. Pathogenesis of idiopathic scoliosis. Experimental study in rats. *Spine (Phila Pa 1976).* **1999**, *24*, 1985-1989.
222. Turgut, M.; Sargin, H.; Onol, B.; Açikgöz, B. Changes in end-plate vascularity after Nd: YAG laser application to the guinea pig intervertebral disc. *Acta Neurochir (Wien).* **1998**, *140*, 819-825; discussion 825-826.
223. Pedrini-Mille, A.; Weinstein, J. N.; Found, E. M.; Chung, C. B.; Goel,

V. K. Stimulation of dorsal root ganglia and degradation of rabbit annulus fibrosus. *Spine (Phila Pa 1976).* **1990**, *15*, 1252-1256.

224. Puustjärvi, K.; Lammi, M.; Helminen, H.; Inkinen, R.; Tammi, M. Proteoglycans in the intervertebral disc of young dogs following strenuous running exercise. *Connect Tissue Res.* **1994**, *30*, 225-240.
225. Puustjärvi, K.; Lammi, M.; Kiviranta, I.; Helminen, H. J.; Tammi, M. Proteoglycan synthesis in canine intervertebral discs after long-distance running training. *J Orthop Res.* **1993**, *11*, 738-746.
226. Säämänen, A. M.; Puustjärvi, K.; Ilves, K.; Lammi, M.; Kiviranta, I.; Jurvelin, J.; Helminen, H. J.; Tammi, M. Effect of running exercise on proteoglycans and collagen content in the intervertebral disc of young dogs. *Int J Sports Med.* **1993**, *14*, 48-51.
227. Lerer, A.; Nykamp, S. G.; Harriss, A. B.; Gibson, T. W.; Koch, T. G.; Brown, S. H. MRI-based relationships between spine pathology, intervertebral disc degeneration, and muscle fatty infiltration in chondrodystrophic and non-chondrodystrophic dogs. *Spine J.* **2015**, *15*, 2433-2439.
228. Smolders, L. A.; Bergknut, N.; Grinwis, G. C.; Hagman, R.; Lagerstedt, A. S.; Hazewinkel, H. A.; Tryfonidou, M. A.; Meij, B. P. Intervertebral disc degeneration in the dog. Part 2: chondrodystrophic and non-chondrodystrophic breeds. *Vet J.* **2013**, *195*, 292-299.
229. Bergknut, N.; Rutges, J. P.; Kranenburg, H. J.; Smolders, L. A.; Hagman, R.; Smidt, H. J.; Lagerstedt, A. S.; Penning, L. C.; Voorhout, G.; Hazewinkel, H. A.; Grinwis, G. C.; Creemers, L. B.; Meij, B. P.; Dhert, W. J. The dog as an animal model for intervertebral disc degeneration? *Spine (Phila Pa 1976).* **2012**, *37*, 351-358.
230. Ohnishi, T.; Sudo, H.; Tsujimoto, T.; Iwasaki, N. Age-related spontaneous lumbar intervertebral disc degeneration in a mouse model. *J Orthop Res.* **2018**, *36*, 224-232.
231. Tajerian, M.; Alvarado, S.; Millecamps, M.; Dashwood, T.; Anderson, K. M.; Haglund, L.; Ouellet, J.; Szyf, M.; Stone, L. S. DNA methylation of SPARC and chronic low back pain. *Mol Pain.* **2011**, *7*, 65.
232. Boyd, L. M.; Richardson, W. J.; Allen, K. D.; Flahiff, C.; Jing, L.; Li, Y.; Chen, J.; Setton, L. A. Early-onset degeneration of the intervertebral disc and vertebral end plate in mice deficient in type IX collagen. *Arthritis Rheum.* **2008**, *58*, 164-171.
233. van Ooij, A. Analysis of porous ingrowth in intervertebral disc prostheses: a nonhuman primate model. *Spine (Phila Pa 1976).* **2003**, *28*, 2304.
234. Modic, M. T.; Masaryk, T. J.; Ross, J. S.; Carter, J. R. Imaging of degenerative disk disease. *Radiology.* **1988**, *168*, 177-186.
235. Kimura, T.; Nakata, K.; Tsumaki, N.; Miyamoto, S.; Matsui, Y.; Ebara, S.; Ochi, T. Progressive degeneration of articular cartilage and intervertebral discs. An experimental study in transgenic mice bearing a type IX collagen mutation. *Int Orthop.* **1996**, *20*, 177-181.
236. Watanabe, H.; Nakata, K.; Kimata, K.; Nakanishi, I.; Yamada, Y. Dwarfism and age-associated spinal degeneration of heterozygote cmd mice defective in aggrecan. *Proc Natl Acad Sci U S A.* **1997**, *94*, 6943-6947.
237. Watanabe, H.; Yamada, Y. Chondrodysplasia of gene knockout mice for aggrecan and link protein. *Glycoconj J.* **2002**, *19*, 269-273.
238. Mason, R. M.; Palfrey, A. J. Intervertebral disc degeneration in adult mice with hereditary kyphoscoliosis. *J Orthop Res.* **1984**, *2*, 333-338.
239. Sahlman, J.; Inkinen, R.; Hirvonen, T.; Lammi, M. J.; Lammi, P. E.; Nieminen, J.; Lapveteläinen, T.; Prockop, D. J.; Arita, M.; Li, S. W.; Hyttinen, M. M.; Helminen, H. J.; Puustjärvi, K. Premature vertebral endplate ossification and mild disc degeneration in mice after inactivation of one allele belonging to the Col2a1 gene for type II collagen. *Spine (Phila Pa 1976).* **2001**, *26*, 2558-2565.
240. Hamrick, M. W.; Pennington, C.; Byron, C. D. Bone architecture and disc degeneration in the lumbar spine of mice lacking GDF-8 (myostatin). *J Orthop Res.* **2003**, *21*, 1025-1032.
241. Sweet, H. O.; Green, M. C. Progressive ankylosis, a new skeletal mutation in the mouse. *J Hered.* **1981**, *72*, 87-93.
242. Furuya, S.; Ohtsuki, T.; Yabe, Y.; Hosoda, Y. Ultrastructural study on calcification of cartilage: comparing ICR and twy mice. *J Bone Miner Metab.* **2000**, *18*, 140-147.
243. Hammer, R. E.; Maika, S. D.; Richardson, J. A.; Tang, J. P.; Taurog, J. D. Spontaneous inflammatory disease in transgenic rats expressing HLA-B27 and human beta 2m: an animal model of HLA-B27-associated human disorders. *Cell.* **1990**, *63*, 1099-1112.
244. Gruber, H. E.; Ashraf, N.; Kilburn, J.; Williams, C.; Norton, H. J.; Gordon, B. E.; Hanley, E. N., Jr. Vertebral endplate architecture and vascularization: application of micro-computerized tomography, a vascular tracer, and immunocytochemistry in analyses of disc degeneration in the aging sand rat. *Spine (Phila Pa 1976).* **2005**, *30*, 2593-2600.
245. Cole, T. C.; Ghosh, P.; Taylor, T. K. Variations of the proteoglycans of the canine intervertebral disc with ageing. *Biochim Biophys Acta.* **1986**, *880*, 209-219.
246. Ghosh, P.; Taylor, T. K.; Braund, K. G.; Larsen, L. H. The collagenous and non-collagenous protein of the canine intervertebral disc and their variation with age, spinal level and breed. *Gerontology.* **1976**, *22*, 124-134.
247. Melrose, J.; Taylor, T. K.; Ghosh, P. Variation in intervertebral disc serine proteinase inhibitory proteins with ageing in a chondrodystrophoid (beagle) and a non-chondrodystrophoid (greyhound) canine breed. *Gerontology.* **1996**, *42*, 322-329.
248. Togni, A.; Kranenburg, H. J.; Morgan, J. P.; Steffen, F. Radiographic and MRI characteristics of lumbar disseminated idiopathic spinal hyperostosis and spondylosis deformans in dogs. *J Small Anim Pract.* **2014**, *55*, 343-349.
249. Silberberg, R.; Gerritsen, G. Aging changes in intervertebral discs and spondylosis in Chinese hamsters. *Diabetes.* **1976**, *25*, 477-483.
250. Grootaert, M. O. J.; Finigan, A.; Figg, N. L.; Uryga, A. K.; Bennett, M. R. SIRT6 protects smooth muscle cells from senescence and reduces atherosclerosis. *Circ Res.* **2021**, *128*, 474-491.
251. Nasto, L. A.; Wang, D.; Robinson, A. R.; Clauson, C. L.; Ngo, K.; Dong, Q.; Roughley, P.; Epperly, M.; Huq, S. M.; Pola, E.; Sowa, G.; Robbins, P. D.; Kang, J.; Niedernhofer, L. J.; Vo, N. V. Genotoxic stress accelerates age-associated degenerative changes in intervertebral discs. *Mech Ageing Dev.* **2013**, *134*, 35-42.
252. Han, Y.; Zhou, C. M.; Shen, H.; Tan, J.; Dong, Q.; Zhang, L.; McGowan, S. J.; Zhao, J.; Sowa, G. A.; Kang, J. D.; Niedernhofer, L. J.; Robbins, P. D.; Vo, N. N. Attenuation of ataxia telangiectasia mutated signalling mitigates age-associated intervertebral disc degeneration. *Aging Cell.* **2020**, *19*, e13162.
253. Vo, N.; Seo, H. Y.; Robinson, A.; Sowa, G.; Bentley, D.; Taylor, L.; Studer, R.; Usas, A.; Huard, J.; Alber, S.; Watkins, S. C.; Lee, J.; Coehlo, P.; Wang, D.; Loppini, M.; Robbins, P. D.; Niedernhofer, L. J.; Kang, J. Accelerated aging of intervertebral discs in a mouse model of progeria. *J Orthop Res.* **2010**, *28*, 1600-1607.
254. Bradshaw, A. D.; Sage, E. H. SPARC, a matricellular protein that functions in cellular differentiation and tissue response to injury. *J Clin Invest.* **2001**, *107*, 1049-1054.
255. Millecamps, M.; Tajerian, M.; Sage, E. H.; Stone, L. S. Behavioral signs of chronic back pain in the SPARC-null mouse. *Spine (Phila Pa 1976).* **2011**, *36*, 95-102.

256. Millecamps, M.; Tajerian, M.; Naso, L.; Sage, H. E.; Stone, L. S. Lumbar intervertebral disc degeneration associated with axial and radiating low back pain in ageing SPARC-null mice. *Pain.* **2012**, *153*, 1167-1179.
257. Taunton, J. E.; Ryan, M. B.; Clement, D. B.; McKenzie, D. C.; Lloyd-Smith, D. R.; Zumbo, B. D. A retrospective case-control analysis of 2002 running injuries. *Br J Sports Med.* **2002**, *36*, 95-101.
258. Luoma, K.; Riihimäki, H.; Luukkonen, R.; Raininko, R.; Viikari-Juntura, E.; Lamminen, A. Low back pain in relation to lumbar disc degeneration. *Spine (Phila Pa 1976).* **2000**, *25*, 487-492.
259. Dubravcic-Simunjak, S.; Pecina, M.; Kuipers, H.; Moran, J.; Haspl, M. The incidence of injuries in elite junior figure skaters. *Am J Sports Med.* **2003**, *31*, 511-517.
260. Chen, S.; Lv, X.; Hu, B.; Zhao, L.; Li, S.; Li, Z.; Qing, X.; Liu, H.; Xu, J.; Shao, Z. Critical contribution of RIPK1 mediated mitochondrial dysfunction and oxidative stress to compression-induced rat nucleus pulposus cells necroptosis and apoptosis. *Apoptosis.* **2018**, *23*, 299-313.
261. Hu, Y.; Huang, L.; Shen, M.; Liu, Y.; Liu, G.; Wu, Y.; Ding, F.; Ma, K.; Wang, W.; Zhang, Y.; Shao, Z.; Cai, X.; Xiong, L. Pioglitazone protects compression-mediated apoptosis in nucleus pulposus mesenchymal stem cells by suppressing oxidative stress. *Oxid Med Cell Longev.* **2019**, *2019*, 4764071.
262. Huang, D.; Peng, Y.; Li, Z.; Chen, S.; Deng, X.; Shao, Z.; Ma, K. Compression-induced senescence of nucleus pulposus cells by promoting mitophagy activation via the PINK1/PARKIN pathway. *J Cell Mol Med.* **2020**, *24*, 5850-5864.
263. Xiang, Q.; Kang, L.; Wang, J.; Liao, Z.; Song, Y.; Zhao, K.; Wang, K.; Yang, C.; Zhang, Y. CircRNA-CIDN mitigated compression loading-induced damage in human nucleus pulposus cells via miR-34a-5p/SIRT1 axis. *EBioMedicine.* **2020**, *53*, 102679.
264. Lundin, O.; Ekström, L.; Hellström, M.; Holm, S.; Swärd, L. Exposure of the porcine spine to mechanical compression: differences in injury pattern between adolescents and adults. *Eur Spine J.* **2000**, **9**, 466-471.
265. Thoreson, O.; Baranto, A.; Ekström, L.; Holm, S.; Hellström, M.; Swärd, L. The immediate effect of repeated loading on the compressive strength of young porcine lumbar spine. *Knee Surg Sports Traumatol Arthrosc.* **2010**, *18*, 694-701.
266. Cassidy, J. D.; Yong-Hing, K.; Kirkaldy-Willis, W. H.; Wilkinson, A. A. A study of the effects of bipedism and upright posture on the lumbosacral spine and paravertebral muscles of the Wistar rat. *Spine (Phila Pa 1976).* **1988**, *13*, 301-308.
267. Peng, B.; Hou, S.; Shi, Q.; Jia, L. The relationship between cartilage end-plate calcification and disc degeneration: an experimental study. *Chin Med J (Engl).* **2001**, *114*, 308-312.
268. Stokes, I. A.; Counts, D. F.; Frymoyer, J. W. Experimental instability in the rabbit lumbar spine. *Spine (Phila Pa 1976). 1989*, *14*, 68-72.
269. Kaigle, A. M.; Holm, S. H.; Hansson, T. H. Experimental instability in the lumbar spine. *Spine (Phila Pa 1976).* **1995**, *20*, 421-430.
270. Hadjipavlou, A. G.; Simmons, J. W.; Yang, J. P.; Bi, L. X.; Ansari, G. A.; Kaphalia, B. S.; Simmons, D. J.; Nicodemus, C. L.; Necessary, J. T.; Lane, R.; Esch, O. Torsional injury resulting in disc degeneration: I. An in vivo rabbit model. *J Spinal Disord.* **1998**, *11*, 312-317.
271. Higuchi, M.; Abe, K.; Kaneda, K. Changes in the nucleus pulposus of the intervertebral disc in bipedal mice. A light and electron microscopic study. *Clin Orthop Relat Res.* **1983**, 251-257.
272. Hutton, W. C.; Yoon, S. T.; Elmer, W. A.; Li, J.; Murakami, H.; Minamide, A.; Akamaru, T. Effect of tail suspension (or simulated weightlessness) on the lumbar intervertebral disc: study of proteoglycans and collagen. *Spine (Phila Pa 1976).* **2002**, *27*, 1286-1290.
273. Stokes, I. A.; McBride, C. A.; Aronsson, D. D.; Roughley, P. J. Metabolic effects of angulation, compression, and reduced mobility on annulus fibrosis in a model of altered mechanical environment in scoliosis. *Spine Deform.* **2013**, *1*, 161-170.
274. Pedrini-Mille, A.; Maynard, J. A.; Durnova, G. N.; Kaplansky, A. S.; Pedrini, V. A.; Chung, C. B.; Fedler-Troester, J. Effects of microgravity on the composition of the intervertebral disk. *J Appl Physiol (1985).* **1992**, *73*, 26S-32S.
275. Bailey, J. F.; Hargens, A. R.; Cheng, K. K.; Lotz, J. C. Effect of microgravity on the biomechanical properties of lumbar and caudal intervertebral discs in mice. *J Biomech.* **2014**, *47*, 2983-2988.
276. Zheng, L.; Cao, Y.; Ni, S.; Qi, H.; Ling, Z.; Xu, X.; Zou, X.; Wu, T.; Deng, R.; Hu, B.; Gao, B.; Chen, H.; Li, Y.; Zhu, J.; Tintani, F.; Demehri, S.; Jain, A.; Kebaish, K. M.; Liao, S.; Séguin, C. A.; Crane, J. L.; Wan, M.; Lu, H.; Sponseller, P. D.; Riley, L. H., 3rd; Zhou, X.; Hu, J.; Cao, X. Ciliary parathyroid hormone signaling activates transforming growth factor-β to maintain intervertebral disc homeostasis during aging. *Bone Res.* **2018**, *6*, 21.
277. Xiao, Z. F.; Su, G. Y.; Hou, Y.; Chen, S. D.; Zhao, B. D.; He, J. B.; Zhang, J. H.; Chen, Y. J.; Lin, D. K. Mechanics and biology interact in intervertebral disc degeneration: a novel composite mouse model. *Calcif Tissue Int.* **2020**, *106*, 401-414.
278. Fu, F.; Bao, R.; Yao, S.; Zhou, C.; Luo, H.; Zhang, Z.; Zhang, H.; Li, Y.; Yan, S.; Yu, H.; Du, W.; Yang, Y.; Jin, H.; Tong, P.; Sun, Z. T.; Yue, M.; Chen, D.; Wu, C.; Ruan, H. Aberrant spinal mechanical loading stress triggers intervertebral disc degeneration by inducing pyroptosis and nerve ingrowth. *Sci Rep.* **2021**, *11*, 772.
279. Chen, L. H.; Lai, P. L.; Tai, C. L.; Niu, C. C.; Fu, T. S.; Chen, W. J. The effect of interspinous ligament integrity on adjacent segment instability after lumbar instrumentation and laminectomy--an experimental study in porcine model. *Biomed Mater Eng.* **2006**, *16*, 261-267.
280. Tai, C. L.; Hsieh, P. H.; Chen, W. P.; Chen, L. H.; Chen, W. J.; Lai, P. L. Biomechanical comparison of lumbar spine instability between laminectomy and bilateral laminotomy for spinal stenosis syndrome - an experimental study in porcine model. *BMC Musculoskelet Disord.* **2008**, *9*, 84.
281. Kim, J.; Yang, S. J.; Kim, H.; Kim, Y.; Park, J. B.; Dubose, C.; Lim, T. H. Effect of shear force on intervertebral disc (IVD) degeneration: an in vivo rat study. *Ann Biomed Eng.* **2012**, *40*, 1996-2004.
282. Xia, D. D.; Lin, S. L.; Wang, X. Y.; Wang, Y. L.; Xu, H. M.; Zhou, F.; Tan, J. Effects of shear force on intervertebral disc: an in vivo rabbit study. *Eur Spine J.* **2015**, *24*, 1711-1719.
283. Court, C.; Colliou, O. K.; Chin, J. R.; Liebenberg, E.; Bradford, D. S.; Lotz, J. C. The effect of static in vivo bending on the murine intervertebral disc. *Spine J.* **2001**, *1*, 239-245.
284. Gullbrand, S. E.; Peterson, J.; Ahlborn, J.; Mastropolo, R.; Fricker, A.; Roberts, T. T.; Abousayed, M.; Lawrence, J. P.; Glennon, J. C.; Ledet, E. H. ISSLS Prize Winner: dynamic loading-induced convective transport enhances intervertebral disc nutrition. *Spine (Phila Pa 1976).* **2015**, *40*, 1158-1164.
285. Holguin, N.; Uzer, G.; Chiang, F. P.; Rubin, C.; Judex, S. Brief daily exposure to low-intensity vibration mitigates the degradation of the intervertebral disc in a frequency-specific manner. *J Appl Physiol (1985).* **2011**, *111*, 1846-1853.
286. Yasuoka, H.; Asazuma, T.; Nakanishi, K.; Yoshihara, Y.; Sugihara, A.; Tomiya, M.; Okabayashi, T.; Nemoto, K. Effects of reloading after simulated microgravity on proteoglycan metabolism in the nucleus pulposus and anulus fibrosus of the lumbar intervertebral disc: an

experimental study using a rat tail suspension model. *Spine (Phila Pa 1976).* **2007**, *32*, E734-740.

287. Jensen, G. M. Biomechanics of the lumbar intervertebral disk: a review. *Phys Ther.* **1980**, *60*, 765-773.
288. Court, C.; Chin, J. R.; Liebenberg, E.; Colliou, O. K.; Lotz, J. C. Biological and mechanical consequences of transient intervertebral disc bending. *Eur Spine J.* **2007**, *16*, 1899-1906.
289. Barbir, A.; Godburn, K. E.; Michalek, A. J.; Lai, A.; Monsey, R. D.; Iatridis, J. C. Effects of torsion on intervertebral disc gene expression and biomechanics, using a rat tail model. *Spine (Phila Pa 1976).* **2011**, *36*, 607-614.
290. Lotz, J. C.; Colliou, O. K.; Chin, J. R.; Duncan, N. A.; Liebenberg, E. Compression-induced degeneration of the intervertebral disc: an in vivo mouse model and finite-element study. *Spine (Phila Pa 1976).* **1998**, *23*, 2493-2506.
291. Kawakami, M.; Hashizume, H.; Nishi, H.; Matsumoto, T.; Tamaki, T.; Kuribayashi, K. Comparison of neuropathic pain induced by the application of normal and mechanically compressed nucleus pulposus to lumbar nerve roots in the rat. *J Orthop Res.* **2003**, *21*, 535-539.
292. Liu, Z.; Zhou, Q.; Zheng, J.; Li, C.; Zhang, W.; Zhang, X. A novel in vivo mouse intervertebral disc degeneration model induced by compressive suture. *Exp Cell Res.* **2021**, *398*, 112359.
293. Hutton, W. C.; Toribatake, Y.; Elmer, W. A.; Ganey, T. M.; Tomita, K.; Whitesides, T. E. The effect of compressive force applied to the intervertebral disc in vivo. A study of proteoglycans and collagen. *Spine (Phila Pa 1976).* **1998**, *23*, 2524-2537.
294. Osterman, K.; Osterman, H. Experimental lumbar spondylolisthesis in growing rabbits. *Clin Orthop Relat Res.* **1996**, 274-280.
295. Lipson, S. J.; Muir, H. Vertebral osteophyte formation in experimental disc degeneration. Morphologic and proteoglycan changes over time. *Arthritis Rheum.* **1980**, *23*, 319-324.
296. Lipson, S. J.; Muir, H. 1980 Volvo award in basic science. Proteoglycans in experimental intervertebral disc degeneration. *Spine (Phila Pa 1976).* **1981**, *6*, 194-210.
297. Latorre, A.; Albareda, J.; Castiella, T.; Lasierra, J. M.; Seral, F. Experimental model of multidirectional disc hernia in rats. *Int Orthop.* **1998**, *22*, 44-48.
298. Kim, K. S.; Yoon, S. T.; Li, J.; Park, J. S.; Hutton, W. C. Disc degeneration in the rabbit: a biochemical and radiological comparison between four disc injury models. *Spine (Phila Pa 1976).* **2005**, *30*, 33-37.
299. Urayama, S. Histological and ultrastructural study of degeneration of the lumbar intervertebral disc in the rabbit following nucleotomy, with special reference to the topographical distribution pattern of the degeneration. *Nihon Seikeigeka Gakkai Zasshi.* **1986**, *60*, 649-662.
300. Takaishi, H.; Nemoto, O.; Shiota, M.; Kikuchi, T.; Yamada, H.; Yamagishi, M.; Yabe, Y. Type-II collagen gene expression is transiently upregulated in experimentally induced degeneration of rabbit intervertebral disc. *J Orthop Res.* **1997**, *15*, 528-538.
301. Melrose, J.; Ghosh, P.; Taylor, T. K.; Hall, A.; Osti, O. L.; Vernon-Roberts, B.; Fraser, R. D. A longitudinal study of the matrix changes induced in the intervertebral disc by surgical damage to the annulus fibrosus. *J Orthop Res.* **1992**, *10*, 665-676.
302. Melrose, J.; Ghosh, P.; Taylor, T. K.; Latham, J.; Moore, R. Topographical variation in the catabolism of aggrecan in an ovine annular lesion model of experimental disc degeneration. *J Spinal Disord.* **1997**, *10*, 55-67.
303. Melrose, J.; Taylor, T. K.; Ghosh, P. The serine proteinase inhibitory proteins of the chondrodystrophoid (beagle) and non-chondrodystrophoid (greyhound) canine intervertebral disc. *Electrophoresis.* **1997**, *18*, 1059-1063.
304. Fazzalari, N. L.; Costi, J. J.; Hearn, T. C.; Fraser, R. D.; Vernon-Roberts, B.; Hutchinson, J.; Manthey, B. A.; Parkinson, I. H.; Sinclair, C. Mechanical and pathologic consequences of induced concentric anular tears in an ovine model. *Spine (Phila Pa 1976).* **2001**, *26*, 2575-2581.
305. Schollum, M. L.; Appleyard, R. C.; Little, C. B.; Melrose, J. A detailed microscopic examination of alterations in normal anular structure induced by mechanical destabilization in an ovine model of disc degeneration. *Spine (Phila Pa 1976).* **2010**, *35*, 1965-1973.
306. Kaigle, A. M.; Holm, S. H.; Hansson, T. H. 1997 Volvo Award winner in biomechanical studies. Kinematic behavior of the porcine lumbar spine: a chronic lesion model. *Spine (Phila Pa 1976).* **1997**, *22*, 2796-2806.
307. Zhu, J.; Xia, K.; Yu, W.; Wang, Y.; Hua, J.; Liu, B.; Gong, Z.; Wang, J.; Xu, A.; You, Z.; Chen, Q.; Li, F.; Tao, H.; Liang, C. Sustained release of GDF5 from a designed coacervate attenuates disc degeneration in a rat model. *Acta Biomater.* **2019**, *86*, 300-311.
308. Olsewski, J. M.; Schendel, M. J.; Wallace, L. J.; Ogilvie, J. W.; Gundry, C. R. Magnetic resonance imaging and biological changes in injured intervertebral discs under normal and increased mechanical demands. *Spine (Phila Pa 1976).* **1996**, *21*, 1945-1951.
309. Aoki, Y.; Akeda, K.; An, H.; Muehleman, C.; Takahashi, K.; Moriya, H.; Masuda, K. Nerve fiber ingrowth into scar tissue formed following nucleus pulposus extrusion in the rabbit anular-puncture disc degeneration model: effects of depth of puncture. *Spine (Phila Pa 1976).* **2006**, *31*, E774-780.
310. Masuda, K.; Imai, Y.; Okuma, M.; Muehleman, C.; Nakagawa, K.; Akeda, K.; Thonar, E.; Andersson, G.; An, H. S. Osteogenic protein-1 injection into a degenerated disc induces the restoration of disc height and structural changes in the rabbit anular puncture model. *Spine (Phila Pa 1976).* **2006**, *31*, 742-754.
311. Mwale, F.; Masuda, K.; Pichika, R.; Epure, L. M.; Yoshikawa, T.; Hemmad, A.; Roughley, P. J.; Antoniou, J. The efficacy of Link N as a mediator of repair in a rabbit model of intervertebral disc degeneration. *Arthritis Res Ther.* **2011**, *13*, R120.
312. Liu, Y.; Lin, J.; Wu, X.; Guo, X.; Sun, H.; Yu, B.; Shen, J.; Bai, J.; Chen, Z.; Yang, H.; Geng, D.; Mao, H. Aspirin-mediated attenuation of intervertebral disc degeneration by ameliorating reactive oxygen species in vivo and in vitro. *Oxid Med Cell Longev.* **2019**, *2019*, 7189854.
313. Han, B.; Zhu, K.; Li, F. C.; Xiao, Y. X.; Feng, J.; Shi, Z. L.; Lin, M.; Wang, J.; Chen, Q. X. A simple disc degeneration model induced by percutaneous needle puncture in the rat tail. *Spine (Phila Pa 1976).* **2008**, *33*, 1925-1934.
314. Makino, H.; Seki, S.; Yahara, Y.; Shiozawa, S.; Aikawa, Y.; Motomura, H.; Nogami, M.; Watanabe, K.; Sainoh, T.; Ito, H.; Tsumaki, N.; Kawaguchi, Y.; Yamazaki, M.; Kimura, T. A selective inhibition of c-Fos/activator protein-1 as a potential therapeutic target for intervertebral disc degeneration and associated pain. *Sci Rep.* **2017**, *7*, 16983.
315. Henriksson, H. B.; Svanvik, T.; Jonsson, M.; Hagman, M.; Horn, M.; Lindahl, A.; Brisby, H. Transplantation of human mesenchymal stems cells into intervertebral discs in a xenogeneic porcine model. *Spine (Phila Pa 1976).* **2009**, *34*, 141-148.
316. van Heeswijk, V. M.; Thambyah, A.; Robertson, P. A.; Broom, N. D. Does an annular puncture influence the herniation path?: An in vitro mechanical and structural investigation. *Spine (Phila Pa 1976).* **2018**, *43*, 467-476.
317. Piazza, M.; Peck, S. H.; Gullbrand, S. E.; Bendigo, J. R.; Arginteanu, T.;

Zhang, Y.; Smith, H. E.; Malhotra, N. R.; Smith, L. J. Quantitative MRI correlates with histological grade in a percutaneous needle injury mouse model of disc degeneration. *J Orthop Res.* **2018**, *36*, 2771-2779.
318. Liang, H.; Ma, S. Y.; Feng, G.; Shen, F. H.; Joshua Li, X. Therapeutic effects of adenovirus-mediated growth and differentiation factor-5 in a mice disc degeneration model induced by annulus needle puncture. *Spine J.* **2010**, *10*, 32-41.
319. Hu, M. H.; Yang, K. C.; Chen, Y. J.; Sun, Y. H.; Lin, F. H.; Yang, S. H. Optimization of puncture injury to rat caudal disc for mimicking early degeneration of intervertebral disc. *J Orthop Res.* **2018**, *36*, 202-211.
320. Zhang, H.; La Marca, F.; Hollister, S. J.; Goldstein, S. A.; Lin, C. Y. Developing consistently reproducible intervertebral disc degeneration at rat caudal spine by using needle puncture. *J Neurosurg Spine.* **2009**, *10*, 522-530.
321. Hsieh, A. H.; Hwang, D.; Ryan, D. A.; Freeman, A. K.; Kim, H. Degenerative anular changes induced by puncture are associated with insufficiency of disc biomechanical function. *Spine (Phila Pa 1976).* **2009**, *34*, 998-1005.
322. Zhang, K. B.; Zheng, Z. M.; Liu, H.; Liu, X. G. The effects of punctured nucleus pulposus on lumbar radicular pain in rats: a behavioral and immunohistochemical study. *J Neurosurg Spine.* **2009**, *11*, 492-500.
323. Zhang, H.; Wang, L.; Park, J. B.; Park, P.; Yang, V. C.; Hollister, S. J.; La Marca, F.; Lin, C. Y. Intradiscal injection of simvastatin retards progression of intervertebral disc degeneration induced by stab injury. *Arthritis Res Ther.* **2009**, *11*, R172.
324. Sadamasu, A.; Sakuma, Y.; Suzuki, M.; Orita, S.; Yamauchi, K.; Inoue, G.; Aoki, Y.; Ishikawa, T.; Miyagi, M.; Kamoda, H.; Kubota, G.; Oikawa, Y.; Inage, K.; Sainoh, T.; Sato, J.; Nakamura, J.; Toyone, T.; Takahashi, K.; Ohtori, S. Upregulation of NaV1.7 in dorsal root ganglia after intervertebral disc injury in rats. *Spine (Phila Pa 1976).* **2014**, *39*, E421-426.
325. Sato, M.; Inage, K.; Sakuma, Y.; Sato, J.; Orita, S.; Yamauchi, K.; Eguchi, Y.; Ochiai, N.; Kuniyoshi, K.; Aoki, Y.; Nakamura, J.; Miyagi, M.; Suzuki, M.; Kubota, G.; Sainoh, T.; Fujimoto, K.; Shiga, Y.; Abe, K.; Kanamoto, H.; Inoue, G.; Takahashi, K.; Ohtori, S. Anti-RANKL antibodies decrease CGRP expression in dorsal root ganglion neurons innervating injured lumbar intervertebral discs in rats. *Eur Spine J.* **2015**, *24*, 2017-2022.
326. Horii, M.; Orita, S.; Nagata, M.; Takaso, M.; Yamauchi, K.; Yamashita, M.; Inoue, G.; Eguchi, Y.; Ochiai, N.; Kishida, S.; Aoki, Y.; Ishikawa, T.; Arai, G.; Miyagi, M.; Kamoda, H.; Kuniyoshi, K.; Suzuki, M.; Nakamura, J.; Toyone, T.; Takahashi, K.; Ohtori, S. Direct application of the tumor necrosis factor-α inhibitor, etanercept, into a punctured intervertebral disc decreases calcitonin gene-related peptide expression in rat dorsal root ganglion neurons. *Spine (Phila Pa 1976).* **2011**, *36*, E80-85.
327. Li, D.; Yang, H.; Huang, Y.; Wu, Y.; Sun, T.; Li, X. Lumbar intervertebral disc puncture under C-arm fluoroscopy: a new rat model of lumbar intervertebral disc degeneration. *Exp Anim.* **2014**, *63*, 227-234.
328. Liu, W.; Xia, P.; Feng, J.; Kang, L.; Huang, M.; Wang, K.; Song, Y.; Li, S.; Wu, X.; Yang, S.; Yang, C. MicroRNA-132 upregulation promotes matrix degradation in intervertebral disc degeneration. *Exp Cell Res.* **2017**, *359*, 39-49.
329. Liao, J. C. Cell therapy using bone marrow-derived stem cell overexpressing BMP-7 for degenerative discs in a rat tail disc model. *Int J Mol Sci.* **2016**, *17*, 147.
330. Tian, Z.; Ma, X.; Yasen, M.; Mauck, R. L.; Qin, L.; Shofer, F. S.; Smith, L. J.; Pacifici, M.; Enomoto-Iwamoto, M.; Zhang, Y. Intervertebral disc degeneration in a percutaneous mouse tail injury model. *Am J Phys Med Rehabil.* **2018**, *97*, 170-177.
331. Zhang, C.; Smith, M. P.; Zhou, G. K.; Lai, A.; Hoy, R. C.; Mroz, V.; Torre, O. M.; Laudier, D. M.; Bradley, E. W.; Westendorf, J. J.; Iatridis, J. C.; Illien-Jünger, S. Phlpp1 is associated with human intervertebral disc degeneration and its deficiency promotes healing after needle puncture injury in mice. *Cell Death Dis.* **2019**, *10*, 754.
332. Xiao, L.; Ding, M.; Zhang, Y.; Chordia, M.; Pan, D.; Shimer, A.; Shen, F.; Glover, D.; Jin, L.; Li, X. A novel modality for functional imaging in acute intervertebral disk herniation via tracking leukocyte infiltration. *Mol Imaging Biol.* **2017**, *19*, 703-713.
333. Tam, V.; Rogers, I.; Chan, D.; Leung, V. Y.; Cheung, K. M. A comparison of intravenous and intradiscal delivery of multipotential stem cells on the healing of injured intervertebral disk. *J Orthop Res.* **2014**, *32*, 819-825.
334. Yang, F.; Leung, V. Y.; Luk, K. D.; Chan, D.; Cheung, K. M. Injury-induced sequential transformation of notochordal nucleus pulposus to chondrogenic and fibrocartilaginous phenotype in the mouse. *J Pathol.* **2009**, *218*, 113-121.
335. Ohta, R.; Tanaka, N.; Nakanishi, K.; Kamei, N.; Nakamae, T.; Izumi, B.; Fujioka, Y.; Ochi, M. Heme oxygenase-1 modulates degeneration of the intervertebral disc after puncture in Bach 1 deficient mice. *Eur Spine J.* **2012**, *21*, 1748-1757.
336. Xin, L.; Xu, W.; Yu, L.; Fan, S.; Wang, W.; Yu, F.; Wang, Z. Effects of annulus defects and implantation of poly(lactic-co-glycolic acid) (PLGA)/fibrin gel scaffolds on nerves ingrowth in a rabbit model of annular injury disc degeneration. *J Orthop Surg Res.* **2017**, *12*, 73.
337. Sobajima, S.; Kompel, J. F.; Kim, J. S.; Wallach, C. J.; Robertson, D. D.; Vogt, M. T.; Kang, J. D.; Gilbertson, L. G. A slowly progressive and reproducible animal model of intervertebral disc degeneration characterized by MRI, X-ray, and histology. *Spine (Phila Pa 1976).* **2005**, *30*, 15-24.
338. Jacobs, L.; Vo, N.; Coelho, J. P.; Dong, Q.; Bechara, B.; Woods, B.; Hempen, E.; Hartman, R.; Preuss, H.; Balk, J.; Kang, J.; Sowa, G. Glucosamine supplementation demonstrates a negative effect on intervertebral disc matrix in an animal model of disc degeneration. *Spine (Phila Pa 1976).* **2013**, *38*, 984-990.
339. Xin, L.; Zhang, C.; Zhong, F.; Fan, S.; Wang, W.; Wang, Z. Minimal invasive annulotomy for induction of disc degeneration and implantation of poly (lactic-co-glycolic acid) (PLGA) plugs for annular repair in a rabbit model. *Eur J Med Res.* **2016**, *21*, 7.
340. Ashinsky, B. G.; Gullbrand, S. E.; Bonnevie, E. D.; Mandalapu, S. A.; Wang, C.; Elliott, D. M.; Han, L.; Mauck, R. L.; Smith, H. E. Multiscale and multimodal structure-function analysis of intervertebral disc degeneration in a rabbit model. *Osteoarthritis Cartilage.* **2019**, **27**, 1860-1869.
341. Shi, P.; Chee, A.; Liu, W.; Chou, P. H.; Zhu, J.; An, H. S. Therapeutic effects of cell therapy with neonatal human dermal fibroblasts and rabbit dermal fibroblasts on disc degeneration and inflammation. *Spine J.* **2019**, *19*, 171-181.
342. Zhou, R. P.; Zhang, Z. M.; Wang, L.; Huang, M. J.; Zheng, X. C.; Cui, Y. N.; Yin, M.; Wang, X. K.; Yao, N. Z.; Chen, T. Y.; Chen, J.; Bai, X. C.; Jin, D. D. Establishing a disc degeneration model using computed tomography-guided percutaneous puncture technique in the rabbit. *J Surg Res.* **2013**, *181*, e65-74.
343. Luo, T. D.; Marquez-Lara, A.; Zabarsky, Z. K.; Vines, J. B.; Mowry, K. C.; Jinnah, A. H.; Ma, X.; Berwick, B. W.; Willey, J. S.; Li, Z.; Smith, T. L.; O'Gara, T. J. A percutaneous, minimally invasive annulus fibrosus

needle puncture model of intervertebral disc degeneration in rabbits. *J Orthop Surg (Hong Kong).* **2018**, *26*, 2309499018792715.

344. Luo, T. D.; Vines, J. B.; Zabarsky, Z. K.; Mowry, K. C.; Marquez-Lara, A.; Jinnah, A. H.; Ma, X.; Berwick, B. W.; Willey, J. S.; Smith, T. L.; Li, Z.; O'Gara, T. J. Evaluation of percutaneous intradiscal amniotic suspension allograft in a rabbit model of intervertebral disc degeneration. *Spine (Phila Pa 1976).* **2019**, *44*, E329-E337.
345. Kim, D. W.; Chun, H. J.; Lee, S. K. Percutaneous needle puncture technique to create a rabbit model with traumatic degenerative disk disease. *World Neurosurg.* **2015**, *84*, 438-445.
346. Chun, H. J.; Kim, Y. S.; Kim, B. K.; Kim, E. H.; Kim, J. H.; Do, B. R.; Hwang, S. J.; Hwang, J. Y.; Lee, Y. K. Transplantation of human adipose-derived stem cells in a rabbit model of traumatic degeneration of lumbar discs. *World Neurosurg.* **2012**, *78*, 364-371.
347. Yang, H.; Wu, J.; Liu, J.; Ebraheim, M.; Castillo, S.; Liu, X.; Tang, T.; Ebraheim, N. A. Transplanted mesenchymal stem cells with pure fibrinous gelatin-transforming growth factor-beta1 decrease rabbit intervertebral disc degeneration. *Spine J.* **2010**, *10*, 802-810.
348. Chik, T. K.; Ma, X. Y.; Choy, T. H.; Li, Y. Y.; Diao, H. J.; Teng, W. K.; Han, S. J.; Cheung, K. M.; Chan, B. P. Photochemically crosslinked collagen annulus plug: a potential solution solving the leakage problem of cell-based therapies for disc degeneration. *Acta Biomater.* **2013**, *9*, 8128-8139.
349. Li, Z.; Zhang, K.; Li, X.; Pan, H.; Li, S.; Chen, F.; Zhang, J.; Zheng, Z.; Wang, J.; Liu, H. Wnt5a suppresses inflammation-driven intervertebral disc degeneration via a TNF-α/NF-κB-Wnt5a negative-feedback loop. *Osteoarthritis Cartilage.* **2018**, *26*, 966-977.
350. Elliott, D. M.; Yerramalli, C. S.; Beckstein, J. C.; Boxberger, J. I.; Johannessen, W.; Vresilovic, E. J. The effect of relative needle diameter in puncture and sham injection animal models of degeneration. *Spine (Phila Pa 1976).* **2008**, *33*, 588-596.
351. Chen, T.; Cheng, X.; Wang, J.; Feng, X.; Zhang, L. Time-Course investigation of intervertebral disc degeneration induced by different sizes of needle punctures in rat tail disc. *Med Sci Monit.* **2018**, *24*, 6456-6465.
352. Cunha, C.; Lamas, S.; Gonçalves, R. M.; Barbosa, M. A. Joint analysis of IVD herniation and degeneration by rat caudal needle puncture model. *J Orthop Res.* **2017**, *35*, 258-268.
353. Martin, J. T.; Gorth, D. J.; Beattie, E. E.; Harfe, B. D.; Smith, L. J.; Elliott, D. M. Needle puncture injury causes acute and long-term mechanical deficiency in a mouse model of intervertebral disc degeneration. *J Orthop Res.* **2013**, *31*, 1276-1282.
354. Omlor, G. W.; Lorenz, S.; Nerlich, A. G.; Guehring, T.; Richter, W. Disc cell therapy with bone-marrow-derived autologous mesenchymal stromal cells in a large porcine disc degeneration model. *Eur Spine J.* **2018**, *27*, 2639-2649.
355. Omlor, G. W.; Nerlich, A. G.; Lorenz, H.; Bruckner, T.; Richter, W.; Pfeiffer, M.; Gühring, T. Injection of a polymerized hyaluronic acid/collagen hydrogel matrix in an in vivo porcine disc degeneration model. *Eur Spine J.* **2012**, *21*, 1700-1708.
356. Omlor, G. W.; Nerlich, A. G.; Wilke, H. J.; Pfeiffer, M.; Lorenz, H.; Schaaf-Keim, M.; Bertram, H.; Richter, W.; Carstens, C.; Guehring, T. A new porcine in vivo animal model of disc degeneration: response of anulus fibrosus cells, chondrocyte-like nucleus pulposus cells, and notochordal nucleus pulposus cells to partial nucleotomy. *Spine (Phila Pa 1976).* **2009**, *34*, 2730-2739.
357. Yoon, S. H.; Miyazaki, M.; Hong, S. W.; Tow, B.; Morishita, Y.; Hu, M.; Ahn, S. J.; Wang, J. C. A porcine model of intervertebral disc degeneration induced by annular injury characterized with magnetic resonance imaging and histopathological findings. Laboratory investigation. *J Neurosurg Spine.* **2008**, *8*, 450-457.
358. Issy, A. C.; Castania, V.; Silveira, J. W.; Nogueira-Barbosa, M. H.; Salmon, C. E.; Del-Bel, E.; Defino, H. L. Does a small size needle puncture cause intervertebral disc changes? *Acta Cir Bras.* **2015**, *30*, 574-579.
359. Keorochana, G.; Johnson, J. S.; Taghavi, C. E.; Liao, J. C.; Lee, K. B.; Yoo, J. H.; Ngo, S. S.; Wang, J. C. The effect of needle size inducing degeneration in the rat caudal disc: evaluation using radiograph, magnetic resonance imaging, histology, and immunohistochemistry. *Spine J.* **2010**, *10*, 1014-1023.
360. Zhang, H.; Yang, S.; Wang, L.; Park, P.; La Marca, F.; Hollister, S. J.; Lin, C. Y. Time course investigation of intervertebral disc degeneration produced by needle-stab injury of the rat caudal spine: laboratory investigation. *J Neurosurg Spine.* **2011**, *15*, 404-413.
361. Yan, J.; Yang, S.; Sun, H.; Guo, D.; Wu, B.; Ji, F.; Zhou, D. Effects of releasing recombinant human growth and differentiation factor-5 from poly(lactic-co-glycolic acid) microspheres for repair of the rat degenerated intervertebral disc. *J Biomater Appl.* **2014**, *29*, 72-80.
362. Than, K. D.; Rahman, S. U.; Wang, L.; Khan, A.; Kyere, K. A.; Than, T. T.; Miyata, Y.; Park, Y. S.; La Marca, F.; Kim, H. M.; Zhang, H.; Park, P.; Lin, C. Y. Intradiscal injection of simvastatin results in radiologic, histologic, and genetic evidence of disc regeneration in a rat model of degenerative disc disease. *Spine J.* **2014**, *14*, 1017-1028.
363. Castania, V.; Issy, A. C.; Silveira, J. W.; Ferreira, F. R.; Titze-de-Almeida, S. S.; Resende, F. F.; Ferreira, N. R.; Titze-de-Almeida, R.; Defino, H. L.; Del Bel, E. The presence of the neuronal nitric oxide synthase isoform in the intervertebral disk. *Neurotox Res.* **2017**, *31*, 148-161.
364. Li, L.; Zhou, Z.; Li, J.; Fang, J.; Qing, Y.; Tian, T.; Zhang, S.; Wu, G.; Scotti, A.; Cai, K.; Zhu, W. Diffusion kurtosis imaging provides quantitative assessment of the microstructure changes of disc degeneration: an in vivo experimental study. *Eur Spine J.* **2019**, *28*, 1005-1013.
365. Zhan, S.; Wang, K.; Song, Y.; Li, S.; Yin, H.; Luo, R.; Liao, Z.; Wu, X.; Zhang, Y.; Yang, C. Long non-coding RNA HOTAIR modulates intervertebral disc degenerative changes via Wnt/β-catenin pathway. *Arthritis Res Ther.* **2019**, *21*, 201.
366. Zou, F.; Jiang, J.; Lu, F.; Ma, X.; Xia, X.; Wang, L.; Wang, H. Efficacy of intradiscal hepatocyte growth factor injection for the treatment of intervertebral disc degeneration. *Mol Med Rep.* **2013**, *8*, 118-122.
367. Grunert, P.; Hudson, K. D.; Macielak, M. R.; Aronowitz, E.; Borde, B. H.; Alimi, M.; Njoku, I.; Ballon, D.; Tsiouris, A. J.; Bonassar, L. J.; Härtl, R. Assessment of intervertebral disc degeneration based on quantitative magnetic resonance imaging analysis: an in vivo study. *Spine (Phila Pa 1976).* **2014**, *39*, E369-378.
368. Jiang, L. B.; Liu, H. X.; Zhou, Y. L.; Sheng, S. R.; Xu, H. Z.; Xue, E. X. An ultrastructural study of chondroptosis: programmed cell death in degenerative intervertebral discs in vivo. *J Anat.* **2017**, *231*, 129-139.
369. Chiang, E. R.; Ma, H. L.; Wang, J. P.; Chang, M. C.; Liu, C. L.; Chen, T. H.; Hung, S. C. Use of allogeneic hypoxic mesenchymal stem cells for treating disc degeneration in rabbits. *J Orthop Res.* **2019**, *37*, 1440-1450.
370. Li, Z.; Liu, H.; Yang, H.; Wang, J.; Wang, H.; Zhang, K.; Ding, W.; Zheng, Z. Both expression of cytokines and posterior annulus fibrosus rupture are essential for pain behavior changes induced by degenerative intervertebral disc: An experimental study in rats. *J Orthop Res.* **2014**, *32*, 262-272.

371. Ohnishi, T.; Sudo, H.; Iwasaki, K.; Tsujimoto, T.; Ito, Y. M.; Iwasaki, N. In vivo mouse intervertebral disc degeneration model based on a new histological classification. *PLoS One.* **2016**, *11*, e0160486.
372. Arai, I.; Mao, G. P.; Otani, K.; Konno, S.; Kikuchi, S.; Olmarker, K. Indomethacin blocks the nucleus pulposus-induced effects on nerve root function. An experimental study in dogs with assessment of nerve conduction and blood flow following experimental disc herniation. *Eur Spine J.* **2004**, *13*, 691-694.
373. Kawakami, M.; Matsumoto, T.; Tamaki, T. Roles of thromboxane A2 and leukotriene B4 in radicular pain induced by herniated nucleus pulposus. *J Orthop Res.* **2001**, *19*, 472-477.
374. Kiester, D. P.; Williams, J. M.; Andersson, G. B.; Thonar, E. J.; McNeill, T. W. The dose-related effect of intradiscal chymopapain on rabbit intervertebral discs. *Spine (Phila Pa 1976).* **1994**, *19*, 747-751.
375. Ushirozako, H.; Yoshida, G.; Togawa, D.; Omura, T.; Hasegawa, T.; Yamato, Y.; Banno, T.; Arima, H.; Oe, S.; Mihara, Y.; Yamada, T.; Natsume, T.; Ogawa, S.; Awaga, Y.; Takamatsu, H.; Matsuyama, Y. Brain activation in a cynomolgus macaque model of chymopapain-induced discogenic low back pain: a preliminary study. *Spine Surg Relat Res.* **2019**, *3*, 368-376.
376. Wardlaw, D.; Rithchie, I. K.; Sabboubeh, A. F.; Vavdha, M.; Downing, M.; Eastmond, C. J. Prospective randomized trial of chemonucleolysis compared with surgery for soft disc herniation with 1-year, intermediate, and long-term outcome: part II: the radiological outcome. *Spine (Phila Pa 1976).* **2013**, *38*, E1058-1064.
377. Haro, H.; Nishiga, M.; Ishii, D.; Shimomoto, T.; Kato, T.; Takenouchi, O.; Koyanagi, S.; Ohba, T.; Komori, H. Experimental chemonucleolysis with recombinant human matrix metalloproteinase 7 in human herniated discs and dogs. *Spine J.* **2014**, *14*, 1280-1290.
378. Ishibashi, K.; Iwai, H.; Koga, H. Chemonucleolysis with chondroitin sulfate ABC endolyase as a novel minimally invasive treatment for patients with lumbar intervertebral disc herniation. *J Spine Surg.* **2019**, *5*, S115-S121.
379. Wu, B.; Meng, C.; Wang, H.; Jia, C.; Zhao, Y. Changes of proteoglycan and collagen II of the adjacent intervertebral disc in the cervical instability models. *Biomed Pharmacother.* **2016**, *84*, 754-758.
380. Borem, R.; Walters, J.; Madeline, A.; Madeline, L.; Gill, S.; Easley, J.; Mercuri, J. Characterization of chondroitinase-induced lumbar intervertebral disc degeneration in a sheep model intended for assessing biomaterials. *J Biomed Mater Res A.* **2021**, *109*, 1232-1246.
381. Gullbrand, S. E.; Malhotra, N. R.; Schaer, T. P.; Zawacki, Z.; Martin, J. T.; Bendigo, J. R.; Milby, A. H.; Dodge, G. R.; Vresilovic, E. J.; Elliott, D. M.; Mauck, R. L.; Smith, L. J. A large animal model that recapitulates the spectrum of human intervertebral disc degeneration. *Osteoarthritis Cartilage.* **2017**, *25*, 146-156.
382. Boxberger, J. I.; Orlansky, A. S.; Sen, S.; Elliott, D. M. Reduced nucleus pulposus glycosaminoglycan content alters intervertebral disc dynamic viscoelastic mechanics. *J Biomech.* **2009**, *42*, 1941-1946.
383. Masters, K. S.; Shah, D. N.; Leinwand, L. A.; Anseth, K. S. Crosslinked hyaluronan scaffolds as a biologically active carrier for valvular interstitial cells. *Biomaterials.* **2005**, *26*, 2517-2525.
384. MacBarb, R. F.; Makris, E. A.; Hu, J. C.; Athanasiou, K. A. A chondroitinase-ABC and TGF-β1 treatment regimen for enhancing the mechanical properties of tissue-engineered fibrocartilage. *Acta Biomater.* **2013**, *9*, 4626-4634.
385. Huey, D. J.; Athanasiou, K. A. Maturational growth of self-assembled, functional menisci as a result of TGF-β1 and enzymatic chondroitinase-ABC stimulation. *Biomaterials.* **2011**, *32*, 2052-2058.
386. Jiang, E. Y.; Sloan, S. R., Jr.; Wipplinger, C.; Kirnaz, S.; Härtl, R.; Bonassar, L. J. Proteoglycan removal by chondroitinase ABC improves injectable collagen gel adhesion to annulus fibrosus. *Acta Biomater.* **2019**, *97*, 428-436.
387. Mahmoud, M.; Kokozidou, M.; Auffarth, A.; Schulze-Tanzil, G. The relationship between diabetes mellitus type II and intervertebral disc degeneration in diabetic rodent models: a systematic and comprehensive review. *Cells.* **2020**, *9*, 2208.
388. Piccirilli, M.; Tarantino, R.; Anichini, G.; Delfini, R. Multiple disc herniations in a type II diabetic patient: case report and review of the literature. *J Neurosurg Sci.* **2008**, *52*, 83-85.
389. Illien-Junger, S.; Grosjean, F.; Laudier, D. M.; Vlassara, H.; Striker, G. E.; Iatridis, J. C. Combined anti-inflammatory and anti-AGE drug treatments have a protective effect on intervertebral discs in mice with diabetes. *PLoS One.* **2013**, *8*, e64302.
390. Hanssen, N. M. J.; Teraa, M.; Scheijen, J.; Van de Waarenburg, M.; Gremmels, H.; Stehouwer, C. D. A.; Verhaar, M. C.; Schalkwijk, C. G. Plasma methylglyoxal levels are associated with amputations and mortality in severe limb ischemia patients with and without diabetes. *Diabetes Care.* **2021**, *44*, 157-163.
391. Cannata, F.; Vadalà, G.; Ambrosio, L.; Fallucca, S.; Napoli, N.; Papalia, R.; Pozzilli, P.; Denaro, V. Intervertebral disc degeneration: A focus on obesity and type 2 diabetes. *Diabetes Metab Res Rev.* **2020**, *36*, e3224.
392. Song, Y.; Wang, Y.; Zhang, Y.; Geng, W.; Liu, W.; Gao, Y.; Li, S.; Wang, K.; Wu, X.; Kang, L.; Yang, C. Advanced glycation end products regulate anabolic and catabolic activities via NLRP3-inflammasome activation in human nucleus pulposus cells. *J Cell Mol Med.* **2017**, *21*, 1373-1387.
393. Illien-Jünger, S.; Lu, Y.; Qureshi, S. A.; Hecht, A. C.; Cai, W.; Vlassara, H.; Striker, G. E.; Iatridis, J. C. Chronic ingestion of advanced glycation end products induces degenerative spinal changes and hypertrophy in aging pre-diabetic mice. *PLoS One.* **2015**, *10*, e0116625.
394. Wang, J.; Hu, J.; Chen, X.; Huang, C.; Lin, J.; Shao, Z.; Gu, M.; Wu, Y.; Tian, N.; Gao, W.; Zhou, Y.; Wang, X.; Zhang, X. BRD4 inhibition regulates MAPK, NF-κB signals, and autophagy to suppress MMP-13 expression in diabetic intervertebral disc degeneration. *FASEB J.* **2019**, *33*, 11555-11566.
395. Hu, Y.; Shao, Z.; Cai, X.; Liu, Y.; Shen, M.; Yao, Y.; Yuan, T.; Wang, W.; Ding, F.; Xiong, L. Mitochondrial pathway is involved in advanced glycation end products-induced apoptosis of rabbit annulus fibrosus cells. *Spine (Phila Pa 1976).* **2019**, *44*, E585-E595.
396. Luo, R.; Song, Y.; Liao, Z.; Yin, H.; Zhan, S.; Wang, K.; Li, S.; Li, G.; Ma, L.; Lu, S.; Zhang, Y.; Yang, C. Impaired calcium homeostasis via advanced glycation end products promotes apoptosis through endoplasmic reticulum stress in human nucleus pulposus cells and exacerbates intervertebral disc degeneration in rats. *FEBS J.* **2019**, *286*, 4356-4373.
397. Liao, Z.; Luo, R.; Li, G.; Song, Y.; Zhan, S.; Zhao, K.; Hua, W.; Zhang, Y.; Wu, X.; Yang, C. Exosomes from mesenchymal stem cells modulate endoplasmic reticulum stress to protect against nucleus pulposus cell death and ameliorate intervertebral disc degeneration in vivo. *Theranostics.* **2019**, *9*, 4084-4100.
398. Lee, M.; Kim, B. J.; Lim, E. J.; Back, S. K.; Lee, J. H.; Yu, S. W.; Hong, S. H.; Kim, J. H.; Lee, S. H.; Jung, W. W.; Sul, D.; Na, H. S. Complete Freund's adjuvant-induced intervertebral discitis as an animal model for discogenic low back pain. *Anesth Analg.* **2009**, *109*, 1287-1296.
399. Luan, S.; Wan, Q.; Luo, H.; Li, X.; Ke, S.; Lin, C.; Wu, Y.; Wu, S.; Ma, C. Running exercise alleviates pain and promotes cell proliferation in

a rat model of intervertebral disc degeneration. *Int J Mol Sci.* **2015**, *16*, 2130-2144.

400. Jung, W. W.; Kim, H. S.; Shon, J. R.; Lee, M.; Lee, S. H.; Sul, D.; Na, H. S.; Kim, J. H.; Kim, B. J. Intervertebral disc degeneration-induced expression of pain-related molecules: glial cell-derived neurotropic factor as a key factor. *J Neurosurg Anesthesiol.* **2011**, *23*, 329-334.
401. Oegema, T. R., Jr.; Johnson, S. L.; Aguiar, D. J.; Ogilvie, J. W. Fibronectin and its fragments increase with degeneration in the human intervertebral disc. *Spine (Phila Pa 1976).* **2000**, *25*, 2742-2747.
402. Tiaden, A. N.; Klawitter, M.; Lux, V.; Mirsaidi, A.; Bahrenberg, G.; Glanz, S.; Quero, L.; Liebscher, T.; Wuertz, K.; Ehrmann, M.; Richards, P. J. Detrimental role for human high temperature requirement serine protease A1 (HTRA1) in the pathogenesis of intervertebral disc (IVD) degeneration. *J Biol Chem.* **2012**, *287*, 21335-21345.
403. Schmidli, M. R.; Sadowska, A.; Cvitas, I.; Gantenbein, B.; Lischer, H. E. L.; Forterre, S.; Hitzl, W.; Forterre, F.; Wuertz-Kozak, K. Fibronectin fragments and inflammation during canine intervertebral disc disease. *Front Vet Sci.* **2020**, *7*, 547644.
404. Krock, E.; Rosenzweig, D. H.; Currie, J. B.; Bisson, D. G.; Ouellet, J. A.; Haglund, L. Toll-like Receptor Activation Induces Degeneration of Human Intervertebral Discs. *Sci Rep.* **2017**, *7*, 17184.
405. Liu, H. F.; Zhang, H.; Qiao, G. X.; Ning, B.; Hu, Y. L.; Wang, D. C.; Hu, Y. G. A novel rabbit disc degeneration model induced by fibronectin fragment. *Joint Bone Spine.* **2013**, *80*, 301-306.
406. Greg Anderson, D.; Li, X.; Tannoury, T.; Beck, G.; Balian, G. A fibronectin fragment stimulates intervertebral disc degeneration in vivo. *Spine (Phila Pa 1976).* **2003**, *28*, 2338-2345.
407. Khan, A. N.; Jacobsen, H. E.; Khan, J.; Filippi, C. G.; Levine, M.; Lehman, R. A., Jr.; Riew, K. D.; Lenke, L. G.; Chahine, N. O. Inflammatory biomarkers of low back pain and disc degeneration: a review. *Ann N Y Acad Sci.* **2017**, *1410*, 68-84.
408. Cosamalón-Gan, I.; Cosamalón-Gan, T.; Mattos-Piaggio, G.; Villar-Suárez, V.; García-Cosamalón, J.; Vega-Álvarez, J. A. Inflammation in the intervertebral disc herniation. *Neurocirugia (Astur : Engl Ed).* **2021**, *32*, 21-35.
409. Kim, H.; Hong, J. Y.; Lee, J.; Jeon, W. J.; Ha, I. H. IL-1β promotes disc degeneration and inflammation through direct injection of intervertebral disc in a rat lumbar disc herniation model. *Spine J.* **2021**, *21*, 1031-1041.
410. Glant, T. T.; Mikecz, K.; Arzoumanian, A.; Poole, A. R. Proteoglycan-induced arthritis in BALB/c mice. Clinical features and histopathology. *Arthritis Rheum.* **1987**, *30*, 201-212.
411. Mikecz, K.; Glant, T. T.; Poole, A. R. Immunity to cartilage proteoglycans in BALB/c mice with progressive polyarthritis and ankylosing spondylitis induced by injection of human cartilage proteoglycan. *Arthritis Rheum.* **1987**, *30*, 306-318.
412. Leroux, J. Y.; Guerassimov, A.; Cartman, A.; Delaunay, N.; Webber, C.; Rosenberg, L. C.; Banerjee, S.; Poole, A. R. Immunity to the G1 globular domain of the cartilage proteoglycan aggrecan can induce inflammatory erosive polyarthritis and spondylitis in BALB/c mice but immunity to G1 is inhibited by covalently bound keratan sulfate in vitro and in vivo. *J Clin Invest.* **1996**, *97*, 621-632.
413. Shi, S.; Ciurli, C.; Cartman, A.; Pidoux, I.; Poole, A. R.; Zhang, Y. Experimental immunity to the G1 domain of the proteoglycan versican induces spondylitis and sacroiliitis, of a kind seen in human spondylarthropathies. *Arthritis Rheum.* **2003**, *48*, 2903-2915.
414. Tseng, H. W.; Glant, T. T.; Brown, M. A.; Kenna, T. J.; Thomas, G. P.; Pettit, A. R. Early anti-inflammatory intervention ameliorates axial disease in the proteoglycan-induced spondylitis mouse model of ankylosing spondylitis. *BMC Musculoskelet Disord.* **2017**, *18*, 228.
415. Zhou, C.; Cha, T.; Wang, W.; Guo, R.; Li, G. Investigation of alterations in the lumbar disc biomechanics at the adjacent segments after spinal fusion using a combined in vivo and in silico approach. *Ann Biomed Eng.* **2021**, *49*, 601-616.
416. Oppenheimer, J. H.; DeCastro, I.; McDonnell, D. E. Minimally invasive spine technology and minimally invasive spine surgery: a historical review. *Neurosurg Focus.* **2009**, *27*, E9.
417. Loenen, A. C. Y.; Noriega, D. C.; Ruiz Wills, C.; Noailly, J.; Nunley, P. D.; Kirchner, R.; Ito, K.; van Rietbergen, B. Misaligned spinal rods can induce high internal forces consistent with those observed to cause screw pullout and disc degeneration. *Spine J.* **2021**, *21*, 528-537.
418. Liu, Y.; Luo, X.; Zhou, J.; Li, N.; Peng, S.; Rong, P.; Wang, W. Prognosis of posterior osteophyte after anterior cervical decompression and fusion in patients with cervical spondylotic myelopathy using three-dimensional computed tomography study. *Eur Spine J.* **2016**, *25*, 1861-1868.
419. Phillips, F. M.; Reuben, J.; Wetzel, F. T. Intervertebral disc degeneration adjacent to a lumbar fusion. An experimental rabbit model. *J Bone Joint Surg Br.* **2002**, *84*, 289-294.
420. Foster, M. R.; Allen, M. J.; Schoonmaker, J. E.; Yuan, H. A.; Kanazawa, A.; Park, S. A.; Liu, B. Characterization of a developing lumbar arthrodesis in a sheep model with quantitative instability. *Spine J.* **2002**, *2*, 244-250.
421. Holmes, C.; Elder, B. D.; Ishida, W.; Perdomo-Pantoja, A.; Locke, J.; Cottrill, E.; Lo, S. L.; Witham, T. F. Comparing the efficacy of syngeneic iliac and femoral allografts with iliac crest autograft in a rat model of lumbar spinal fusion. *J Orthop Surg Res.* **2020**, *15*, 410.
422. Kroeber, M.; Unglaub, F.; Guehring, T.; Nerlich, A.; Hadi, T.; Lotz, J.; Carstens, C. Effects of controlled dynamic disc distraction on degenerated intervertebral discs: an in vivo study on the rabbit lumbar spine model. *Spine (Phila Pa 1976).* **2005**, *30*, 181-187.
423. Pearce, R. H.; Grimmer, B. J.; Adams, M. E. Degeneration and the chemical composition of the human lumbar intervertebral disc. *J Orthop Res.* **1987**, *5*, 198-205.
424. Huang, Y. C.; Xiao, J.; Leung, V. Y.; Lu, W. W.; Hu, Y.; Luk, K. D. K. Lumbar intervertebral disc allograft transplantation: the revascularisation pattern. *Eur Spine J.* **2018**, *27*, 728-736.
425. Flouzat-Lachaniette, C. H.; Jullien, N.; Bouthors, C.; Beohou, E.; Laurent, B.; Bierling, P.; Dubory, A.; Rouard, H. A novel in vivo porcine model of intervertebral disc degeneration induced by cryoinjury. *Int Orthop.* **2018**, *42*, 2263-2272.
426. Holm, S.; Baranto, A.; Kaigle Holm, A.; Ekström, L.; Swärd, L.; Hansson, T.; Hansson, H. A. Reactive changes in the adolescent porcine spine with disc degeneration due to endplate injury. *Vet Comp Orthop Traumatol.* **2007**, *20*, 12-17.
427. Kawchuk, G. N.; Kaigle, A. M.; Holm, S. H.; Rod Fauvel, O.; Ekström, L.; Hansson, T. The diagnostic performance of vertebral displacement measurements derived from ultrasonic indentation in an in vivo model of degenerative disc disease. *Spine (Phila Pa 1976).* **2001**, *26*, 1348-1355.
428. Yuan, W.; Che, W.; Jiang, Y. Q.; Yuan, F. L.; Wang, H. R.; Zheng, G. L.; Li, X. L.; Dong, J. Establishment of intervertebral disc degeneration model induced by ischemic sub-endplate in rat tail. *Spine J.* **2015**, *15*, 1050-1059.
429. Yin, S.; Du, H.; Zhao, W.; Ma, S.; Zhang, M.; Guan, M.; Liu, M. Inhibition of both endplate nutritional pathways results in intervertebral disc degeneration in a goat model. *J Orthop Surg Res.* **2019**,

14, 138.
430. Peng, B.; Wu, W.; Hou, S.; Li, P.; Zhang, C.; Yang, Y. The pathogenesis of discogenic low back pain. *J Bone Joint Surg Br.* **2005**, *87*, 62-67.
431. Fagan, A. B.; Sarvestani, G.; Moore, R. J.; Fraser, R. D.; Vernon-Roberts, B.; Blumbergs, P. C. Innervation of anulus tears: an experimental animal study. *Spine (Phila Pa 1976).* **2010**, *35*, 1200-1205.
432. Freemont, A. J.; Watkins, A.; Le Maitre, C.; Baird, P.; Jeziorska, M.; Knight, M. T.; Ross, E. R.; O'Brien, J. P.; Hoyland, J. A. Nerve growth factor expression and innervation of the painful intervertebral disc. *J Pathol.* **2002**, *197*, 286-292.
433. Stefanakis, M.; Al-Abbasi, M.; Harding, I.; Pollintine, P.; Dolan, P.; Tarlton, J.; Adams, M. A. Annulus fissures are mechanically and chemically conducive to the ingrowth of nerves and blood vessels. *Spine (Phila Pa 1976).* **2012**, *37*, 1883-1891.
434. Johnson, W. E.; Sivan, S.; Wright, K. T.; Eisenstein, S. M.; Maroudas, A.; Roberts, S. Human intervertebral disc cells promote nerve growth over substrata of human intervertebral disc aggrecan. *Spine (Phila Pa 1976).* **2006**, *31*, 1187-1193.
435. Melrose, J.; Roberts, S.; Smith, S.; Menage, J.; Ghosh, P. Increased nerve and blood vessel ingrowth associated with proteoglycan depletion in an ovine anular lesion model of experimental disc degeneration. *Spine (Phila Pa 1976).* **2002**, *27*, 1278-1285.
436. Shi, C.; Das, V.; Li, X.; Kc, R.; Qiu, S.; I, O. S.; Ripper, R. L.; Kroin, J. S.; Mwale, F.; Wallace, A. A.; Zhu, B.; Zhao, L.; van Wijnen, A. J.; Ji, M.; Lu, J.; Votta-Velis, G.; Yuan, W.; Im, H. J. Development of an in vivo mouse model of discogenic low back pain. *J Cell Physiol.* **2018**, *233*, 6589-6602.
437. McMorran, J. G.; Gregory, D. E. The influence of axial compression on the cellular and mechanical function of spinal tissues; emphasis on the nucleus pulposus and annulus fibrosus: a review. *J Biomech Eng.* **2021**, *143*, 050802.
438. Borem, R.; Madeline, A.; Vela, R., Jr.; Gill, S.; Mercuri, J. Multi-laminate annulus fibrosus repair scaffold with an interlamellar matrix enhances impact resistance, prevents herniation and assists in restoring spinal kinematics. *J Mech Behav Biomed Mater.* **2019**, *95*, 41-52.
439. Torre, O. M.; Evashwick-Rogler, T. W.; Nasser, P.; Iatridis, J. C. Biomechanical test protocols to detect minor injury effects in intervertebral discs. *J Mech Behav Biomed Mater.* **2019**, *95*, 13-20.
440. 440. Li, J.; Yuan, X.; Li, F.; Wang, F.; Li, Y.; Wang, E.; Yang, X.; Xiang, Y.; Song, E. A novel full endoscopic annular repair technique combined with autologous conditioned plasma intradiscal injection: a new safe serial therapeutic model for the treatment of lumbar disc herniation. *Ann Palliat Med.* **2021**, *10*, 292-301.
441. Ren, C.; Qin, R.; Li, Y.; Wang, P. Microendoscopic discectomy combined with annular suture versus percutaneous transforaminal endoscopic discectomy for lumbar disc herniation: a prospective observational study. *Pain Physician.* **2020**, *23*, E713-E721.
442. Miller, L. E.; McGirt, M. J.; Garfin, S. R.; Bono, C. M. Association of annular defect width after lumbar discectomy with risk of symptom recurrence and reoperation: systematic review and meta-analysis of comparative studies. *Spine (Phila Pa 1976).* **2018**, *43*, E308-E315.
443. Peredo, A. P.; Gullbrand, S. E.; Smith, H. E.; Mauck, R. L. Putting the pieces in place: mobilizing cellular players to improve annulus fibrosus repair. *Tissue Eng Part B Rev.* **2020**. doi: 10.1089/ten.TEB.2020.0196.
444. Lequin, M. B.; Barth, M.; Thomė, C.; Bouma, G. J. Primary limited lumbar discectomy with an annulus closure device: one-year clinical and radiographic results from a prospective, multi-center study. *Korean J Spine.* **2012**, *9*, 340-347.
445. Strenge, K. B.; DiPaola, C. P.; Miller, L. E.; Hill, C. P.; Whitmore, R. G. Multicenter study of lumbar discectomy with Barricaid annular closure device for prevention of lumbar disc reherniation in US patients: A historically controlled post-market study protocol. *Medicine (Baltimore).* **2019**, *98*, e16953.
446. Kienzler, J. C.; Fandino, J.; Van de Kelft, E.; Eustacchio, S.; Bouma, G. J. Risk factors for early reherniation after lumbar discectomy with or without annular closure: results of a multicenter randomized controlled study. *Acta Neurochir (Wien).* **2021**, *163*, 259-268.
447. Miller, L. E.; Allen, R. T.; Duhon, B.; Radcliff, K. E. Expert review with meta-analysis of randomized and nonrandomized controlled studies of Barricaid annular closure in patients at high risk for lumbar disc reherniation. *Expert Rev Med Devices.* **2020**, *17*, 461-469.
448. Thomé, C.; Klassen, P. D.; Bouma, G. J.; Kuršumović, A.; Fandino, J.; Barth, M.; Arts, M.; van den Brink, W.; Bostelmann, R.; Hegewald, A.; Heidecke, V.; Vajkoczy, P.; Fröhlich, S.; Wolfs, J.; Assaker, R.; Van de Kelft, E.; Köhler, H. P.; Jadik, S.; Eustacchio, S.; Hes, R.; Martens, F. Annular closure in lumbar microdiscectomy for prevention of reherniation: a randomized clinical trial. *Spine J.* **2018**, *18*, 2278-2287.
449. Choy, W. J.; Phan, K.; Diwan, A. D.; Ong, C. S.; Mobbs, R. J. Annular closure device for disc herniation: meta-analysis of clinical outcome and complications. *BMC Musculoskelet Disord.* **2018**, *19*, 290.
450. Bailey, A.; Araghi, A.; Blumenthal, S.; Huffmon, G. V. Prospective, multicenter, randomized, controlled study of anular repair in lumbar discectomy: two-year follow-up. *Spine (Phila Pa 1976).* **2013**, *38*, 1161-1169.
451. Bouma, G. J.; Ardeshiri, A.; Miller, L. E.; Van de Kelft, E.; Bostelmann, R.; Klassen, P. D.; Flüh, C.; Kuršumović, A. Clinical performance of a bone-anchored annular closure device in older adults. *Clin Interv Aging.* **2019**, *14*, 1085-1094.
452. Likhitpanichkul, M.; Dreischarf, M.; Illien-Junger, S.; Walter, B. A.; Nukaga, T.; Long, R. G.; Sakai, D.; Hecht, A. C.; Iatridis, J. C. Fibrin-genipin adhesive hydrogel for annulus fibrosus repair: performance evaluation with large animal organ culture, in situ biomechanics, and in vivo degradation tests. *Eur Cell Mater.* **2014**, *28*, 25-37; discussion 37-38.
453. DiStefano, T. J.; Shmukler, J. O.; Danias, G.; Di Pauli von Treuheim, T.; Hom, W. W.; Goldberg, D. A.; Laudier, D. M.; Nasser, P. R.; Hecht, A. C.; Nicoll, S. B.; Iatridis, J. C. Development of a two-part biomaterial adhesive strategy for annulus fibrosus repair and ex vivo evaluation of implant herniation risk. *Biomaterials.* **2020**, *258*, 120309.
454. Ghobril, C.; Grinstaff, M. W. The chemistry and engineering of polymeric hydrogel adhesives for wound closure: a tutorial. *Chem Soc Rev.* **2015**, *44*, 1820-1835.
455. Chapter 1 - Introduction and Adhesion Theories. In *Adhesives Technology Handbook (Second Edition)*, Ebnesajjad, S., ed. William Andrew Publishing: Norwich, NY, **2009**; pp 1-19.
456. Li, X.; Wang, Y.; Xu, F.; Zhang, F.; Xu, Y.; Tang, L.; Webster, T. J. Artemisinin loaded mPEG-PCL nanoparticle based photosensitive gelatin methacrylate hydrogels for the treatment of gentamicin induced hearing loss. *Int J Nanomedicine.* **2020**, *15*, 4591-4606.
457. Ügdüler, S.; De Somer, T.; Van Geem, K. M.; Roosen, M.; Kulawig, A.; Leineweber, R.; De Meester, S. Towards a better understanding of delamination of multilayer flexible packaging films by carboxylic acids. *ChemSusChem.* **2021**. doi: 10.1002/cssc.202002877.
458. Benz, K.; Stippich, C.; Fischer, L.; Möhl, K.; Weber, K.; Lang, J.; Steffen, F.; Beintner, B.; Gaissmaier, C.; Mollenhauer, J. A. Intervertebral disc cell- and hydrogel-supported and spontaneous intervertebral disc repair in nucleotomized sheep. *Eur Spine J.* **2012**, *21*,

1758-1768.

459. Tsujimoto, T.; Sudo, H.; Todoh, M.; Yamada, K.; Iwasaki, K.; Ohnishi, T.; Hirohama, N.; Nonoyama, T.; Ukeba, D.; Ura, K.; Ito, Y. M.; Iwasaki, N. An acellular bioresorbable ultra-purified alginate gel promotes intervertebral disc repair: A preclinical proof-of-concept study. *EBioMedicine.* **2018**, *37*, 521-534.
460. Doench, I.; Ahn Tran, T.; David, L.; Montembault, A.; Viguier, E.; Gorzelanny, C.; Sudre, G.; Cachon, T.; Louback-Mohamed, M.; Horbelt, N.; Peniche-Covas, C.; Osorio-Madrazo, A. Cellulose nanofiber-reinforced chitosan hydrogel composites for intervertebral disc tissue repair. *Biomimetics (Basel).* **2019**, *4*, 19.
461. Long, R. G.; Zderic, I.; Gueorguiev, B.; Ferguson, S. J.; Alini, M.; Grad, S.; Iatridis, J. C. Effects of level, loading rate, injury and repair on biomechanical response of ovine cervical intervertebral discs. *Ann Biomed Eng.* **2018**, *46*, 1911-1920.
462. Fujii, K.; Lai, A.; Korda, N.; Hom, W. W.; Evashwick-Rogler, T. W.; Nasser, P.; Hecht, A. C.; Iatridis, J. C. Ex-vivo biomechanics of repaired rat intervertebral discs using genipin crosslinked fibrin adhesive hydrogel. *J Biomech.* **2020**, *113*, 110100.
463. Peng, Y.; Huang, D.; Li, J.; Liu, S.; Qing, X.; Shao, Z. Genipin-crosslinked decellularized annulus fibrosus hydrogels induces tissue-specific differentiation of bone mesenchymal stem cells and intervertebral disc regeneration. *J Tissue Eng Regen Med.* **2020**, *14*, 497-509.
464. Cruz, M. A.; McAnany, S.; Gupta, N.; Long, R. G.; Nasser, P.; Eglin, D.; Hecht, A. C.; Illien-Junger, S.; Iatridis, J. C. Structural and chemical modification to improve adhesive and material properties of fibrin-genipin for repair of annulus fibrosus defects in intervertebral disks. *J Biomech Eng.* **2017**, *139*, 0845011-0845017.
465. Sharabi, M.; Wertheimer, S.; Wade, K. R.; Galbusera, F.; Benayahu, D.; Wilke, H. J.; Haj-Ali, R. Towards intervertebral disc engineering: Bio-mimetics of form and function of the annulus fibrosus lamellae. *J Mech Behav Biomed Mater.* **2019**, *94*, 298-307.
466. Shamsah, A. H.; Cartmell, S. H.; Richardson, S. M.; Bosworth, L. A. Tissue engineering the annulus fibrosus using 3D rings of electrospun PCL:PLLA angle-ply nanofiber sheets. *Front Bioeng Biotechnol.* **2019**, *7*, 437.
467. Gluais, M.; Clouet, J.; Fusellier, M.; Decante, C.; Moraru, C.; Dutilleul, M.; Veziers, J.; Lesoeur, J.; Dumas, D.; Abadie, J.; Hamel, A.; Bord, E.; Chew, S. Y.; Guicheux, J.; Le Visage, C. In vitro and in vivo evaluation of an electrospun-aligned microfibrous implant for annulus fibrosus repair. *Biomaterials.* **2019**, *205*, 81-93.
468. Tavakoli, J.; Elliott, D. M.; Costi, J. J. The ultra-structural organization of the elastic network in the intra- and inter-lamellar matrix of the intervertebral disc. *Acta Biomater.* **2017**, *58*, 269-277.
469. Park, S. H.; Gil, E. S.; Mandal, B. B.; Cho, H.; Kluge, J. A.; Min, B. H.; Kaplan, D. L. Annulus fibrosus tissue engineering using lamellar silk scaffolds. *J Tissue Eng Regen Med.* **2012**, *6* Suppl 3, s24-33.
470. Bhattacharjee, M.; Miot, S.; Gorecka, A.; Singha, K.; Loparic, M.; Dickinson, S.; Das, A.; Bhavesh, N. S.; Ray, A. R.; Martin, I.; Ghosh, S. Oriented lamellar silk fibrous scaffolds to drive cartilage matrix orientation: towards annulus fibrosus tissue engineering. *Acta Biomater.* **2012**, *8*, 3313-3325.
471. Bhunia, B. K.; Kaplan, D. L.; Mandal, B. B. Silk-based multilayered angle-ply annulus fibrosus construct to recapitulate form and function of the intervertebral disc. *Proc Natl Acad Sci U S A.* **2018**, *115*, 477-482.
472. Bowles, R. D.; Gebhard, H. H.; Härtl, R.; Bonassar, L. J. Tissue-engineered intervertebral discs produce new matrix, maintain disc height, and restore biomechanical function to the rodent spine. *Proc Natl Acad Sci U S A.* **2011**, *108*, 13106-13111.
473. De Pieri, A.; Byerley, A. M.; Musumeci, C. R.; Salemizadehparizi, F.; Vanderhorst, M. A.; Wuertz-Kozak, K. Electrospinning and 3D bioprinting for intervertebral disc tissue engineering. *JOR Spine.* **2020**, *3*, e1117.
474. Beckett, L. E.; Lewis, J. T.; Tonge, T. K.; Korley, L. T. J. Enhancement of the mechanical properties of hydrogels with continuous fibrous reinforcement. *ACS Biomater Sci Eng.* **2020**, *6*, 5453-5473.
475. Alexeev, D.; Cui, S.; Grad, S.; Li, Z.; Ferguson, S. J. Mechanical and biological characterization of a composite annulus fibrosus repair strategy in an endplate delamination model. *JOR Spine.* **2020**, *3*, e1107.
476. Xiao, L.; Wu, M.; Yan, F.; Xie, Y.; Liu, Z.; Huang, H.; Yang, Z.; Yao, S.; Cai, L. A radial 3D polycaprolactone nanofiber scaffold modified by biomineralization and silk fibroin coating promote bone regeneration in vivo. *Int J Biol Macromol.* **2021**, *172*, 19-29.
477. Liu, W.; Thomopoulos, S.; Xia, Y. Electrospun nanofibers for regenerative medicine. *Adv Healthc Mater.* **2012**, *1*, 10-25.
478. Parham, S.; Kharazi, A. Z.; Bakhsheshi-Rad, H. R.; Ghayour, H.; Ismail, A. F.; Nur, H.; Berto, F. Electrospun nano-fibers for biomedical and tissue engineering applications: a comprehensive review. *Materials (Basel).* **2020**, *13*, 2153.
479. Zhou, P.; Chu, G.; Yuan, Z.; Wang, H.; Zhang, W.; Mao, Y.; Zhu, X.; Chen, W.; Yang, H.; Li, B. Regulation of differentiation of annulus fibrosus-derived stem cells using heterogeneous electrospun fibrous scaffolds. *J Orthop Translat.* **2021**, *26*, 171-180.
480. Ma, J.; He, Y.; Liu, X.; Chen, W.; Wang, A.; Lin, C. Y.; Mo, X.; Ye, X. A novel electrospun-aligned nanoyarn/three-dimensional porous nanofibrous hybrid scaffold for annulus fibrosus tissue engineering. *Int J Nanomedicine.* **2018**, *13*, 1553-1567.
481. Xu, H.; Xu, B.; Yang, Q.; Li, X.; Ma, X.; Xia, Q.; Zhang, Y.; Zhang, C.; Wu, Y.; Zhang, Y. Comparison of decellularization protocols for preparing a decellularized porcine annulus fibrosus scaffold. *PLoS One.* **2014**, *9*, e86723.
482. Saldin, L. T.; Cramer, M. C.; Velankar, S. S.; White, L. J.; Badylak, S. F. Extracellular matrix hydrogels from decellularized tissues: Structure and function. *Acta Biomater.* **2017**, *49*, 1-15.
483. D'Este, M.; Eglin, D.; Alini, M. Lessons to be learned and future directions for intervertebral disc biomaterials. *Acta Biomater.* **2018**, *78*, 13-22.
484. McGuire, R.; Borem, R.; Mercuri, J. The fabrication and characterization of a multi-laminate, angle-ply collagen patch for annulus fibrosus repair. *J Tissue Eng Regen Med.* **2017**, *11*, 3488-3493.
485. Liu, C.; Xiao, L.; Zhang, Y.; Zhao, Q.; Xu, H. Regeneration of annulus fibrosus tissue using a DAFM/PECUU-blended electrospun scaffold. *J Biomater Sci Polym Ed.* **2020**, *31*, 2347-2361.
486. Chen, H.; Han, Q.; Wang, C.; Liu, Y.; Chen, B.; Wang, J. Porous scaffold design for additive manufacturing in orthopedics: a review. *Front Bioeng Biotechnol.* **2020**, *8*, 609.
487. Lutzweiler, G.; Ndreu Halili, A.; Engin Vrana, N. The overview of porous, bioactive scaffolds as instructive biomaterials for tissue regeneration and their clinical translation. *Pharmaceutics.* **2020**, *12*, 602.
488. Chen, X.; Fan, H.; Deng, X.; Wu, L.; Yi, T.; Gu, L.; Zhou, C.; Fan, Y.; Zhang, X. Scaffold structural microenvironmental cues to guide tissue regeneration in bone tissue applications. *Nanomaterials (Basel).* **2018**, *8*, 960.
489. Griffon, D. J.; Sedighi, M. R.; Schaeffer, D. V.; Eurell, J. A.; Johnson, A. L. Chitosan scaffolds: interconnective pore size and cartilage

engineering. *Acta Biomater.* **2006**, *2*, 313-320.
490. Nava, M. M.; Draghi, L.; Giordano, C.; Pietrabissa, R. The effect of scaffold pore size in cartilage tissue engineering. *J Appl Biomater Funct Mater.* **2016**, *14*, e223-229.
491. Xu, H.; Xu, B.; Yang, Q.; Li, X.; Ma, X.; Xia, Q.; Zhang, C.; Wu, Y. Fabrication and analysis of a novel tissue engineered composite biphasic scaffold for annulus fibrosus and nucleus pulposus. *Zhongguo Xiu Fu Chong Jian Wai Ke Za Zhi.* **2013**, *27*, 475-480.
492. Xu, B.; Xu, H.; Wu, Y.; Li, X.; Zhang, Y.; Ma, X.; Yang, Q. Intervertebral disc tissue engineering with natural extracellular matrix-derived biphasic composite scaffolds. *PLoS One.* **2015**, *10*, e0124774.
493. Oh, S. H.; Kim, T. H.; Im, G. I.; Lee, J. H. Investigation of pore size effect on chondrogenic differentiation of adipose stem cells using a pore size gradient scaffold. *Biomacromolecules.* **2010**, *11*, 1948-1955.
494. Nehrer, S.; Breinan, H. A.; Ramappa, A.; Young, G.; Shortkroff, S.; Louie, L. K.; Sledge, C. B.; Yannas, I. V.; Spector, M. Matrix collagen type and pore size influence behaviour of seeded canine chondrocytes. *Biomaterials.* **1997**, *18*, 769-776.
495. Im, G. I.; Ko, J. Y.; Lee, J. H. Chondrogenesis of adipose stem cells in a porous polymer scaffold: influence of the pore size. *Cell Transplant.* **2012**, *21*, 2397-2405.
496. Kim, H. Y.; Kim, H. N.; Lee, S. J.; Song, J. E.; Kwon, S. Y.; Chung, J. W.; Lee, D.; Khang, G. Effect of pore sizes of PLGA scaffolds on mechanical properties and cell behaviour for nucleus pulposus regeneration in vivo. *J Tissue Eng Regen Med.* **2017**, *11*, 44-57.
497. Chou, P. H.; Chee, A.; Shi, P.; Lin, C. L.; Zhao, Y.; Zhang, L.; An, H. S. Small molecule antagonist of C-C chemokine receptor 1 (CCR1) reduces disc inflammation in the rabbit model. *Spine J.* **2020**, *20*, 2025-2036.
498. Zhang, W.; Nie, L.; Guo, Y. J.; Han, L. X.; Wang, X.; Zhao, H.; Han, Y. G.; Zhang, Y. Q.; Cheng, L. Th17 cell frequency and IL-17 concentration correlate with pre- and postoperative pain sensation in patients with intervertebral disk degeneration. *Orthopedics.* **2014**, *37*, e685-691.
499. Kawakubo, A.; Uchida, K.; Miyagi, M.; Nakawaki, M.; Satoh, M.; Sekiguchi, H.; Yokozeki, Y.; Inoue, G.; Takaso, M. Investigation of resident and recruited macrophages following disc injury in mice. *J Orthop Res.* **2020**, *38*, 1703-1709.
500. Sussman, E. M.; Halpin, M. C.; Muster, J.; Moon, R. T.; Ratner, B. D. Porous implants modulate healing and induce shifts in local macrophage polarization in the foreign body reaction. *Ann Biomed Eng.* **2014**, *42*, 1508-1516.
501. Zhu, Y.; Hideyoshi, S.; Jiang, H.; Matsumura, Y.; Dziki, J. L.; LoPresti, S. T.; Huleihel, L.; Faria, G. N. F.; Fuhrman, L. C.; Lodono, R.; Badylak, S. F.; Wagner, W. R. Injectable, porous, biohybrid hydrogels incorporating decellularized tissue components for soft tissue applications. *Acta Biomater.* **2018**, *73*, 112-126.
502. Veiseh, O.; Doloff, J. C.; Ma, M.; Vegas, A. J.; Tam, H. H.; Bader, A. R.; Li, J.; Langan, E.; Wyckoff, J.; Loo, W. S.; Jhunjhunwala, S.; Chiu, A.; Siebert, S.; Tang, K.; Hollister-Lock, J.; Aresta-Dasilva, S.; Bochenek, M.; Mendoza-Elias, J.; Wang, Y.; Qi, M.; Lavin, D. M.; Chen, M.; Dholakia, N.; Thakrar, R.; Lacík, I.; Weir, G. C.; Oberholzer, J.; Greiner, D. L.; Langer, R.; Anderson, D. G. Size- and shape-dependent foreign body immune response to materials implanted in rodents and non-human primates. *Nat Mater.* **2015**, *14*, 643-651.
503. Jia, Y.; Yang, W.; Zhang, K.; Qiu, S.; Xu, J.; Wang, C.; Chai, Y. Nanofiber arrangement regulates peripheral nerve regeneration through differential modulation of macrophage phenotypes. *Acta Biomater.* **2019**, *83*, 291-301.
504. McWhorter, F. Y.; Wang, T.; Nguyen, P.; Chung, T.; Liu, W. F. Modulation of macrophage phenotype by cell shape. *Proc Natl Acad Sci U S A.* **2013**, *110*, 17253-17258.
505. Tylek, T.; Blum, C.; Hrynevich, A.; Schlegelmilch, K.; Schilling, T.; Dalton, P. D.; Groll, J. Precisely defined fiber scaffolds with 40 μm porosity induce elongation driven M2-like polarization of human macrophages. *Biofabrication.* **2020**, *12*, 025007.
506. Roberts, S.; Evans, H.; Trivedi, J.; Menage, J. Histology and pathology of the human intervertebral disc. *J Bone Joint Surg Am.* **2006**, *88* Suppl 2, 10-14.
507. Shen, J.; Xu, S.; Zhou, H.; Liu, H.; Jiang, W.; Hao, J.; Hu, Z. IL-1β induces apoptosis and autophagy via mitochondria pathway in human degenerative nucleus pulposus cells. *Sci Rep.* **2017**, *7*, 41067.
508. Sivan, S. S.; Wachtel, E.; Roughley, P. Structure, function, aging and turnover of aggrecan in the intervertebral disc. *Biochim Biophys Acta.* **2014**, *1840*, 3181-3189.
509. Tengblad, A.; Pearce, R. H.; Grimmer, B. J. Demonstration of link protein in proteoglycan aggregates from human intervertebral disc. *Biochem J.* **1984**, *222*, 85-92.
510. Roughley, P.; Martens, D.; Rantakokko, J.; Alini, M.; Mwale, F.; Antoniou, J. The involvement of aggrecan polymorphism in degeneration of human intervertebral disc and articular cartilage. *Eur Cell Mater.* **2006**, *11*, 1-7; discussion 7.
511. Ray, C. D. The PDN prosthetic disc-nucleus device. *Eur Spine J.* **2002**, *11* Suppl 2, S137-142.
512. Ceylan, A.; Aşik, I.; Özgencil, G. E.; Erken, B. Clinical results of intradiscal hydrogel administration (GelStix) in lumbar degenerative disc disease. *Turk J Med Sci.* **2019**, *49*, 1634-1639.
513. Durdag, E.; Ayden, O.; Albayrak, S.; Atci, I. B.; Armagan, E. Fragmentation to epidural space: first documented complication of Gelstix(TM.). *Turk Neurosurg.* **2014**, *24*, 602-605.
514. Coric, D.; Mummaneni, P. V. Nucleus replacement technologies. *J Neurosurg Spine.* **2008**, *8*, 115-120.
515. Berlemann, U.; Schwarzenbach, O. An injectable nucleus replacement as an adjunct to microdiscectomy: 2 year follow-up in a pilot clinical study. *Eur Spine J.* **2009**, *18*, 1706-1712.
516. Eysel, P.; Rompe, J.; Schoenmayr, R.; Zoellner, J. Biomechanical behaviour of a prosthetic lumbar nucleus. *Acta Neurochir (Wien).* **1999**, *141*, 1083-1087.
517. Scholz, B.; Kinzelmann, C.; Benz, K.; Mollenhauer, J.; Wurst, H.; Schlosshauer, B. Suppression of adverse angiogenesis in an albumin-based hydrogel for articular cartilage and intervertebral disc regeneration. *Eur Cell Mater.* **2010**, *20*, 24-36; discussion 36-37.
518. Tschugg, A.; Michnacs, F.; Strowitzki, M.; Meisel, H. J.; Thomé, C. A prospective multicenter phase I/II clinical trial to evaluate safety and efficacy of NOVOCART disc plus autologous disc chondrocyte transplantation in the treatment of nucleotomized and degenerative lumbar disc to avoid secondary disease: study protocol for a randomized controlled trial. *Trials.* **2016**, *17*, 108.
519. Choi, U. Y.; Joshi, H. P.; Payne, S.; Kim, K. T.; Kyung, J. W.; Choi, H.; Cooke, M. J.; Kwon, S. Y.; Roh, E. J.; Sohn, S.; Shoichet, M. S.; Han, I. An injectable hyaluronan-methylcellulose (HAMC) hydrogel combined with Wharton's jelly-derived mesenchymal stromal cells (WJ-MSCs) promotes degenerative disc repair. *Int J Mol Sci.* **2020**, *21*, 7391.
520. Häckel, S.; Zolfaghar, M.; Du, J.; Hoppe, S.; Benneker, L. M.; Garstka, N.; Peroglio, M.; Alini, M.; Grad, S.; Yayon, A.; Li, Z. Fibrin-hyaluronic acid hydrogel (RegenoGel) with fibroblast growth factor-18 for in vitro

3D culture of human and bovine nucleus pulposus cells. *Int J Mol Sci.* **2019**, *20*, 5036.

521. Ukeba, D.; Sudo, H.; Tsujimoto, T.; Ura, K.; Yamada, K.; Iwasaki, N. Bone marrow mesenchymal stem cells combined with ultra-purified alginate gel as a regenerative therapeutic strategy after discectomy for degenerated intervertebral discs. *EBioMedicine.* **2020**, *53*, 102698.
522. Alinejad, Y.; Adoungotchodo, A.; Grant, M. P.; Epure, L. M.; Antoniou, J.; Mwale, F.; Lerouge, S. Injectable chitosan hydrogels with enhanced mechanical properties for nucleus pulposus regeneration. *Tissue Eng Part A.* **2019**, *25*, 303-313.
523. Gan, Y.; Li, S.; Li, P.; Xu, Y.; Wang, L.; Zhao, C.; Ouyang, B.; Tu, B.; Zhang, C.; Luo, L.; Luo, X.; Mo, X.; Zhou, Q. A controlled release codelivery system of MSCs encapsulated in dextran/gelatin hydrogel with tgf-β3-loaded nanoparticles for nucleus pulposus regeneration. *Stem Cells Int.* **2016**, *2016*, 9042019.
524. Nguyen, N. T.; Milani, A. H.; Jennings, J.; Adlam, D. J.; Freemont, A. J.; Hoyland, J. A.; Saunders, B. R. Highly compressive and stretchable poly(ethylene glycol) based hydrogels synthesised using pH-responsive nanogels without free-radical chemistry. *Nanoscale.* **2019**, *11*, 7921-7930.
525. Leone, G.; Consumi, M.; Lamponi, S.; Bonechi, C.; Tamasi, G.; Donati, A.; Rossi, C.; Magnani, A. Thixotropic PVA hydrogel enclosing a hydrophilic PVP core as nucleus pulposus substitute. *Mater Sci Eng C Mater Biol Appl.* **2019**, *98*, 696-704.
526. Schmocker, A.; Khoushabi, A.; Frauchiger, D. A.; Gantenbein, B.; Schizas, C.; Moser, C.; Bourban, P. E.; Pioletti, D. P. A photopolymerized composite hydrogel and surgical implanting tool for a nucleus pulposus replacement. *Biomaterials.* **2016**, *88*, 110-119.
527. Peng, Y.; Huang, D.; Liu, S.; Li, J.; Qing, X.; Shao, Z. Biomaterials-induced stem cells specific differentiation into intervertebral disc lineage cells. *Front Bioeng Biotechnol.* **2020**, *8*, 56.
528. Chen, P.; Ning, L.; Qiu, P.; Mo, J.; Mei, S.; Xia, C.; Zhang, J.; Lin, X.; Fan, S. Photo-crosslinked gelatin-hyaluronic acid methacrylate hydrogel-committed nucleus pulposus-like differentiation of adipose stromal cells for intervertebral disc repair. *J Tissue Eng Regen Med.* **2019**, *13*, 682-693.
529. Binch, A. L. A.; Ratcliffe, L. P. D.; Milani, A. H.; Saunders, B. R.; Armes, S. P.; Hoyland, J. A. Site-directed differentiation of human adipose-derived mesenchymal stem cells to nucleus pulposus cells using an injectable hydroxyl-functional diblock copolymer worm gel. *Biomacromolecules.* **2021**, *22*, 837-845.
530. Wang, Z.; Liu, H.; Luo, W.; Cai, T.; Li, Z.; Liu, Y.; Gao, W.; Wan, Q.; Wang, X.; Wang, J.; Wang, Y.; Yang, X. Regeneration of skeletal system with genipin crosslinked biomaterials. *J Tissue Eng.* **2020**, *11*, 2041731420974861.
531. Panebianco, C. J.; DiStefano, T. J.; Mui, B.; Hom, W. W.; Iatridis, J. C. Crosslinker concentration controls TGFβ-3 release and annulus fibrosus cell apoptosis in genipin-crosslinked fibrin hydrogels. *Eur Cell Mater.* **2020**, *39*, 211-226.
532. Zhou, X.; Wang, J.; Fang, W.; Tao, Y.; Zhao, T.; Xia, K.; Liang, C.; Hua, J.; Li, F.; Chen, Q. Genipin cross-linked type II collagen/chondroitin sulfate composite hydrogel-like cell delivery system induces differentiation of adipose-derived stem cells and regenerates degenerated nucleus pulposus. *Acta Biomater.* **2018**, *71*, 496-509.
533. Wu, X.; Liu, Y.; Guo, X.; Zhou, W.; Wang, L.; Shi, J.; Tao, Y.; Zhu, M.; Geng, D.; Yang, H.; Mao, H. Prolactin inhibits the progression of intervertebral disc degeneration through inactivation of the NF-κB pathway in rats. *Cell Death Dis.* **2018**, *9*, 98.
534. Issy, A. C.; Castania, V.; Castania, M.; Salmon, C. E.; Nogueira-Barbosa, M. H.; Bel, E. D.; Defino, H. L. Experimental model of intervertebral disc degeneration by needle puncture in Wistar rats. *Braz J Med Biol Res.* **2013**, *46*, 235-244.
535. Alfredo Uquillas, J.; Kishore, V.; Akkus, O. Genipin crosslinking elevates the strength of electrochemically aligned collagen to the level of tendons. *J Mech Behav Biomed Mater.* **2012**, *15*, 176-189.
536. Censi, R.; Di Martino, P.; Vermonden, T.; Hennink, W. E. Hydrogels for protein delivery in tissue engineering. *J Control Release.* **2012**, *161*, 680-692.
537. Francisco, A. T.; Mancino, R. J.; Bowles, R. D.; Brunger, J. M.; Tainter, D. M.; Chen, Y. T.; Richardson, W. J.; Guilak, F.; Setton, L. A. Injectable laminin-functionalized hydrogel for nucleus pulposus regeneration. *Biomaterials.* **2013**, *34*, 7381-7388.
538. Zhu, Y.; Tan, J.; Zhu, H.; Lin, G.; Yin, F.; Wang, L.; Song, K.; Wang, Y.; Zhou, G.; Yi, W. Development of kartogenin-conjugated chitosan-hyaluronic acid hydrogel for nucleus pulposus regeneration. *Biomater Sci.* **2017**, *5*, 784-791.
539. Sulaiman, S. B.; Idrus, R. B. H.; Hwei, N. M. Gelatin microsphere for cartilage tissue engineering: current and future strategies. *Polymers (Basel).* **2020**, *12*, 2404.
540. Leong, W.; Wang, D. A. Cell-laden polymeric microspheres for biomedical applications. *Trends Biotechnol.* **2015**, *33*, 653-666.
541. Patel, K. S.; Patel, M. B. Preparation and evaluation of chitosan microspheres containing nicorandil. *Int J Pharm Investig.* **2014**, *4*, 32-37.
542. Wang, X.; Wenk, E.; Matsumoto, A.; Meinel, L.; Li, C.; Kaplan, D. L. Silk microspheres for encapsulation and controlled release. *J Control Release.* **2007**, *117*, 360-370.
543. Saravanan, M.; Bhaskar, K.; Maharajan, G.; Pillai, K. S. Development of gelatin microspheres loaded with diclofenac sodium for intra-articular administration. *J Drug Target.* **2011**, *19*, 96-103.
544. Dhamecha, D.; Movsas, R.; Sano, U.; Menon, J. U. Applications of alginate microspheres in therapeutics delivery and cell culture: Past, present and future. *Int J Pharm.* **2019**, *569*, 118627.
545. Xu, H.; Sun, M.; Wang, C.; Xia, K.; Xiao, S.; Wang, Y.; Ying, L.; Yu, C.; Yang, Q.; He, Y.; Liu, A.; Chen, L. Growth differentiation factor-5-gelatin methacryloyl injectable microspheres laden with adipose-derived stem cells for repair of disc degeneration. *Biofabrication.* **2020**, *13*, 015010.
546. Xu, H.; Sun, M.; Wang, C.; Xia, K.; Xiao, S.; Wang, Y.; Ying, L.; Yu, C.; Yang, Q.; He, Y.; Liu, A.; Chen, L. GDF5-GelMA injectable microspheres laden with adipose-derived stem cells for disc degeneration repair. *Biofabrication.* **2020**. doi: 10.1088/1758-5090/abc4d3.
547. Feng, G.; Zhang, Z.; Dang, M.; Rambhia, K. J.; Ma, P. X. Nanofibrous spongy microspheres to deliver rabbit mesenchymal stem cells and anti-miR-199a to regenerate nucleus pulposus and prevent calcification. *Biomaterials.* **2020**, *256*, 120213.
548. Xia, K.; Zhu, J.; Hua, J.; Gong, Z.; Yu, C.; Zhou, X.; Wang, J.; Huang, X.; Yu, W.; Li, L.; Gao, J.; Chen, Q.; Li, F.; Liang, C. Intradiscal injection of induced pluripotent stem cell-derived nucleus pulposus-like cell-seeded polymeric microspheres promotes rat disc regeneration. *Stem Cells Int.* **2019**, *2019*, 6806540.
549. Shan, Z.; Lin, X.; Wang, S.; Zhang, X.; Pang, Y.; Li, S.; Yu, T.; Fan, S.; Zhao, F. An injectable nucleus pulposus cell-modified decellularized scaffold: biocompatible material for prevention of disc degeneration. *Oncotarget.* **2017**, *8*, 40276-40288.
550. Liang, C. Z.; Li, H.; Tao, Y. Q.; Peng, L. H.; Gao, J. Q.; Wu, J. J.; Li, F. C.; Hua, J. M.; Chen, Q. X. Dual release of dexamethasone and TGF-β3

from polymeric microspheres for stem cell matrix accumulation in a rat disc degeneration model. *Acta Biomater.* **2013**, *9*, 9423-9433.
551. Wu, D.; Yu, Y.; Zhao, C.; Shou, X.; Piao, Y.; Zhao, X.; Zhao, Y.; Wang, S. NK-cell-encapsulated porous microspheres via microfluidic electrospray for tumor immunotherapy. *ACS Appl Mater Interfaces.* **2019**, *11*, 33716-33724.
552. Jo, Y. K.; Lee, D. Biopolymer microparticles prepared by microfluidics for biomedical applications. *Small.* **2020**, *16*, e1903736.
553. McMasters, J.; Panitch, A. Collagen-binding nanoparticles for extracellular anti-inflammatory peptide delivery decrease platelet activation, promote endothelial migration, and suppress inflammation. *Acta Biomater.* **2017**, *49*, 78-88.
554. Sangtani, A.; Nag, O. K.; Field, L. D.; Breger, J. C.; Delehanty, J. B. Multifunctional nanoparticle composites: progress in the use of soft and hard nanoparticles for drug delivery and imaging. *Wiley Interdiscip Rev Nanomed Nanobiotechnol.* **2017**, *9*.
555. Ji, M. L.; Jiang, H.; Zhang, X. J.; Shi, P. L.; Li, C.; Wu, H.; Wu, X. T.; Wang, Y. T.; Wang, C.; Lu, J. Preclinical development of a microRNA-based therapy for intervertebral disc degeneration. *Nat Commun.* **2018**, *9*, 5051.
556. Liang, C.; Li, H.; Li, C.; Yang, Z.; Zhou, X.; Tao, Y.; Xiao, Y.; Li, F.; Chen, Q. Fabrication of a layered microstructured polymeric microspheres as a cell carrier for nucleus pulposus regeneration. *J Biomater Sci Polym Ed.* **2012**, *23*, 2287-2302.
557. van der Meel, R.; Vehmeijer, L. J.; Kok, R. J.; Storm, G.; van Gaal, E. V. Ligand-targeted particulate nanomedicines undergoing clinical evaluation: current status. *Adv Drug Deliv Rev.* **2013**, *65*, 1284-1298.
558. Lammers, T.; Kiessling, F.; Hennink, W. E.; Storm, G. Drug targeting to tumors: principles, pitfalls and (pre-) clinical progress. *J Control Release.* **2012**, *161*, 175-187.
559. Xiao, S.; Tang, Y.; Lv, Z.; Lin, Y.; Chen, L. Nanomedicine - advantages for their use in rheumatoid arthritis theranostics. *J Control Release.* **2019**, *316*, 302-316.
560. Nadra, I.; Boccaccini, A. R.; Philippidis, P.; Whelan, L. C.; McCarthy, G. M.; Haskard, D. O.; Landis, R. C. Effect of particle size on hydroxyapatite crystal-induced tumor necrosis factor alpha secretion by macrophages. *Atherosclerosis.* **2008**, *196*, 98-105.
561. Pradal, J.; Maudens, P.; Gabay, C.; Seemayer, C. A.; Jordan, O.; Allémann, E. Effect of particle size on the biodistribution of nano- and microparticles following intra-articular injection in mice. *Int J Pharm.* **2016**, *498*, 119-129.
562. Patel, S.; Kim, J.; Herrera, M.; Mukherjee, A.; Kabanov, A. V.; Sahay, G. Brief update on endocytosis of nanomedicines. *Adv Drug Deliv Rev.* **2019**, *144*, 90-111.
563. Yameen, B.; Choi, W. I.; Vilos, C.; Swami, A.; Shi, J.; Farokhzad, O. C. Insight into nanoparticle cellular uptake and intracellular targeting. *J Control Release.* **2014**, *190*, 485-499.
564. Kang, M. L.; Ko, J. Y.; Kim, J. E.; Im, G. I. Intra-articular delivery of kartogenin-conjugated chitosan nano/microparticles for cartilage regeneration. *Biomaterials.* **2014**, *35*, 9984-9994.
565. Chen, Z.; Liu, D.; Wang, J.; Wu, L.; Li, W.; Chen, J.; Cai, B. C.; Cheng, H. Development of nanoparticles-in-microparticles system for improved local retention after intra-articular injection. *Drug Deliv.* **2014**, *21*, 342-350.
566. Abrego, G.; Alvarado, H.; Souto, E. B.; Guevara, B.; Bellowa, L. H.; Garduño, M. L.; Garcia, M. L.; Calpena, A. C. Biopharmaceutical profile of hydrogels containing pranoprofen-loaded PLGA nanoparticles for skin administration: In vitro, ex vivo and in vivo characterization. *Int J Pharm.* **2016**, *501*, 350-361.
567. Shirazi-Adl, A.; Taheri, M.; Urban, J. P. Analysis of cell viability in intervertebral disc: Effect of endplate permeability on cell population. *J Biomech.* **2010**, *43*, 1330-1336.
568. Bowles, R. D.; Williams, R. M.; Zipfel, W. R.; Bonassar, L. J. Self-assembly of aligned tissue-engineered annulus fibrosus and intervertebral disc composite via collagen gel contraction. *Tissue Eng Part A.* **2010**, *16*, 1339-1348.
569. Mizuno, H.; Roy, A. K.; Zaporojan, V.; Vacanti, C. A.; Ueda, M.; Bonassar, L. J. Biomechanical and biochemical characterization of composite tissue-engineered intervertebral discs. *Biomaterials.* **2006**, *27*, 362-370.
570. Iatridis, J. C. Tissue engineering: Function follows form. *Nat Mater.* **2009**, *8*, 923-924.
571. Nerurkar, N. L.; Elliott, D. M.; Mauck, R. L. Mechanical design criteria for intervertebral disc tissue engineering. *J Biomech.* **2010**, *43*, 1017-1030.
572. Luk, K. D.; Ruan, D. K.; Chow, D. H.; Leong, J. C. Intervertebral disc autografting in a bipedal animal model. *Clin Orthop Relat Res.* **1997**, 13-26.
573. Frick, S. L.; Hanley, E. N., Jr.; Meyer, R. A., Jr.; Ramp, W. K.; Chapman, T. M. Lumbar intervertebral disc transfer. A canine study. *Spine (Phila Pa 1976).* **1994**, *19*, 1826-1834; discussion 1834-1835.
574. Chan, S. C.; Lam, S.; Leung, V. Y.; Chan, D.; Luk, K. D.; Cheung, K. M. Minimizing cryopreservation-induced loss of disc cell activity for storage of whole intervertebral discs. *Eur Cell Mater.* **2010**, *19*, 273-283.
575. Ruan, D.; He, Q.; Ding, Y.; Hou, L.; Li, J.; Luk, K. D. Intervertebral disc transplantation in the treatment of degenerative spine disease: a preliminary study. *Lancet.* **2007**, *369*, 993-999.
576. Ding, Y.; Ruan, D. K.; He, Q.; Hou, L. S.; Lin, J. N.; Cui, H. P. Imaging evaluation and relative significance in cases of cervical disk allografting: radiographic character after total disk transplantation. *Clinical spine surgery.* **2016**, *29*, E488-E495.
577. Tumialán, L. M.; Ponton, R. P.; Garvin, A.; Gluf, W. M. Arthroplasty in the military: a preliminary experience with ProDisc-C and ProDisc-L. *Neurosurg Focus.* **2010**, *28*, E18.
578. Yue, J. J.; Mo, F. F. Clinical study to evaluate the safety and effectiveness of the Aesculap Activ-L artificial disc in the treatment of degenerative disc disease. *BMC Surg.* **2010**, *10*, 14.
579. Plais, N.; Thevenot, X.; Cogniet, A.; Rigal, J.; Le Huec, J. C. Maverick total disc arthroplasty performs well at 10 years follow-up: a prospective study with HRQL and balance analysis. *Eur Spine J.* **2018**, *27*, 720-727.
580. Gornet, M. F.; Burkus, J. K.; Dryer, R. F.; Peloza, J. H.; Schranck, F. W.; Copay, A. G. Lumbar disc arthroplasty versus anterior lumbar interbody fusion: 5-year outcomes for patients in the Maverick disc investigational device exemption study. *J Neurosurg Spine.* **2019**, *31*, 347-356.
581. Sandhu, F. A.; Dowlati, E.; Garica, R. Lumbar Arthroplasty: Past, Present, and Future. *Neurosurgery.* **2020**, *86*, 155-169.
582. Austen, S.; Punt, I. M.; Cleutjens, J. P.; Willems, P. C.; Kurtz, S. M.; MacDonald, D. W.; van Rhijn, L. W.; van Ooij, A. Clinical, radiological, histological and retrieval findings of Activ-L and Mobidisc total disc replacements: a study of two patients. *Eur Spine J.* **2012**, *21* Suppl 4, S513-520.
583. Yue, J. J.; Garcia, R.; Blumenthal, S.; Coric, D.; Patel, V. V.; Dinh, D. H.; Buttermann, G. R.; Deutsch, H.; Miller, L. E.; Persaud, E. J.; Ferko, N. C. Five-year results of a randomized controlled trial for lumbar artificial

discs in single-level degenerative disc disease. *Spine (Phila Pa 1976).* **2019**, *44*, 1685-1696.

584. Aunoble, S.; Donkersloot, P.; Le Huec, J. C. Dislocations with intervertebral disc prosthesis: two case reports. *Eur Spine J.* **2004**, *13*, 464-467.
585. Shim, C. S.; Lee, S.; Maeng, D. H.; Lee, S. H. Vertical split fracture of the vertebral body following total disc replacement using ProDisc: report of two cases. *J Spinal Disord Tech.* **2005**, *18*, 465-469.
586. François, J.; Coessens, R.; Lauweryns, P. Early removal of a Maverick disc prosthesis: surgical findings and morphological changes. *Acta Orthop Belg.* **2007**, *73*, 122-127.
587. Zeh, A.; Becker, C.; Planert, M.; Lattke, P.; Wohlrab, D. Time-dependent release of cobalt and chromium ions into the serum following implantation of the metal-on-metal Maverick type artificial lumbar disc (Medtronic Sofamor Danek). *Arch Orthop Trauma Surg.* **2009**, *129*, 741-746.
588. Gornet, M. F.; Burkus, J. K.; Harper, M. L.; Chan, F. W.; Skipor, A. K.; Jacobs, J. J. Prospective study on serum metal levels in patients with metal-on-metal lumbar disc arthroplasty. *Eur Spine J.* **2013**, *22*, 741-746.
589. Natu, S.; Sidaginamale, R. P.; Gandhi, J.; Langton, D. J.; Nargol, A. V. Adverse reactions to metal debris: histopathological features of periprosthetic soft tissue reactions seen in association with failed metal on metal hip arthroplasties. *J Clin Pathol.* **2012**, *65*, 409-418.
590. Sasso, R. C.; Kenneth Burkus, J.; LeHuec, J. C. Retrograde ejaculation after anterior lumbar interbody fusion: transperitoneal versus retroperitoneal exposure. *Spine (Phila Pa 1976).* **2003**, *28*, 1023-1026.
591. Tropiano, P.; Huang, R. C.; Girardi, F. P.; Cammisa, F. P., Jr.; Marnay, T. Lumbar total disc replacement. Surgical technique. *J Bone Joint Surg Am.* **2006**, *88 Suppl 1 Pt 1*, 50-64.
592. Härtl, R.; Joeris, A.; McGuire, R. A. Comparison of the safety outcomes between two surgical approaches for anterior lumbar fusion surgery: anterior lumbar interbody fusion (ALIF) and extreme lateral interbody fusion (ELIF). *Eur Spine J.* **2016**, *25*, 1484-1521.
593. Brau, S. A.; Spoonamore, M. J.; Snyder, L.; Gilbert, C.; Rhonda, G.; Williams, L. A.; Watkins, R. G. Nerve monitoring changes related to iliac artery compression during anterior lumbar spine surgery. *Spine J.* **2003**, *3*, 351-355.
594. Cui, X. D.; Li, H. T.; Zhang, W.; Zhang, L. L.; Luo, Z. P.; Yang, H. L. Mid- to long-term results of total disc replacement for lumbar degenerative disc disease: a systematic review. *J Orthop Surg Res.* **2018**, *13*, 326.
595. Salzmann, S. N.; Shue, J.; Hughes, A. P. Lateral lumbar interbody fusion-outcomes and complications. *Curr Rev Musculoskelet Med.* **2017**, *10*, 539-546.
596. Martin, J. T.; Milby, A. H.; Chiaro, J. A.; Kim, D. H.; Hebela, N. M.; Smith, L. J.; Elliott, D. M.; Mauck, R. L. Translation of an engineered nanofibrous disc-like angle-ply structure for intervertebral disc replacement in a small animal model. *Acta Biomater.* **2014**, *10*, 2473-2481.
597. Norbertczak, H. T.; Ingham, E.; Fermor, H. L.; Wilcox, R. K. Decellularized intervertebral discs: a potential replacement for degenerate human discs. *Tissue Eng Part C Methods.* **2020**, *26*, 565-576.
598. Hensley, A.; Rames, J.; Casler, V.; Rood, C.; Walters, J.; Fernandez, C.; Gill, S.; Mercuri, J. J. Decellularization and characterization of a whole intervertebral disk xenograft scaffold. *J Biomed Mater Res A.* **2018**, *106*, 2412-2423.
599. Moriguchi, Y.; Mojica-Santiago, J.; Grunert, P.; Pennicooke, B.; Berlin, C.; Khair, T.; Navarro-Ramirez, R.; Ricart Arbona, R. J.; Nguyen, J.; Härtl, R.; Bonassar, L. J. Total disc replacement using tissue-engineered intervertebral discs in the canine cervical spine. *PLoS One.* **2017**, *12*, e0185716.
600. Grunert, P.; Borde, B. H.; Towne, S. B.; Moriguchi, Y.; Hudson, K. D.; Bonassar, L. J.; Härtl, R. Riboflavin crosslinked high-density collagen gel for the repair of annular defects in intervertebral discs: An in vivo study. *Acta Biomater.* **2015**, *26*, 215-224.
601. Sloan, S. R., Jr.; Wipplinger, C.; Kirnaz, S.; Navarro-Ramirez, R.; Schmidt, F.; McCloskey, D.; Pannellini, T.; Schiavinato, A.; Härtl, R.; Bonassar, L. J. Combined nucleus pulposus augmentation and annulus fibrosus repair prevents acute intervertebral disc degeneration after discectomy. *Sci Transl Med.* **2020**, *12*, eaay2380.
602. Pennicooke, B.; Hussain, I.; Berlin, C.; Sloan, S. R.; Borde, B.; Moriguchi, Y.; Lang, G.; Navarro-Ramirez, R.; Cheetham, J.; Bonassar, L. J.; Härtl, R. Annulus fibrosus repair using high-density collagen gel: an in vivo ovine model. *Spine (Phila Pa 1976).* **2018**, *43*, E208-E215.
603. Zhang, Y.; Drapeau, S.; An, H. S.; Markova, D.; Lenart, B. A.; Anderson, D. G. Histological features of the degenerating intervertebral disc in a goat disc-injury model. *Spine (Phila Pa 1976).* **2011**, *36*, 1519-1527.
604. Matta, A.; Karim, M. Z.; Gerami, H.; Jun, P.; Funabashi, M.; Kawchuk, G.; Goldstein, A.; Foltz, W.; Sussman, M.; Eek, B. C.; Erwin, W. M. NTG-101: a novel molecular therapy that halts the progression of degenerative disc disease. *Sci Rep.* **2018**, *8*, 16809.
605. Long, R. G.; Ferguson, S. J.; Benneker, L. M.; Sakai, D.; Li, Z.; Pandit, A.; Grijpma, D. W.; Eglin, D.; Zeiter, S.; Schmid, T.; Eberli, U.; Nehrbass, D.; Di Pauli von Treuheim, T.; Alini, M.; Iatridis, J. C.; Grad, S. Morphological and biomechanical effects of annulus fibrosus injury and repair in an ovine cervical model. *JOR Spine.* **2020**, *3*, e1074.
606. Liu, W.; Liu, D.; Zheng, J.; Shi, P.; Chou, P. H.; Oh, C.; Chen, D.; An, H. S.; Chee, A. Annulus fibrosus cells express and utilize C-C chemokine receptor 5 (CCR5) for migration. *Spine J.* **2017**, *17*, 720-726.
607. Huang, B. R.; Bau, D. T.; Chen, T. S.; Chuang, I. C.; Tsai, C. F.; Chang, P. C.; Hsu, H. C.; Lu, D. Y. Pro-inflammatory stimuli influence expression of intercellular adhesion molecule 1 in human anulus fibrosus cells through FAK/ERK/GSK3 and PKCδ signaling pathways. *Int J Mol Sci.* **2018**, *20*, 77.
608. Stich, S.; Möller, A.; Cabraja, M.; Krüger, J. P.; Hondke, S.; Endres, M.; Ringe, J.; Sittinger, M. Chemokine CCL25 induces migration and extracellular matrix production of anulus fibrosus-derived cells. *Int J Mol Sci.* **2018**, *19*, 2207.
609. Zhou, Z.; Zeiter, S.; Schmid, T.; Sakai, D.; Iatridis, J. C.; Zhou, G.; Richards, R. G.; Alini, M.; Grad, S.; Li, Z. Effect of the CCL5-releasing fibrin gel for intervertebral disc regeneration. *Cartilage.* **2020**, *11*, 169-180.
610. Magge, S. N.; Malik, S. Z.; Royo, N. C.; Chen, H. I.; Yu, L.; Snyder, E. Y.; O'Rourke, D. M.; Watson, D. J. Role of monocyte chemoattractant protein-1 (MCP-1/CCL2) in migration of neural progenitor cells toward glial tumors. *J Neurosci Res.* **2009**, *87*, 1547-1555.
611. Wang, L.; Li, H.; Lin, J.; He, R.; Chen, M.; Zhang, Y.; Liao, Z.; Zhang, C. CCR2 improves homing and engraftment of adipose-derived stem cells in dystrophic mice. *Stem Cell Res Ther.* **2021**, *12*, 12.
612. Frapin, L.; Clouet, J.; Chédeville, C.; Moraru, C.; Samarut, E.; Henry, N.; André, M.; Bord, E.; Halgand, B.; Lesoeur, J.; Fusellier, M.; Guicheux, J.; Le Visage, C. Controlled release of biological factors for endogenous progenitor cell migration and intervertebral disc extracellular matrix remodelling. *Biomaterials.* **2020**, *253*, 120107.
613. Watanabe, Y.; Tsuchiya, A.; Seino, S.; Kawata, Y.; Kojima, Y.; Ikarashi,

S.; Starkey Lewis, P. J.; Lu, W. Y.; Kikuta, J.; Kawai, H.; Yamagiwa, S.; Forbes, S. J.; Ishii, M.; Terai, S. Mesenchymal stem cells and induced bone marrow-derived macrophages synergistically improve liver fibrosis in mice. *Stem Cells Transl Med.* **2019**, *8*, 271-284.
614. Wang, Q.; Zhang, F.; Lei, Y.; Liu, P.; Liu, C.; Tao, Y. microRNA-322/424 promotes liver fibrosis by regulating angiogenesis through targeting CUL2/HIF-1α pathway. *Life Sci.* **2021**, *266*, 118819.
615. Liu, W.; Wang, L.; Zhang, J.; Qiao, L.; Liu, Y.; Yang, X.; Zhang, J.; Zheng, W.; Ma, Z. Purification of recombinant human chemokine CCL2 in E. coli and its function in ovarian cancer. *3 Biotech.* **2021**, *11*, 8.
616. Liu, W.; Wang, W.; Zhang, N.; Di, W. The role of CCL20-CCR6 axis in ovarian cancer metastasis. *Onco Targets Ther.* **2020**, *13*, 12739-12750.
617. Korbecki, J.; Kojder, K.; Simińska, D.; Bohatyrewicz, R.; Gutowska, I.; Chlubek, D.; Baranowska-Bosiacka, I. CC chemokines in a tumor: a review of pro-cancer and anti-cancer properties of the ligands of receptors CCR1, CCR2, CCR3, and CCR4. *Int J Mol Sci.* **2020**, *21*, 8412.
618. Raghu, H.; Lepus, C. M.; Wang, Q.; Wong, H. H.; Lingampalli, N.; Oliviero, F.; Punzi, L.; Giori, N. J.; Goodman, S. B.; Chu, C. R.; Sokolove, J. B.; Robinson, W. H. CCL2/CCR2, but not CCL5/CCR5, mediates monocyte recruitment, inflammation and cartilage destruction in osteoarthritis. *Ann Rheum Dis.* **2017**, *76*, 914-922.
619. Schwager, J.; Richard, N.; Fowler, A.; Seifert, N.; Raederstorff, D. Carnosol and related substances modulate chemokine and cytokine production in macrophages and chondrocytes. *Molecules.* **2016**, *21*, 465.
620. Hingert, D.; Barreto Henriksson, H.; Baranto, A.; Brisby, H. BMP-3 promotes matrix production in co-cultured stem cells and disc cells from low back pain patients. *Tissue Eng Part A.* **2020**, *26*, 47-56.
621. Elmasry, S.; Asfour, S.; de Rivero Vaccari, J. P.; Travascio, F. A computational model for investigating the effects of changes in bioavailability of insulin-like growth factor-1 on the homeostasis of the intervertebral disc. *Comput Biol Med.* **2016**, *78*, 126-137.
622. Takegami, K.; An, H. S.; Kumano, F.; Chiba, K.; Thonar, E. J.; Singh, K.; Masuda, K. Osteogenic protein-1 is most effective in stimulating nucleus pulposus and annulus fibrosus cells to repair their matrix after chondroitinase ABC-induced in vitro chemonucleolysis. *Spine J.* **2005**, *5*, 231-238.
623. Wallach, C. J.; Kim, J. S.; Sobajima, S.; Lattermann, C.; Oxner, W. M.; McFadden, K.; Robbins, P. D.; Gilbertson, L. G.; Kang, J. D. Safety assessment of intradiscal gene transfer: a pilot study. *Spine J.* **2006**, *6*, 107-112.
624. Cho, H.; Lee, S.; Park, S. H.; Huang, J.; Hasty, K. A.; Kim, S. J. Synergistic effect of combined growth factors in porcine intervertebral disc degeneration. *Connect Tissue Res.* **2013**, *54*, 181-186.
625. Vadalà, G.; Mozetic, P.; Rainer, A.; Centola, M.; Loppini, M.; Trombetta, M.; Denaro, V. Bioactive electrospun scaffold for annulus fibrosus repair and regeneration. *Eur Spine J.* **2012**, *21* Suppl 1, S20-26.
626. Murata, K.; Kokubun, T.; Onitsuka, K.; Oka, Y.; Kano, T.; Morishita, Y.; Ozone, K.; Kuwabara, N.; Nishimoto, J.; Isho, T.; Takayanagi, K.; Kanemura, N. Controlling joint instability after anterior cruciate ligament transection inhibits transforming growth factor-beta-mediated osteophyte formation. *Osteoarthritis Cartilage.* **2019**, *27*, 1185-1196.
627. Kaneko, H.; Ishijima, M.; Futami, I.; Tomikawa-Ichikawa, N.; Kosaki, K.; Sadatsuki, R.; Yamada, Y.; Kurosawa, H.; Kaneko, K.; Arikawa-Hirasawa, E. Synovial perlecan is required for osteophyte formation in knee osteoarthritis. *Matrix Biol.* **2013**, *32*, 178-187.
628. Fuller, E. S.; Shu, C.; Smith, M. M.; Little, C. B.; Melrose, J. Hyaluronan oligosaccharides stimulate matrix metalloproteinase and anabolic gene expression in vitro by intervertebral disc cells and annular repair in vivo. *J Tissue Eng Regen Med.* **2018**, *12*, e216-e226.
629. Binch, A. L. A.; Fitzgerald, J. C.; Growney, E. A.; Barry, F. Cell-based strategies for IVD repair: clinical progress and translational obstacles. *Nat Rev Rheumatol.* **2021**, *17*, 158-175.
630. Chen, S.; Deng, X.; Ma, K.; Zhao, L.; Huang, D.; Li, Z.; Shao, Z. Icariin improves the viability and function of cryopreserved human nucleus pulposus-derived mesenchymal stem cells. *Oxid Med Cell Longev.* **2018**, *2018*, 3459612.
631. Li, Z.; Chen, S.; Ma, K.; Lv, X.; Lin, H.; Hu, B.; He, R.; Shao, Z. CsA attenuates compression-induced nucleus pulposus mesenchymal stem cells apoptosis via alleviating mitochondrial dysfunction and oxidative stress. *Life Sci.* **2018**, *205*, 26-37.
632. Pas, H. I.; Winters, M.; Haisma, H. J.; Koenis, M. J.; Tol, J. L.; Moen, M. H. Stem cell injections in knee osteoarthritis: a systematic review of the literature. *Br J Sports Med.* **2017**, *51*, 1125-1133.
633. Song, H. G.; Rumma, R. T.; Ozaki, C. K.; Edelman, E. R.; Chen, C. S. Vascular tissue engineering: progress, challenges, and clinical promise. *Cell Stem Cell.* **2018**, *22*, 340-354.
634. Jin, J. Stem Cell Treatments. *JAMA.* **2017**, *317*, 330.
635. Sackett, S. D.; Brown, M. E.; Tremmel, D. M.; Ellis, T.; Burlingham, W. J.; Odorico, J. S. Modulation of human allogeneic and syngeneic pluripotent stem cells and immunological implications for transplantation. *Transplant Rev (Orlando).* **2016**, *30*, 61-70.
636. Xiao, L.; Huang, R.; Zhang, Y.; Li, T.; Dai, J.; Nannapuneni, N.; Chastanet, T. R.; Chen, M.; Shen, F. H.; Jin, L.; Dorn, H. C.; Li, X. A new formyl peptide receptor-1 antagonist conjugated fullerene nanoparticle for targeted treatment of degenerative disc diseases. *ACS Appl Mater Interfaces.* **2019**, *11*, 38405-38416.
637. Qu, Y.; Wang, Z.; Zhou, H.; Kang, M.; Dong, R.; Zhao, J. Oligosaccharide nanomedicine of alginate sodium improves therapeutic results of posterior lumbar interbody fusion with cages for degenerative lumbar disease in osteoporosis patients by downregulating serum miR-155. *Int J Nanomedicine.* **2017**, *12*, 8459-8469.
638. Robinson, K.; Platt, S.; Bibi, K.; Banovic, F.; Barber, R.; Howerth, E. W.; Madsen, G. A pilot study on the safety of a novel antioxidant nanoparticle delivery system and its indirect effects on cytokine levels in four dogs. *Front Vet Sci.* **2020**, *7*, 447.
639. Tryfonidou, M. A.; de Vries, G.; Hennink, W. E.; Creemers, L. B. "Old Drugs, New Tricks" - local controlled drug release systems for treatment of degenerative joint disease. *Adv Drug Deliv Rev.* **2020**, *160*, 170-185.
640. van Tulder, M.; Koes, B.; Bombardier, C. Low back pain. *Best Pract Res Clin Rheumatol.* **2002**, *16*, 761-775.
641. van Tulder, M.; Koes, B. Low back pain (chronic). *Clin Evid.* **2006**, 1634-1653.
642. van Tulder, M.; Becker, A.; Bekkering, T.; Breen, A.; del Real, M. T.; Hutchinson, A.; Koes, B.; Laerum, E.; Malmivaara, A.; COST B13 Working Group on Guidelines for the Management of Acute Low Back Pain in Primary Care. Chapter 3. European guidelines for the management of acute nonspecific low back pain in primary care. *Eur Spine J.* **2006**, *15 Suppl 2*, S169-191.
643. Lyu, F. J.; Cui, H.; Pan, H.; Mc Cheung, K.; Cao, X.; Iatridis, J. C.; Zheng, Z. Painful intervertebral disc degeneration and inflammation: from laboratory evidence to clinical interventions. *Bone Res.* **2021**, *9*, 7.
644. Mosley, G. E.; Evashwick-Rogler, T. W.; Lai, A.; Iatridis, J. C. Looking beyond the intervertebral disc: the need for behavioral assays in models of discogenic pain. *Ann N Y Acad Sci.* **2017**, *1409*, 51-66.

645. Kambiz, S.; Baas, M.; Duraku, L. S.; Kerver, A. L.; Koning, A. H.; Walbeehm, E. T.; Ruigrok, T. J. Innervation mapping of the hind paw of the rat using Evans Blue extravasation, Optical Surface Mapping and CASAM. *J Neurosci Methods.* **2014**, *229*, 15-27.
646. Símaro, G. V.; Lemos, M.; Mangabeira da Silva, J. J.; Ribeiro, V. P.; Arruda, C.; Schneider, A. H.; Wagner de Souza Wanderley, C.; Carneiro, L. J.; Mariano, R. L.; Ambrósio, S. R.; Faloni de Andrade, S.; Banderó-Filho, V. C.; Sasse, A.; Sheridan, H.; Andrade, E. S. M. L.; Bastos, J. K. Antinociceptive and anti-inflammatory activities of Copaifera pubiflora Benth oleoresin and its major metabolite ent-hardwickiic acid. *J Ethnopharmacol.* **2021**, *271*, 113883.
647. Molstad, D. H. H.; Bradley, E. W. Pain and Activity Measurements. *Methods Mol Biol.* **2021**, *2221*, 291-299.
648. Heinsinger, N. M.; Spagnuolo, G.; Allahyari, R. V.; Galer, S.; Fox, T.; Jaffe, D. A.; Thomas, S. J.; Iacovitti, L.; Lepore, A. C. Facial grimace testing as an assay of neuropathic pain-related behavior in a mouse model of cervical spinal cord injury. *Exp Neurol.* **2020**, *334*, 113468.
649. Deuis, J. R.; Dvorakova, L. S.; Vetter, I. Methods used to evaluate pain behaviors in rodents. *Front Mol Neurosci.* **2017**, *10*, 284.
650. Chaplan, S. R.; Bach, F. W.; Pogrel, J. W.; Chung, J. M.; Yaksh, T. L. Quantitative assessment of tactile allodynia in the rat paw. *J Neurosci Methods.* **1994**, *53*, 55-63.
651. Evans, D. W.; De Nunzio, A. M. Controlled manual loading of body tissues: towards the next generation of pressure algometer. *Chiropr Man Therap.* **2020**, *28*, 51.
652. Plinsinga, M. L.; Meeus, M.; Brink, M. S.; Heugen, N.; van Wilgen, P. Evidence of widespread mechanical hyperalgesia but not exercise induced analgesia in athletes with mild patellar tendinopathy compared to pain-free matched controls: a blinded exploratory study. *Am J Phys Med Rehabil.* **2020**. doi: 10.1097/PHM.0000000000001673.
653. Ilnytska, O.; Lyzogubov, V. V.; Stevens, M. J.; Drel, V. R.; Mashtalir, N.; Pacher, P.; Yorek, M. A.; Obrosova, I. G. Poly(ADP-ribose) polymerase inhibition alleviates experimental diabetic sensory neuropathy. *Diabetes.* **2006**, *55*, 1686-1694.
654. Yalcin, I.; Charlet, A.; Freund-Mercier, M. J.; Barrot, M.; Poisbeau, P. Differentiating thermal allodynia and hyperalgesia using dynamic hot and cold plate in rodents. *J Pain.* **2009**, *10*, 767-773.
655. Bannon, A. W.; Malmberg, A. B. Models of nociception: hot-plate, tail-flick, and formalin tests in rodents. *Curr Protoc Neurosci.* **2007**, Chapter 8, Unit 8.9.
656. Driscoll, C.; Chanalaris, A.; Knights, C.; Ismail, H.; Sacitharan, P. K.; Gentry, C.; Bevan, S.; Vincent, T. L. Nociceptive sensitizers are regulated in damaged joint tissues, including articular cartilage, when osteoarthritic mice display pain behavior. *Arthritis Rheumatol.* **2016**, *68*, 857-867.
657. Millecamps, M.; Stone, L. S. Delayed onset of persistent discogenic axial and radiating pain after a single-level lumbar intervertebral disc injury in mice. *Pain.* **2018**, *159*, 1843-1855.
658. Wang, T.; Hurwitz, O.; Shimada, S. G.; Tian, D.; Dai, F.; Zhou, J.; Ma, C.; LaMotte, R. H. Anti-nociceptive effects of bupivacaine-encapsulated PLGA nanoparticles applied to the compressed dorsal root ganglion in mice. *Neurosci Lett.* **2018**, *668*, 154-158.
659. Kim, J. S.; Kroin, J. S.; Li, X.; An, H. S.; Buvanendran, A.; Yan, D.; Tuman, K. J.; van Wijnen, A. J.; Chen, D.; Im, H. J. The rat intervertebral disk degeneration pain model: relationships between biological and structural alterations and pain. *Arthritis Res Ther.* **2011**, *13*, R165.
660. Kinser, A. M.; Sands, W. A.; Stone, M. H. Reliability and validity of a pressure algometer. *J Strength Cond Res.* **2009**, *23*, 312-314.
661. O'Callaghan, J. P.; Holtzman, S. G. Quantification of the analgesic activity of narcotic antagonists by a modified hot-plate procedure. *J Pharmacol Exp Ther.* **1975**, *192*, 497-505.
662. Yoon, C.; Wook, Y. Y.; Sik, N. H.; Ho, K. S.; Mo, C. J. Behavioral signs of ongoing pain and cold allodynia in a rat model of neuropathic pain. *Pain.* **1994**, *59*, 369-376.
663. Tajerian, M.; Millecamps, M.; Stone, L. S. Morphine and clonidine synergize to ameliorate low back pain in mice. *Pain research and treatment.* **2012**, *2012*, 150842.
664. Aono, Y.; Hasegawa, H.; Yamazaki, Y.; Shimada, T.; Fujita, T.; Yamashita, T.; Fukumoto, S. Anti-FGF-23 neutralizing antibodies ameliorate muscle weakness and decreased spontaneous movement of Hyp mice. *J Bone Miner Res.* **2011**, *26*, 803-810.
665. Sluka, K. A.; Rasmussen, L. A. Fatiguing exercise enhances hyperalgesia to muscle inflammation. *Pain.* **2010**, *148*, 188-197.
666. Call, J. A.; McKeehen, J. N.; Novotny, S. A.; Lowe, D. A. Progressive resistance voluntary wheel running in the mdx mouse. *Muscle Nerve.* **2010**, *42*, 871-880.
667. Krock, E.; Millecamps, M.; Currie, J. B.; Stone, L. S.; Haglund, L. Low back pain and disc degeneration are decreased following chronic toll-like receptor 4 inhibition in a mouse model. *Osteoarthritis Cartilage.* **2018**, *26*, 1236-1246.
668. Keshavarzi, S.; Kermanshahi, S.; Karami, L.; Motaghinejad, M.; Motevalian, M.; Sadr, S. Protective role of metformin against methamphetamine induced anxiety, depression, cognition impairment and neurodegeneration in rat: The role of CREB/BDNF and Akt/GSK3 signaling pathways. *Neurotoxicology.* **2019**, *72*, 74-84.
669. Tappe-Theodor, A.; Kuner, R. Studying ongoing and spontaneous pain in rodents--challenges and opportunities. *Eur J Neurosci.* **2014**, *39*, 1881-1890.
670. Denenberg, V. H. Open-field bheavior in the rat: what does it mean? *Ann N Y Acad Sci.* **1969**, *159*, 852-859.
671. Parent, A. J.; Beaudet, N.; Beaudry, H.; Bergeron, J.; Bérubé, P.; Drolet, G.; Sarret, P.; Gendron, L. Increased anxiety-like behaviors in rats experiencing chronic inflammatory pain. *Behav Brain Res.* **2012**, *229*, 160-167.
672. Portfors, C. V. Types and functions of ultrasonic vocalizations in laboratory rats and mice. *J Am Assoc Lab Anim Sci.* **2007**, *46*, 28-34.
673. Williams, W. O.; Riskin, D. K.; Mott, A. K. Ultrasonic sound as an indicator of acute pain in laboratory mice. *J Am Assoc Lab Anim Sci.* **2008**, *47*, 8-10.
674. Langford, D. J.; Bailey, A. L.; Chanda, M. L.; Clarke, S. E.; Drummond, T. E.; Echols, S.; Glick, S.; Ingrao, J.; Klassen-Ross, T.; Lacroix-Fralish, M. L.; Matsumiya, L.; Sorge, R. E.; Sotocinal, S. G.; Tabaka, J. M.; Wong, D.; van den Maagdenberg, A. M.; Ferrari, M. D.; Craig, K. D.; Mogil, J. S. Coding of facial expressions of pain in the laboratory mouse. *Nat Methods.* **2010**, *7*, 447-449.
675. Sotocinal, S. G.; Sorge, R. E.; Zaloum, A.; Tuttle, A. H.; Martin, L. J.; Wieskopf, J. S.; Mapplebeck, J. C.; Wei, P.; Zhan, S.; Zhang, S.; McDougall, J. J.; King, O. D.; Mogil, J. S. The Rat Grimace Scale: a partially automated method for quantifying pain in the laboratory rat via facial expressions. *Mol Pain.* **2011**, *7*, 55.
676. Hohlbaum, K.; Corte, G. M.; Humpenöder, M.; Merle, R.; Thöne-Reineke, C. Reliability of the Mouse Grimace Scale in C57BL/6JRj Mice. *Animals (Basel).* **2020**, *10*, 1648.
677. Miller, A. L.; Leach, M. C. The Mouse Grimace Scale: a clinically useful tool? *PLoS One.* **2015**, *10*, e0136000.

678. Daneshmandi, L.; Barajaa, M.; Tahmasbi Rad, A.; Sydlik, S. A.; Laurencin, C. T. Graphene-based biomaterials for bone regenerative engineering: a comprehensive review of the field and considerations regarding biocompatibility and biodegradation. *Adv Healthc Mater.* **2021**, *10*, e2001414.
679. Rahmati, M.; Mozafari, M. Biocompatibility of alumina-based biomaterials-A review. *J Cell Physiol.* **2019**, *234*, 3321-3335.
680. Patel, H. Blood biocompatibility enhancement of biomaterials by heparin immobilization: a review. *Blood Coagul Fibrinolysis.* **2021**, *32*, 237-247.
681. Huang, H.; Evankovich, J.; Yan, W.; Nace, G.; Zhang, L.; Ross, M.; Liao, X.; Billiar, T.; Xu, J.; Esmon, C. T.; Tsung, A. Endogenous histones function as alarmins in sterile inflammatory liver injury through Toll-like receptor 9 in mice. *Hepatology.* **2011**, *54*, 999-1008.
682. Daly, K. A.; Liu, S.; Agrawal, V.; Brown, B. N.; Johnson, S. A.; Medberry, C. J.; Badylak, S. F. Damage associated molecular patterns within xenogeneic biologic scaffolds and their effects on host remodeling. *Biomaterials.* **2012**, *33*, 91-101.
683. Alsousi, A. A.; Igwe, O. J. Redox-active trace metal-induced release of high mobility group box 1(HMGB1) and inflammatory cytokines in fibroblast-like synovial cells is Toll-like receptor 4 (TLR4) dependent. *Biochim Biophys Acta Mol Basis Dis.* **2018**, *1864*, 3847-3858.
684. Ranzato, E.; Patrone, M.; Pedrazzi, M.; Burlando, B. HMGb1 promotes scratch wound closure of HaCaT keratinocytes via ERK1/2 activation. *Mol Cell Biochem.* **2009**, *332*, 199-205.
685. Fahmy-Garcia, S.; van Driel, M.; Witte-Buoma, J.; Walles, H.; van Leeuwen, J.; van Osch, G.; Farrell, E. NELL-1, HMGB1, and CCN2 enhance migration and vasculogenesis, but not osteogenic differentiation compared to BMP2. *Tissue Eng Part A.* **2018**, *24*, 207-218.
686. Steinke, J. W.; Platts-Mills, T. A.; Commins, S. P. The alpha-gal story: lessons learned from connecting the dots. *J Allergy Clin Immunol.* **2015**, *135*, 589-596; quiz 597.
687. Gabrielli, A.; Candela, M.; Ricciatti, A. M.; Caniglia, M. L.; Wieslander, J. Antibodies to mouse laminin in patients with systemic sclerosis (scleroderma) recognize galactosyl (alpha 1-3)-galactose epitopes. *Clin Exp Immunol.* **1991**, *86*, 367-373.
688. Perea-Gil, I.; Uriarte, J. J.; Prat-Vidal, C.; Gálvez-Montón, C.; Roura, S.; Llucià-Valldeperas, A.; Soler-Botija, C.; Farré, R.; Navajas, D.; Bayes-Genis, A. In vitro comparative study of two decellularization protocols in search of an optimal myocardial scaffold for recellularization. *Am J Transl Res.* **2015**, *7*, 558-573.
689. Ning, L. J.; Jiang, Y. L.; Zhang, C. H.; Zhang, Y.; Yang, J. L.; Cui, J.; Zhang, Y. J.; Yao, X.; Luo, J. C.; Qin, T. W. Fabrication and characterization of a decellularized bovine tendon sheet for tendon reconstruction. *J Biomed Mater Res A.* **2017**, *105*, 2299-2311.
690. Bourgine, P. E.; Pippenger, B. E.; Todorov, A., Jr.; Tchang, L.; Martin, I. Tissue decellularization by activation of programmed cell death. *Biomaterials.* **2013**, *34*, 6099-6108.
691. Limana, F.; Germani, A.; Zacheo, A.; Kajstura, J.; Di Carlo, A.; Borsellino, G.; Leoni, O.; Palumbo, R.; Battistini, L.; Rastaldo, R.; Müller, S.; Pompilio, G.; Anversa, P.; Bianchi, M. E.; Capogrossi, M. C. Exogenous high-mobility group box 1 protein induces myocardial regeneration after infarction via enhanced cardiac C-kit+ cell proliferation and differentiation. *Circ Res.* **2005**, *97*, e73-83.
692. van Steenberghe, M.; Schubert, T.; Xhema, D.; Bouzin, C.; Guiot, Y.; Duisit, J.; Abdelhamid, K.; Gianello, P. Enhanced vascular regeneration with chemically/physically treated bovine/human pericardium in rodents. *J Surg Res.* **2018**, *222*, 167-179.
693. Duisit, J.; Orlando, G.; Debluts, D.; Maistriaux, L.; Xhema, D.; de Bisthoven, Y. J.; Galli, C.; Peloso, A.; Behets, C.; Lengelé, B.; Gianello, P. Decellularization of the porcine ear generates a biocompatible, nonimmunogenic extracellular matrix platform for face subunit bioengineering. *Ann Surg.* **2018**, *267*, 1191-1201.
694. Wang, Z.; Sun, F.; Lu, Y.; Pan, S.; Yang, W.; Zhang, G.; Ma, J.; Shi, H. Rapid preparation of decellularized trachea as a 3D scaffold for organ engineering. *Int J Artif Organs.* **2021**, *44*, 55-64.
695. Naso, F.; Gandaglia, A.; Iop, L.; Spina, M.; Gerosa, G. Alpha-Gal detectors in xenotransplantation research: a word of caution. *Xenotransplantation.* **2012**, *19*, 215-220.
696. Gao, H. W.; Li, S. B.; Sun, W. Q.; Yun, Z. M.; Zhang, X.; Song, J. W.; Zhang, S. K.; Leng, L.; Ji, S. P.; Tan, Y. X.; Gong, F. Quantification of α-Gal antigen removal in the porcine dermal tissue by α-galactosidase. *Tissue Eng Part C Methods.* **2015**, *21*, 1197-1204.
697. Kim, M. S.; Lim, H. G.; Kim, Y. J. Calcification of decellularized and alpha-galactosidase-treated bovine pericardial tissue in an alpha-Gal knock-out mouse implantation model: comparison with primate pericardial tissue. *Eur J Cardiothorac Surg.* **2016**, *49*, 894-900.
698. Katti, D. S.; Lakshmi, S.; Langer, R.; Laurencin, C. T. Toxicity, biodegradation and elimination of polyanhydrides. *Adv Drug Deliv Rev.* **2002**, *54*, 933-961.
699. Cuesta, A.; Del Valle, M. E.; García-Suárez, O.; Viña, E.; Cabo, R.; Vázquez, G.; Cobo, J. L.; Murcia, A.; Alvarez-Vega, M.; García-Cosamalón, J.; Vega, J. A. Acid-sensing ion channels in healthy and degenerated human intervertebral disc. *Connect Tissue Res.* **2014**, *55*, 197-204.
700. Zhou, R. P.; Wu, X. S.; Wang, Z. S.; Xie, Y. Y.; Ge, J. F.; Chen, F. H. Novel insights into acid-sensing ion channels: implications for degenerative diseases. *Aging Dis.* **2016**, *7*, 491-501.
701. Alizadeh, M.; Rezakhani, L.; Khodaei, M.; Soleimannejad, M.; Alizadeh, A. Evaluating the effects of vacuum on the microstructure and biocompatibility of bovine decellularized pericardium. *J Tissue Eng Regen Med.* **2021**, *15*, 116-128.
702. Cheng, J.; Li, J.; Cai, Z.; Xing, Y.; Wang, C.; Guo, L.; Gu, Y. Decellularization of porcine carotid arteries using low-concentration sodium dodecyl sulfate. *Int J Artif Organs.* **2020**. doi: 10.1177/0391398820975420.
703. Wang, C.; Wang, M.; Xu, T.; Zhang, X.; Lin, C.; Gao, W.; Xu, H.; Lei, B.; Mao, C. Engineering bioactive self-healing antibacterial exosomes hydrogel for promoting chronic diabetic wound healing and complete skin regeneration. *Theranostics.* **2019**, 9, 65-76.
704. Liu, S.; Zhou, C.; Mou, S.; Li, J.; Zhou, M.; Zeng, Y.; Luo, C.; Sun, J.; Wang, Z.; Xu, W. Biocompatible graphene oxide-collagen composite aerogel for enhanced stiffness and in situ bone regeneration. *Mater Sci Eng C Mater Biol Appl.* **2019**, *105*, 110137.
705. Liu, Y.; Segura, T. Biomaterials-mediated regulation of macrophage cell fate. *Front Bioeng Biotechnol.* **2020**, *8*, 609297.
706. Lee, J.; Byun, H.; Madhurakkat Perikamana, S. K.; Lee, S.; Shin, H. Current advances in immunomodulatory biomaterials for bone regeneration. *Adv Healthc Mater.* **2019**, *8*, e1801106.
707. Christo, S. N.; Diener, K. R.; Bachhuka, A.; Vasilev, K.; Hayball, J. D. Innate immunity and biomaterials at the nexus: friends or foes. *Biomed Res Int.* **2015**, *2015*, 342304.
708. Varma, D. M.; Lin, H. A.; Long, R. G.; Gold, G. T.; Hecht, A. C.; Iatridis, J. C.; Nicoll, S. B. Thermoresponsive, redox-polymerized cellulosic hydrogels undergo in situ gelation and restore intervertebral disc biomechanics post discectomy. *Eur Cell Mater.* **2018**, *35*, 300-317.

709. Shaha, R. K.; Merkel, D. R.; Anderson, M. P.; Devereaux, E. J.; Patel, R. R.; Torbati, A. H.; Willett, N.; Yakacki, C. M.; Frick, C. P. Biocompatible liquid-crystal elastomers mimic the intervertebral disc. *J Mech Behav Biomed Mater.* **2020**, *107*, 103757.
710. Frith, J. E.; Cameron, A. R.; Menzies, D. J.; Ghosh, P.; Whitehead, D. L.; Gronthos, S.; Zannettino, A. C.; Cooper-White, J. J. An injectable hydrogel incorporating mesenchymal precursor cells and pentosan polysulphate for intervertebral disc regeneration. *Biomaterials.* **2013**, *34*, 9430-9440.
711. Zhu, D.; Cockerill, I.; Su, Y.; Zhang, Z.; Fu, J.; Lee, K. W.; Ma, J.; Okpokwasili, C.; Tang, L.; Zheng, Y.; Qin, Y. X.; Wang, Y. Mechanical strength, biodegradation, and in vitro and in vivo biocompatibility of Zn biomaterials. *ACS Appl Mater Interfaces.* **2019**, *11*, 6809-6819.
712. Huang, Y. C.; Urban, J. P.; Luk, K. D. Intervertebral disc regeneration: do nutrients lead the way? *Nat Rev Rheumatol.* **2014**, *10*, 561-566.
713. Sawamura, K.; Ikeda, T.; Nagae, M.; Okamoto, S.; Mikami, Y.; Hase, H.; Ikoma, K.; Yamada, T.; Sakamoto, H.; Matsuda, K.; Tabata, Y.; Kawata, M.; Kubo, T. Characterization of in vivo effects of platelet-rich plasma and biodegradable gelatin hydrogel microspheres on degenerated intervertebral discs. *Tissue Eng Part A.* **2009**, *15*, 3719-3727.
714. Santos, J. M.; Pereira, S.; Sequeira, D. B.; Messias, A. L.; Martins, J. B.; Cunha, H.; Palma, P. J.; Santos, A. C. Biocompatibility of a bioceramic silicone-based sealer in subcutaneous tissue. *J Oral Sci.* **2019**, *61*, 171-177.
715. Benetti, F.; de Azevedo Queiroz Í, O.; Oliveira, P. H. C.; Conti, L. C.; Azuma, M. M.; Oliveira, S. H. P.; Cintra, L. T. A. Cytotoxicity and biocompatibility of a new bioceramic endodontic sealer containing calcium hydroxide. *Braz Oral Res.* **2019**, *33*, e042.
716. Tukmachev, D.; Forostyak, S.; Koci, Z.; Zaviskova, K.; Vackova, I.; Vyborny, K.; Sandvig, I.; Sandvig, A.; Medberry, C. J.; Badylak, S. F.; Sykova, E.; Kubinova, S. Injectable extracellular matrix hydrogels as scaffolds for spinal cord injury repair. *Tissue Eng Part A.* **2016**, *22*, 306-317.
717. Wolf, M. T.; Daly, K. A.; Brennan-Pierce, E. P.; Johnson, S. A.; Carruthers, C. A.; D'Amore, A.; Nagarkar, S. P.; Velankar, S. S.; Badylak, S. F. A hydrogel derived from decellularized dermal extracellular matrix. *Biomaterials.* **2012**, *33*, 7028-7038.
718. Zhang, C.; Shang, Y.; Chen, X.; Midgley, A. C.; Wang, Z.; Zhu, D.; Wu, J.; Chen, P.; Wu, L.; Wang, X.; Zhang, K.; Wang, H.; Kong, D.; Yang, Z.; Li, Z.; Chen, X. Supramolecular nanofibers containing arginine-glycine-aspartate (RGD) peptides boost therapeutic efficacy of extracellular vesicles in kidney repair. *ACS Nano.* **2020**, *14*, 12133-12147.
719. Ong, S. R.; Trabbic-Carlson, K. A.; Nettles, D. L.; Lim, D. W.; Chilkoti, A.; Setton, L. A. Epitope tagging for tracking elastin-like polypeptides. *Biomaterials.* **2006**, *27*, 1930-1935.
720. Sharma, P.; Brown, S.; Walter, G.; Santra, S.; Moudgil, B. Nanoparticles for bioimaging. *Adv Colloid Interface Sci.* **2006**, *123-126*, 471-485.
721. Frangioni, J. V. In vivo near-infrared fluorescence imaging. *Curr Opin Chem Biol.* **2003**, *7*, 626-634.
722. Jalani, G.; Naccache, R.; Rosenzweig, D. H.; Lerouge, S.; Haglund, L.; Vetrone, F.; Cerruti, M. Real-time, non-invasive monitoring of hydrogel degradation using LiYF4:Yb(3+)/Tm(3+) NIR-to-NIR upconverting nanoparticles. *Nanoscale.* **2015**, *7*, 11255-11262.
723. 723. Sheehan, N. J. Magnetic resonance imaging for low back pain: indications and limitations. *Postgrad Med J.* **2010**, *86*, 374-378.
724. Lai, A.; Chow, D. H.; Siu, W. S.; Holmes, A. D.; Tang, F. H. Reliability of radiographic intervertebral disc height measurement for in vivo rat-tail model. *Med Eng Phys.* **2007**, *29*, 814-819.
725. Masuda, K.; Aota, Y.; Muehleman, C.; Imai, Y.; Okuma, M.; Thonar, E. J.; Andersson, G. B.; An, H. S. A novel rabbit model of mild, reproducible disc degeneration by an anulus needle puncture: correlation between the degree of disc injury and radiological and histological appearances of disc degeneration. *Spine (Phila Pa 1976).* **2005**, *30*, 5-14.
726. Deyo, R. A.; Loeser, J. D.; Bigos, S. J. Herniated lumbar intervertebral disk. *Ann Intern Med.* **1990**, *112*, 598-603.
727. Ng, S. K.; Urquhart, D. M.; Fitzgerald, P. B.; Cicuttini, F. M.; Hussain, S. M.; Fitzgibbon, B. M. The relationship between structural and functional brain changes and altered emotion and cognition in chronic low back pain brain changes: a systematic review of MRI and fMRI studies. *Clin J Pain.* **2018**, *34*, 237-261.
728. Roughley, P. J.; Alini, M.; Antoniou, J. The role of proteoglycans in aging, degeneration and repair of the intervertebral disc. *Biochem Soc Trans.* **2002**, *30*, 869-874.
729. Pfirrmann, C. W.; Metzdorf, A.; Zanetti, M.; Hodler, J.; Boos, N. Magnetic resonance classification of lumbar intervertebral disc degeneration. *Spine (Phila Pa 1976).* **2001**, *26*, 1873-1878.
730. Luoma, K.; Vehmas, T.; Riihimäki, H.; Raininko, R. Disc height and signal intensity of the nucleus pulposus on magnetic resonance imaging as indicators of lumbar disc degeneration. *Spine (Phila Pa 1976).* **2001**, *26*, 680-686.
731. Benneker, L. M.; Heini, P. F.; Anderson, S. E.; Alini, M.; Ito, K. Correlation of radiographic and MRI parameters to morphological and biochemical assessment of intervertebral disc degeneration. *Eur Spine J.* **2005**, *14*, 27-35.
732. Wang, A. M.; Cao, P.; Yee, A.; Chan, D.; Wu, E. X. Detection of extracellular matrix degradation in intervertebral disc degeneration by diffusion magnetic resonance spectroscopy. *Magn Reson Med.* **2015**, *73*, 1703-1712.
733. Yu, L. P.; Qian, W. W.; Yin, G. Y.; Ren, Y. X.; Hu, Z. Y. MRI assessment of lumbar intervertebral disc degeneration with lumbar degenerative disease using the Pfirrmann grading systems. *PLoS One.* **2012**, *7*, e48074.
734. Waldenberg, C.; Hebelka, H.; Brisby, H.; Lagerstrand, K. M. MRI histogram analysis enables objective and continuous classification of intervertebral disc degeneration. *Eur Spine J.* **2018**, *27*, 1042-1048.
735. Hutton, W. C.; Malko, J. A.; Fajman, W. A. Lumbar disc volume measured by MRI: effects of bed rest, horizontal exercise, and vertical loading. *Aviat Space Environ Med.* **2003**, *74*, 73-78.
736. Malko, J. A.; Hutton, W. C.; Giacometti, A. R.; Kater, G.; Greenfield, P.; Boden, S. D.; Silcox, D. H. Do diurnal changes in loading affect the interpretation of MRI scans of the lumbar spine? *J Spinal Disord.* **1996**, *9*, 129-135.
737. Roberts, N.; Hogg, D.; Whitehouse, G. H.; Dangerfield, P. Quantitative analysis of diurnal variation in volume and water content of lumbar intervertebral discs. *Clin Anat.* **1998**, *11*, 1-8.
738. Che, Y. J.; Guo, J. B.; Liang, T.; Chen, X.; Zhang, W.; Yang, H. L.; Luo, Z. P. Assessment of changes in the micro-nano environment of intervertebral disc degeneration based on Pfirrmann grade. *Spine J.* **2019**, *19*, 1242-1253.
739. Jensen, T. S.; Albert, H. B.; Soerensen, J. S.; Manniche, C.; Leboeuf-Yde, C. Natural course of disc morphology in patients with sciatica: an MRI study using a standardized qualitative classification system. *Spine (Phila Pa 1976).* **2006**, *31*, 1605-1612; discussion 1613.
740. Boden, S. D.; Davis, D. O.; Dina, T. S.; Patronas, N. J.; Wiesel, S. W. Abnormal magnetic-resonance scans of the lumbar spine in asymptomatic subjects. A prospective investigation. *J Bone Joint Surg Am.*

1990, *72*, 403-408.
741. Jensen, M. C.; Brant-Zawadzki, M. N.; Obuchowski, N.; Modic, M. T.; Malkasian, D.; Ross, J. S. Magnetic resonance imaging of the lumbar spine in people without back pain. *N Engl J Med.* **1994**, *331*, 69-73.
742. Chavhan, G. B.; Babyn, P. S.; Thomas, B.; Shroff, M. M.; Haacke, E. M. Principles, techniques, and applications of T2*-based MR imaging and its special applications. *Radiographics.* **2009**, *29*, 1433-1449.
743. Foltz, M. H.; Kage, C. C.; Johnson, C. P.; Ellingson, A. M. Noninvasive assessment of biochemical and mechanical properties of lumbar discs through quantitative magnetic resonance imaging in asymptomatic volunteers. *J Biomech Eng.* **2017**, *139*, 1110021-1110027.
744. Samartzis, D.; Borthakur, A.; Belfer, I.; Bow, C.; Lotz, J. C.; Wang, H. Q.; Cheung, K. M.; Carragee, E.; Karppinen, J. Novel diagnostic and prognostic methods for disc degeneration and low back pain. *Spine J.* **2015**, *15*, 1919-1932.
745. Farshad-Amacker, N. A.; Farshad, M.; Winklehner, A.; Andreisek, G. MR imaging of degenerative disc disease. *Eur J Radiol.* **2015**, *84*, 1768-1776.
746. Nguyen, A. M.; Johannessen, W.; Yoder, J. H.; Wheaton, A. J.; Vresilovic, E. J.; Borthakur, A.; Elliott, D. M. Noninvasive quantification of human nucleus pulposus pressure with use of T1rho-weighted magnetic resonance imaging. *J Bone Joint Surg Am.* **2008**, *90*, 796-802.
747. Rong, R.; Zhang, C. Y.; Wang, X. Y. Normal appearance of large field diffusion weighted imaging on 3.0T MRI. *Chin Med Sci J.* **2008**, *23*, 158-161.
748. Ludescher, B.; Effelsberg, J.; Martirosian, P.; Steidle, G.; Markert, B.; Claussen, C.; Schick, F. T2- and diffusion-maps reveal diurnal changes of intervertebral disc composition: an in vivo MRI study at 1.5 Tesla. *J Magn Reson Imaging.* **2008**, *28*, 252-257.
749. Arpinar, V. E.; Rand, S. D.; Klein, A. P.; Maiman, D. J.; Muftuler, L. T. Changes in perfusion and diffusion in the endplate regions of degenerating intervertebral discs: a DCE-MRI study. *Eur Spine J.* **2015**, *24*, 2458-2467.
750. Kealey, S. M.; Aho, T.; Delong, D.; Barboriak, D. P.; Provenzale, J. M.; Eastwood, J. D. Assessment of apparent diffusion coefficient in normal and degenerated intervertebral lumbar disks: initial experience. *Radiology.* **2005**, *235*, 569-574.
751. Li, L. Y.; Wu, X. L.; Roman, R. J.; Fan, F.; Qiu, C. S.; Chen, B. H. Diffusion-weighted 7.0T magnetic resonance imaging in assessment of intervertebral disc degeneration in rats. *Chin Med J (Engl).* **2018**, *131*, 63-68.
752. Paul, C. P. L.; Smit, T. H.; de Graaf, M.; Holewijn, R. M.; Bisschop, A.; van de Ven, P. M.; Mullender, M. G.; Helder, M. N.; Strijkers, G. J. Quantitative MRI in early intervertebral disc degeneration: T1rho correlates better than T2 and ADC with biomechanics, histology and matrix content. *PLoS One.* **2018**, *13*, e0191442.
753. Ward, K. M.; Balaban, R. S. Determination of pH using water protons and chemical exchange dependent saturation transfer (CEST). *Magn Reson Med.* **2000**, *44*, 799-802.
754. Pulickal, T.; Boos, J.; Konieczny, M.; Sawicki, L. M.; Müller-Lutz, A.; Bittersohl, B.; Gerß, J.; Eichner, M.; Wittsack, H. J.; Antoch, G.; Schleich, C. MRI identifies biochemical alterations of intervertebral discs in patients with low back pain and radiculopathy. *Eur Radiol.* **2019**, *29*, 6443-6446.
755. Hang, D.; Li, F.; Che, W.; Wu, X.; Wan, Y.; Wang, J.; Zheng, Y. One-stage positron emission tomography and magnetic resonance imaging to assess mesenchymal stem cell survival in a canine model of intervertebral disc degeneration. *Stem Cells Dev.* **2017**, *26*, 1334-1343.
756. Saldanha, K. J.; Piper, S. L.; Ainslie, K. M.; Kim, H. T.; Majumdar, S. Magnetic resonance imaging of iron oxide labelled stem cells: applications to tissue engineering based regeneration of the intervertebral disc. *Eur Cell Mater.* **2008**, *16*, 17-25.
757. Lalande, C.; Miraux, S.; Derkaoui, S. M.; Mornet, S.; Bareille, R.; Fricain, J. C.; Franconi, J. M.; Le Visage, C.; Letourneur, D.; Amédée, J.; Bouzier-Sore, A. K. Magnetic resonance imaging tracking of human adipose derived stromal cells within three-dimensional scaffolds for bone tissue engineering. *Eur Cell Mater.* **2011**, *21*, 341-354.
758. Martin, J. T.; Milby, A. H.; Ikuta, K.; Poudel, S.; Pfeifer, C. G.; Elliott, D. M.; Smith, H. E.; Mauck, R. L. A radiopaque electrospun scaffold for engineering fibrous musculoskeletal tissues: Scaffold characterization and in vivo applications. *Acta Biomater.* **2015**, *26*, 97-104.
759. Gullbrand, S. E.; Schaer, T. P.; Agarwal, P.; Bendigo, J. R.; Dodge, G. R.; Chen, W.; Elliott, D. M.; Mauck, R. L.; Malhotra, N. R.; Smith, L. J. Translation of an injectable triple-interpenetrating-network hydrogel for intervertebral disc regeneration in a goat model. *Acta Biomater.* **2017**, *60*, 201-209.
760. Nomura, T.; Mochida, J.; Okuma, M.; Nishimura, K.; Sakabe, K. Nucleus pulposus allograft retards intervertebral disc degeneration. *Clin Orthop Relat Res.* **2001**, 94-101.
761. Nishimura, K.; Mochida, J. Percutaneous reinsertion of the nucleus pulposus. An experimental study. *Spine (Phila Pa 1976).* **1998**, *23*, 1531-1538; discussion 1539.
762. Miyazaki, S.; Diwan, A. D.; Kato, K.; Cheng, K.; Bae, W. C.; Sun, Y.; Yamada, J.; Muehleman, C.; Lenz, M. E.; Inoue, N.; Sah, R. L.; Kawakami, M.; Masuda, K. ISSLS PRIZE IN BASIC SCIENCE 2018: Growth differentiation factor-6 attenuated pro-inflammatory molecular changes in the rabbit anular-puncture model and degenerated disc-induced pain generation in the rat xenograft radiculopathy model. *Eur Spine J.* **2018**, *27*, 739-751.
763. Qian, J.; Ge, J.; Yan, Q.; Wu, C.; Yang, H.; Zou, J. Selection of the Optimal Puncture Needle for Induction of a Rat Intervertebral Disc Degeneration Model. *Pain Physician.* **2019**, *22*, 353-360.
764. Chen, Z.; Zhang, W.; Deng, M.; Li, Y.; Zhou, Y. CircGLCE alleviates intervertebral disc degeneration by regulating apoptosis and matrix degradation through the targeting of miR-587/STAP1. *Aging (Albany NY).* **2020**, *12*, 21971-21991.
765. Wang, D.; He, X.; Wang, D.; Peng, P.; Xu, X.; Gao, B.; Zheng, C.; Wang, H.; Jia, H.; Shang, Q.; Sun, Z.; Luo, Z.; Yang, L. Quercetin suppresses apoptosis and attenuates intervertebral disc degeneration via the SIRT1-autophagy pathway. *Front Cell Dev Biol.* **2020**, *8*, 613006.
766. Huang, J. F.; Zheng, X. Q.; Lin, J. L.; Zhang, K.; Tian, H. J.; Zhou, W. X.; Wang, H.; Gao, Z.; Jin, H. M.; Wu, A. M. Sinapic acid inhibits IL-1β-induced apoptosis and catabolism in nucleus pulposus cells and ameliorates intervertebral disk degeneration. *J Inflamm Res.* **2020**, *13*, 883-895.
767. Thompson, J. P.; Pearce, R. H.; Schechter, M. T.; Adams, M. E.; Tsang, I. K.; Bishop, P. B. Preliminary evaluation of a scheme for grading the gross morphology of the human intervertebral disc. *Spine (Phila Pa 1976).* **1990**, *15*, 411-415.
768. Boos, N.; Weissbach, S.; Rohrbach, H.; Weiler, C.; Spratt, K. F.; Nerlich, A. G. Classification of age-related changes in lumbar intervertebral discs: 2002 Volvo Award in basic science. *Spine (Phila Pa 1976).* **2002**, *27*, 2631-2644.
769. Fusellier, M.; Colombier, P.; Lesoeur, J.; Youl, S.; Madec, S.; Gauthier, O.; Hamel, O.; Guicheux, J.; Clouet, J. Longitudinal comparison of

enzyme- and laser-treated intervertebral disc by MRI, X-ray, and histological analyses reveals discrepancies in the progression of disc degeneration: a rabbit study. *Biomed Res Int.* **2016**, *2016*, 5498271.

770. Phillips, K. L.; Jordan-Mahy, N.; Nicklin, M. J.; Le Maitre, C. L. Interleukin-1 receptor antagonist deficient mice provide insights into pathogenesis of human intervertebral disc degeneration. *Ann Rheum Dis.* **2013**, *72*, 1860-1867.
771. Groh, A. M. R.; Fournier, D. E.; Battié, M. C.; Séguin, C. A. Innervation of the human intervertebral disc: a scoping review. *Pain Med.* **2021**, *22*, 1281-1304.
772. Liu, C.; Jin, Z.; Ge, X.; Zhang, Y.; Xu, H. Decellularized annulus fibrosus matrix/chitosan hybrid hydrogels with basic fibroblast growth factor for annulus fibrosus tissue engineering. *Tissue Eng Part A.* **2019**, *25*, 1605-1613.
773. ASTM F2258-05(2015). Standard Test Method for Strength Properties of Tissue Adhesives in Tension. ASTM International: West Conshohocken, PA,2015.
774. ASTM F2255-05(2015). Standard Test Method for Strength Properties of Tissue Adhesives in Lap-Shear by Tension Loading. ASTM International: West Conshohocken, PA,2015.
775. ASTM F2458-05(2015). Standard Test Method for Wound Closure Strength of Tissue Adhesives and Sealants. ASTM International: West Conshohocken, PA,2015.
776. ASTM F2392-04(2015). Standard Test Method for Burst Strength of Surgical Sealants. ASTM International: Conshohocken, PA,2015.
777. Schmitz, T. C.; Salzer, E.; Crispim, J. F.; Fabra, G. T.; LeVisage, C.; Pandit, A.; Tryfonidou, M.; Maitre, C. L.; Ito, K. Characterization of biomaterials intended for use in the nucleus pulposus of degenerated intervertebral discs. *Acta Biomater.* **2020**, *114*, 1-15.
778. Thoreson, O.; Ekström, L.; Hansson, H. A.; Todd, C.; Witwit, W.; Swärd Aminoff, A.; Jonasson, P.; Baranto, A. The effect of repetitive flexion and extension fatigue loading on the young porcine lumbar spine, a feasibility study of MRI and histological analyses. *J Exp Orthop.* **2017**, *4*, 16.
779. Noguchi, M.; Gooyers, C. E.; Karakolis, T.; Noguchi, K.; Callaghan, J. P. Is intervertebral disc pressure linked to herniation?: An in-vitro study using a porcine model. *J Biomech.* **2016**, *49*, 1824-1830.
780. Brown, M. D.; Holmes, D. C.; Heiner, A. D. Measurement of cadaver lumbar spine motion segment stiffness. *Spine (Phila Pa 1976).* **2002**, *27*, 918-922.
781. Newell, N.; Rivera Tapia, D.; Rahman, T.; Lim, S.; O'Connell, G. D.; Holsgrove, T. P. Influence of testing environment and loading rate on intervertebral disc compressive mechanics: An assessment of repeatability at three different laboratories. *JOR Spine.* **2020**, *3*, e21110.
782. Shanks, H. R.; Wu, S.; Nguyen, N. T.; Lu, D.; Saunders, B. R. Including fluorescent nanoparticle probes within injectable gels for remote strain measurements and discrimination between compression and tension. *Soft Matter.* **2021**, *17*, 1048-1055.
783. Iatridis, J. C.; Mente, P. L.; Stokes, I. A.; Aronsson, D. D.; Alini, M. Compression-induced changes in intervertebral disc properties in a rat tail model. *Spine (Phila Pa 1976).* **1999**, *24*, 996-1002.
784. Adams, M. A.; Roughley, P. J. What is intervertebral disc degeneration, and what causes it? *Spine (Phila Pa 1976).* **2006**, *31*, 2151-2161.
785. Shao, Z.; Wang, B.; Shi, Y.; Xie, C.; Huang, C.; Chen, B.; Zhang, H.; Zeng, G.; Liang, H.; Wu, Y.; Zhou, Y.; Tian, N.; Wu, A.; Gao, W.; Wang, X.; Zhang, X. Senolytic agent Quercetin ameliorates intervertebral disc degeneration via the Nrf2/NF-κB axis. *Osteoarthritis Cartilage.* **2021**, *29*, 413-422.
786. Patil, P.; Falabella, M.; Saeed, A.; Lee, D.; Kaufman, B.; Shiva, S.; Croix, C. S.; Van Houten, B.; Niedernhofer, L. J.; Robbins, P. D.; Lee, J.; Gwendolyn, S.; Vo, N. V. Oxidative stress-induced senescence markedly increases disc cell bioenergetics. *Mech Ageing Dev.* **2019**, *180*, 97-106.
787. Rajasekaran, S.; Tangavel, C.; Aiyer, S. N.; Nayagam, S. M.; Raveendran, M.; Demonte, N. L.; Subbaiah, P.; Kanna, R.; Shetty, A. P.; Dharmalingam, K. ISSLS PRIZE IN CLINICAL SCIENCE 2017: Is infection the possible initiator of disc disease? An insight from proteomic analysis. *Eur Spine J.* **2017**, *26*, 1384-1400.
788. Benzakour, T.; Igoumenou, V.; Mavrogenis, A. F.; Benzakour, A. Current concepts for lumbar disc herniation. *Int Orthop.* **2019**, *43*, 841-851.
789. Martin, J. T.; Kim, D. H.; Milby, A. H.; Pfeifer, C. G.; Smith, L. J.; Elliott, D. M.; Smith, H. E.; Mauck, R. L. In vivo performance of an acellular disc-like angle ply structure (DAPS) for total disc replacement in a small animal model. *J Orthop Res.* **2017**, *35*, 23-31.
790. Lim, K. Z.; Daly, C. D.; Ghosh, P.; Jenkin, G.; Oehme, D.; Cooper-White, J.; Naidoo, T.; Goldschlager, T. Ovine lumbar intervertebral disc degeneration model utilizing a lateral retroperitoneal drill bit injury. *J Vis Exp.* **2017**, 55753.
791. Schek, R. M.; Michalek, A. J.; Iatridis, J. C. Genipin-crosslinked fibrin hydrogels as a potential adhesive to augment intervertebral disc annulus repair. *Eur Cell Mater.* **2011**, *21*, 373-383.
792. Fakhoury, J.; Dowling, T. J. Cervical degenerative disc disease. In StatPearls, StatPearls Publishing: Treasure Island (FL), 2021.
793. Ho-Pham, L. T.; Lai, T. Q.; Mai, L. D.; Doan, M. C.; Pham, H. N.; Nguyen, T. V. Prevalence and pattern of radiographic intervertebral disc degeneration in Vietnamese: a population-based study. *Calcif Tissue Int.* **2015**, *96*, 510-517.
794. Zou, F.; Yang, S.; Jiang, J.; Lu, F.; Xia, X.; Ma, X. Adjacent intervertebral disk height decrease phenomenon after single-level transforaminal lumbar interbody fusion of the lumbar spine. *World Neurosurg.* **2019**, *128*, e308-e314.
795. Hei, L.; Ge, Z.; Yuan, W.; Suo, L.; Suo, Z.; Lin, L.; Ding, H.; Qiu, Y. Evaluation of a rabbit model of adjacent intervertebral disc degeneration after fixation and fusion and maintenance in an upright feeding cage. *Neurol Res.* **2021**, *43*, 447-457.
796. Liu, Z.; Zheng, Z.; Qi, J.; Wang, J.; Zhou, Q.; Hu, F.; Liang, J.; Li, C.; Zhang, W.; Zhang, X. CD24 identifies nucleus pulposus progenitors/notochordal cells for disc regeneration. *J Biol Eng.* **2018**, *12*, 35.
797. Yang, S. H.; Hu, M. H.; Wu, C. C.; Chen, C. W.; Sun, Y. H.; Yang, K. C. CD24 expression indicates healthier phenotype and less tendency of cellular senescence in human nucleus pulposus cells. *Artif Cells Nanomed Biotechnol.* **2019**, *47*, 3021-3028.
798. Xunlu, Y.; Minshan, F.; Liguo, Z.; Jiawen, Z.; Xu, W.; Jie, Y.; Shangquan, W.; He, Y.; Long, L.; Tao, H.; Xuepeng, L. Integrative bioinformatics analysis reveals potential gene biomarkers and analysis of function in human degenerative disc annulus fibrosus cells. *Biomed Res Int.* **2019**, *2019*, 9890279.
799. Rutges, J.; Creemers, L. B.; Dhert, W.; Milz, S.; Sakai, D.; Mochida, J.; Alini, M.; Grad, S. Variations in gene and protein expression in human nucleus pulposus in comparison with annulus fibrosus and cartilage cells: potential associations with aging and degeneration. *Osteoarthritis Cartilage.* **2010**, *18*, 416-423.

Received: April 8, 2021
Revised: June 4, 2021
Accepted: June 9, 2021
Available online: June 28, 2021